The Dissertation Committee for Ioana Simona Pavel certifies that this is the approved version of the following dissertation:

Assembly of Gold Nanoparticles by Ribosomal Molecular Machines

Committee:

Karen S. Browning, Supervisor

Angela M. Belcher, Co-Supervisor

David W. Hoffman

John T. McDevitt

John M. Lansdown

Assembly of Gold Nanoparticles by Ribosomal Molecular Machines

by

Ioana Simona Pavel, B.S., M.S.

Dissertation

Presented to the Faculty of the Graduate School of

The University of Texas at Austin

in Partial Fulfillment

of the Requirements

for the Degree of

Doctor of Philosophy

The University of Texas at Austin

May 2005

Dedication

To my family

“Did you ever know that you're my hero,

And ev'rything I would like to be?

I can fly higher than an eagle,

'Cause you are the wind beneath my wings.”

By Larry Henley and Jeff Silbar

Acknowledgements

My journey as a chemist started at the early age of four, when my father introduced me to the magical world of chemistry. Now when I am close to the finish of this immense journey that I started many years ago, I would like to address my respectful thanks and appreciation to all the people who helped me on this path.

Beginning with my teachers in middle school to high school, to my professors at "Babes-Bolyai" University especially Dr. Gabriela Câmpan and to my ex-advisor, Dr. Keith Pannell, who encouraged me and proved that I can do more, I would like to say that I have the utmost respect for you all.

On the 4th of April 2001 I started working in the lab side-by-side with Dr. Karen Browning, who was at that time my co-adviser and later became my adviser. She is the one person who showed me the path for becoming a good and cautious biochemist, a better person and she taught me the quality that I missed the most: patience. She is not only my mentor but also my friend and confidant, the person who always had time for me and my problems. Thank you for not letting me slip along the path and always being there for me. Thank you for all the long discussions that we had.

Also, I would like to thank the other important adviser of mine Dr. Angela M. Belcher for taking a chance with me when I first came into her lab. She had this great idea, which later became my doctoral thesis, and let me pursue it. Three years ago she

left The University of Texas to become a professor at Massachusetts Institute of Technology. I thank her for not leaving me “behind”, always having time for me, the Last Mohican. Thank you for all your help and friendship.

I would also like to acknowledge all my colleagues from Dr. Browning and Dr. Belcher laboratories especially Dr. Esther Ryan, Dr. Leah Allen, Anirvan Chaudhuri, Laura Mayberry, Erin Gooch, and Christine Flynn. I am thankful for our fruitful collaborations and for all the fun we had.

I wish to express special thanks to Dr. Miguel Jose Yacaman and his lab for their help in collecting my TEM data. Special thanks to Dr. John Lansdown for his help with the LA-ICP-MS.

And finally, a big thanks to my family and friends, who were my driving force, the light in the “tunnel” and the re-charger of my batteries.

My doctoral work was a special time as my family and I were blessed with our daughter, Francesca Maria, who is the sunshine in our life and the one that keeps me going. Special thanks to my husband, Alex, for being there for me whenever I felt the need and for being a constant support on whose shoulder I could lean at any given time. My heartfelt gratitude goes to my mother for her help along this journey and thank you for being my best friend all my life. Also, millions of thank to my mother and my mother-in-law for their help, I could have never done this without your help. Lastly, I would also like to thank my brother, Calin, for his joyous spirit, contagious laugh, which lifted my spirits on numerous occasions.

Assembly of Gold Nanoparticles by Ribosomal Molecular Machines

Publication No._____

Ioana Simona Pavel, Ph.D.

The University of Texas at Austin, 2005

Supervisors: Karen S. Browning and Angela M. Belcher

The goal of this work is to develop novel method for organizing gold nanoparticles by linking them to chemically reactive side chains amino acids (e.g., lysine and cysteine) and then incorporating these modified amino acids into a polypeptide through *in vitro* translation of a synthetic mRNA template. The use of this system not only provides a method for the supramolecular assembly of new bio-inorganic heterostructures, using ribosomes as natural molecular machines and an artificial coding template, but also provides a new tool for probing fundamental biological processes (e.g., translation).

Transfer RNA (tRNA) is transcribed *in vitro* from a plasmid-template containing the tRNA gene under control of the T7 promoter. A novel coupled transcription–aminoacylation (CTA) system which prepares large amounts of pure aminoacyl-tRNA in a single reaction mixture was developed. Radiolabeled [^{32}P]-UTP and [^{14}C] or [^{32}S]-amino acid are used to monitor the coupled transcription- aminoacylation reactions. The ability to further modify the tRNA with a biotinylated probe is also demonstrated. The

tRNA synthesized by CTA, or further modified with biotin is shown to retain its functionality in *in vitro* translation, allowing the synthesis and detection of biotin-labeled protein.

Following the charging of the tRNA, the side chain of the amino acid is covalently linked to a gold nanoparticle, i.e. Monomaleido or Mono-sulfo-N-hydroxysuccinimide Nanogolds, either directly or through a heterobifunctional linker, which may vary in length and/or chemical properties, depending on the system used. The result is a novel gold nanoparticle-conjugated tRNA. Each of the steps is verified by mass spectroscopy (ESI and/or MALDI). The attachment of the gold nanoparticle to modified aminoacyl-tRNA is confirmed using High angle annular dark field images (HTEM) and laser ablation inductively coupled plasma mass spectrometry (LA-ICP-MS). The incorporation of the quantum dot-conjugated tRNA into a polypeptide is measured using an *in vitro E. coli* S30 cell-free coupled transcription-translation system, and verified by electrophoresis, laser ablation inductively coupled plasma mass spectrometry (LA-ICP-MS), High angle annular dark field (HAADF) images and electron loss spectroscopy .

Table of Contents

List of Tables xii

List of Figures xiii

CHAPTER 1

INTRODUCTION: 1

1. Overview 1

1. 1. Protein biosynthesis 1

1.2. The Ribosome, A protein factory: 3

1.3. Aminoacyl-tRNA –the code "decipher" 6

1.3.1. Unnatural Aminoacyl-tRNA a new area in modern biochemistry……..8

1.4. Quantum dots 12

1.4.1. Nanotechnology tool for tagging biological substrates 14

1.5. Is it possible to use the ribosome to manufacture an inorganic modified amino acid? 16

1.5.1. My ideal nanodot. 18

CHAPTER 2

LYSINE SYSTEM 20

2.1. Introduction: 20

2.2. Materials and Methods: 22

2.2.1 Enzymes: 22

2.2.1.1. E. coli His^{N}-LysRS: 22

2.2.1.2. E. coli His^{C}-LysRS: 23

2.2.1.3. Human His^N-LysRS: 25

2.2.2. Transfer RNA..... 26

2.2.3. Aminoacyl-tRNA. 27

2.2.4. Coupled Transcription-Aminoacylation Reactions..... 28

2.2.5. Attachment of Cross-Linker [6-aminohexanoic acid (L_2)] to lysyl-tRNA 29

2.2.6. Attachment of nanogold to lysyl-tRNA or linker- lysyl-tRNA 29

2.2.7. Coupled Transcription/Translation 30

2.3 Results and Discussions: 31

2.4. Conclusions: 45

CHAPTER 3

CYSTEINE SYSTEM **46**

3.1. Why we choose this system *versus* lysine or other amino acids systems 46

3.2. Materials and Methods..... 50

3.2.1. *E. coli* His^C-CysRS: 50

3.2.2. Coupled Transcription-Aminoacylation (CTA)..... 51

3.2.3. Attachment of biotin [N-iodoacetyl-N-biotinhexylenediamine] to cysteinyl-tRNA 52

3.2.4. Attachment of Monomaleimido Nanogold (MMA-Au) to cysteinyl-tRNA 53

3.2.5. *In vitro* Coupled Transcription-Translation reactions..... 53

3.2.5.1.Laser Ablation-Inductively Coupled Plasma-Mass Spectrometry-LA-ICP MS..... 55

3.2.5.2. High Angle Annular Dark Field -HAADF. 57

3.3. Results and Discussions: 58

3.4. Conclusions:..... 86

CHAPTER 4

CONCLUSION AND FUTURE WORK **87**

4.1. Conclusions:..... 87

4.2. Future Directions: 90

Appendix..... 93

Protein Sequence:..... 93

E. coli His^N-LysRS protein sequence: 93

DNA sequence of E. coli His^N-LysRS in pET19b:..... 94

E. coli His^C-LysRS protein sequence: 95

DNA sequence of E. coli His^C-LysRS in pET22b:..... 96

Human His^N-LysRS protein sequence:..... 97

DNA Sequence of Human His^N-LysRS in pM368:..... 98

E. coli His^C-CysRS protein sequence: 100

DNA Sequence of E. coli His^C-CysRS in pCysRS09:..... 100

Green Fluorescent Protein (GFP) protein sequence: 102

DNA sequence of GFP in pIVEX2.1:..... 102

Figure 3. 7 106

Figure 3. 8 107

HAADF on Monomaleimido Nanogold ……...108

References:..... 109

Vita ……121

List of Tables

Table 2.1. Comparison of aminoacylation between the native and *in vitro* synthesized lysine specific $tRNA^{lys}$. 34

Table 2.2. Quantitative incorporation of radiolabeled UTP and lysine in tRNA at different time frames 36

Table 2.3. Mass spectroscopy theoretical and experimental data for lysine specific $tRNA^{lys}$, lysyl-$tRNA^{lys}$ and its complexes. 41

Table 3.1. LA-ICP MS Measurement Conditions 56

List of Figures

Figure 1.1. *In vitro* assembly of polypeptides containing quantum dots. 17

Figure 2.1. Two methods of preparation of gold nanoparticle•lysyl $tRNA^{lys}$..... 21

Figure 2.2. Purification of *in vitro* synthesized *E. coli* lysine specific $tRNA^{lys}$. .. 32

Figure 2.3. Coupled Transcription-Aminoacylation for lysine specific $tRNA^{lys}$.. 35

Figure 2.4. Incorporation of radiolabeled [^{32}P] UTP and [^{14}C] lysine in $tRNA^{lys}$ within the two-hour period 37

Figure 2.5. ESI-MS of a mixture of lysine specific tRNA (24630) and lysyl-tRNA (24754). 38

Figure 2.6. ESI-MS on nanocrystal tRNA complex (Au•Lys-tRNA). 40

Figure 2.7. MALDI-MS on nanocrystal tRNA complex (Au•L_2Lys-$tRNA^{lys}$). 41

Figure 2.8. TEM image of nanogold particles attach to ε-amine of a lysyl-tRNA.. 42

Figure 3.1. Model for the assembly of nanoparticles into proteins by molecular machines. 48

Figure 3.2. Method of preparing gold nanoparticles•cysteinyl-tRNA (InAA-tRNA)..... 49

Figure 3.3. Time course of *in vitro* synthesis of [^{32}P] $tRNA^{cys}$ (transcription) and cys-[^{32}P] $tRNA^{cys}$ (CTA). 59

Figure 3.4. Time course of *in vitro* synthesis of [^{35}S]cys-$tRNA^{cys}$. 60

Figure 3.5. *In vitro* translation using tRNAs synthesized by CTA. 65

Figure 3.6. Scheme for purifying the cys-$tRNA^{cys}$. 66

Figure 3.7. Attachment of Monomaleimido gold nanoparticles (Au-MMA) to cysteinyl-$tRNA^{cys}$. Urea Gel Analysis of tRNA. 70

Figure 3.8. *In vitro* translation using gold nanoparticle modified cys-tRNA^{cys} (Au·cys-tRNA^{cys}) and an excess of hydrolyzed Au nanoparticles. . 74

Figure 3.9. *In vitro* translation using gold nanoparticle modified cys-tRNA^{cys} (Au·cys-tRNA^{cys}). 78

Figure 3.10. GFP emission spectra.. 80

Figure 3.11. *In vitro* translation using gold nanoparticle modified cys-tRNA^{cys} (Au·cys-tRNA^{cys}) which was affinity purified Step-Tactin beads... 82

Figure 3.12. Visualization of Au-labeled protein synthesized by *in vitro* translation..... 83

Figure 3.13. Visualization of Au-labeled protein synthesized by *in vitro* translation..... 84

CHAPTER 1

INTRODUCTION:

1. OVERVIEW

The process of synthesizing proteins known as translation is complicated and takes place in three steps: initiation, elongation and termination. Many components are required for the decoding of genetic information into proteins: the ribosome, a molecular machine that makes the peptide bond, messenger RNA (mRNA) to provide the template, aminoacylated transfer RNA (aa-tRNA) to bring the amino acids to be assembled and many other proteins, including aminoacyl-tRNA synthetases and translation initiation, elongation and termination factors. The ribosome is the "stage" where proteins are formed and is a structure where the nucleic acid and protein worlds intersect. The "enzymatic activity" of the ribosome, formation of peptide bonds into protein, is actually carried out in the 28S ribosomal RNA, thus the ribosome is a ribozyme.

1. 1. PROTEIN BIOSYNTHESIS

The translation process takes place in three parts, initiation, elongation and termination. In the initiation step, an initiation complex is formed between the mRNA, a ternary complex composed of initiator met-$tRNA_i$, initiation factor 2 (IF2) and GTP and the small ribosomal subunit. The joining of the large ribosomal subunit is concomitant

with the hydrolysis of the GTP in the ternary complex. The mRNA has to be placed on the 30S subunit so that the start codon is correctly positioned. The selection and positioning of the start site is facilitated by the Shine-Dalgarno nucleotide sequence which is complementary to the 3' end of 16s RNA.[1]

Other initiation factors, IF3 and IF1 also participate in the process. IF3 binds the small subunit preventing the association of ribosomal subunits prematurely [2, 3] and also is involved in the codon-anticodon discrimination between mRNA and initiator RNA.[2] After the IF3 is released, the 50S subunit joins the 30S initiation complex to yield the formation of 70S initiation complex. The function of IF1 is still not clear; there is some thought that IF1 binds to the A-site preventing binding of the initiator tRNA, but crystallographic data shows the initiator tRNA binds to the P-site in the presence or absence of IF1.[4]

The elongation step is the step where the peptide bond is formed, where three elongation factors assist the elongation process: EF-Tu, EF-Ts and EF-G. A ternary complex consisting of EF-Tu, GTP and aa-tRNA brings the amino acids to the ribosome. If the correct amino acid is brought to the ribosome, then the EF-Tu is released accompanied by hydrolysis of GTP to form the EF-Tu•GDP complex and is released from the ribosome. The GDP must be removed by a "recycling" factor, EF-Ts, so that the EF-Tu may bind GTP and form a new complex with another aa-tRNA.

The aa-tRNA is placed in such way in the ribosome that the aminoacyl residue is docked in the transferase center or PFT center and ready for peptide bond formation.[5] The PFT center of the ribosome catalyzes the formation of the peptide bond.

The last stage in the elongation step is translocation. Translocation involves the movement of the mRNA through the ribosome and ejection of empty tRNA. This process is mediated by a protein called EF-G which mimics the EF-Tu-tRNA complex. The EF-G•GTP binds the ribosome and upon hydrolysis to EF-G•GDP facilitates the tRNA-mRNA movement within the ribosome.[6, 7] After the translocation stage is completed, the ribosome is ready to accommodate a new aa-tRNA. The elongation process is continued till one of the three stop codons (UAA, UAG and UGA) is encountered triggering the last step in the translation process.

The last step in translation is called termination and the polypeptide is released and the ribosome is dissociated into its 30S and 50S subunits. This process is mediated by three release factors: RF1 which binds the UAA and UAG stop codons; RF2 that binds the UGA stop codon and RF3 which is thought to be involved in the final translocation and helps the dissociation of the ribosome into its subunits and the release of the deacylated tRNA.[8] The RF1 and RF2 mimic the structure of the tRNA and bind to the stop codons on the mRNA. The release factors transfer a water molecule to the polypeptide chain and cause the nascent polypeptide to be released from the ribosome.

1.2. THE RIBOSOME, A PROTEIN FACTORY:

The prokaryotic ribosome is an efficient molecular machine. A functional 70S ribosome is composed of two subunits, a small subunit with a sedimentation coefficient of 30S and a large subunit with a sedimentation coefficient of 50S and a molecular mass of approximately 2.6 X10^6 Da.[9] *Escherichia coli* ribosomes are composed of proteins

(21 proteins in the 30S subunit and 33 proteins in the 50S subunit) and RNA (16S rRNA in small subunit and 5S and 23S rRNA in large subunit).

In order to better understand how the ribosome works, it is necessary to know a detailed structure. The first high resolution crystals structures for ribosomes were reported in 2000 and several structures have been described.[9-11] The detailed structure of ribosomes opened a new era for elucidating the mechanism of protein synthesis.

The structure of the ribosomal subunits showed that the proteins are situated mostly at the surface, and the inner core is formed from RNA.[9] The main function of the majority of the proteins is to stabilize the 3D structure of the ribosomal RNAs.

The primary function of the ribosome is to "decode" the mRNA and form a protein. To carryout this function ribosomes must use tRNAs to bring the amino acid into the ribosome that corresponds to the codon on the mRNA. This "decoding or deciphering" requires base pairing of the codon on the mRNA with the anticodon on the tRNA in the ribosomes.

Ribosomes have three types of tRNA binding sites, Aminoacyl-, Peptidyl-, and Exit- sites that can accommodate tRNAs. The A-site binds tRNAs carrying amino acids (aminoacylated or aa-tRNA), the P-site binds tRNA that has the growing peptide chain attached and the E site is for the tRNA that has donated its amino acid and is ready to leave the ribosome. The tRNAs bind the ribosome through their acceptor stem in the large subunit and with their anticodon stem (codon-anticodon interaction) in the small subunit. The accuracy of this process is monitored by the correct pairing between the

mRNA codons and the tRNAs anticodons. If the base-pairing is incorrect, the aa-tRNA leaves the ribosome without discharging its amino acid.

The peptidyl-site or P-site is where the tRNA carrying the nascent polypeptide chain waits for the next amino acid to be added to the growing polypeptide chain. Peptide bond formation takes place in the large subunit between the incoming aa-tRNA in the A-site and peptidyl-tRNA in the P-site and is catalyzed by the peptidyl transferase (PFT) activity.[11] The PFT activity is actually the 23S rRNA.[11] The peptidyl-tRNA transfers the peptide chain to the next aa-tRNA. The mechanism of PFT is still not fully understood; however, the carboxyl group from peptidyl-tRNA is attacked by the amino group (α-NH_2) from the incoming aa-tRNA to yield the formation of a tetrahedral intermediate compound with the A2451 nucleotide of 23S rRNA and subsequent formation of the peptide bond.[11-13]

The exit site or E-Site, discovered in the late 1980's is the site where the deacylated tRNA is placed before leaving the ribosome. Except the initiator tRNA which binds directly to the P site, all the other tRNAs move through all three sites starting with the A-site, then P-site, and finally the E-site. The movement of tRNA from one site to the other is called translocation and is catalyzed by elongation factors.

Near the PTF center is a tunnel approximately 100 Å long that is continuous through the large subunit.[11] This tunnel is believed to be the exit tunnel of the nascent protein. The tunnel has an average diameter of 15 Å but in some regions the diameter ranges from 10-20Å. The walls of this tunnel are made from nucleotides of the 23S rRNA and non-globular proteins (L22 and L4).[11, 14-16] From the crystal structures,

one can conclude that the tunnel is too small to permit proteins to fold and therefore it is possible that the proteins begin the folding process only after they exit the tunnel. However, several studies showed that some proteins may exit the ribosome through alternate pathways.[15, 17]

The ribosome's crystal structure brought new perspectives to the understanding of the mechanism of protein biosynthesis. However, many questions regarding the process are still unknown or are not completely understood.[18]

1.3. AMINOACYL-TRNA –THE CODE "DECIPHER"

One of the most important players in protein synthesis is the aminoacyl tRNA. To understand the process of translation it is necessary to comprehend the importance of the aminoacylation process. The aminoacylation process takes place between a tRNA, its cognate amino acids and is catalyzed by a specific aminoacyl-tRNA synthetase to yield the aminoacyl-tRNA (aa-tRNA). The accuracy of this reaction is vital to prevent incorrect amino acids from being placed into the growing polypeptide chain.

The aa-tRNAs are synthesized in a two step process by the cognate aminoacyl-tRNA synthetase. In the first step of aminoacylation, an intermediary aminoacyl adenylate is formed between the amino acid and ATP and then subsequently the activated amino acid is transferred to the 3' end of the tRNA.

This process of aminoacylation is catalyzed by a family of enzymes, the aminoacyl-tRNA synthetase (aaRS). There are ~20 such enzymes, one for each cognate amino acid and are classified into two groups based on their structural features. The

differences between these two classes lies in their catalytic domains; Class I enzymes possess a Rossmann dinucleotide-binding domain as well as HIGH and KMSKS motifs, while Class II enzymes have six anti-parallel β-sheets and three α-helices which are referred to as the αβ active site. Another salient difference between aaRS classes is the way the tRNAs "bind" to the enzymes. Class I aaRS bind to the acceptor stem of tRNA from the minor groove side and acylation take place at 2' hydroxyl group of the 3' adenosine. Meanwhile class II aaRS bind from the major groove side of the stem and acylation takes place at 3' hydroxyl group of the 3'adenosine.[19-21]

An example of a tRNA/aminoacyl-tRNA synthetase pair. *Escherichia coli* cysteinyl-tRNA synthetase (CysRS) is the smallest monomeric synthetase and belongs in subclass Ia of tRNA synthetases.[20, 22] The CysRS has 461 amino acid residues and the HIGH and KMSKS motifs are conserved. These motifs are involved in the activation of cysteine and transfer of active cysteine to 3' CCA end of the tRNA.[23, 24]

All tRNAs have an L-shaped tertiary structure where the acceptor stem and the TψC stem form the short arm of the L-structure and the dihydrouridine (D) stem and anticodon stem forms the long arm of the L-structure. The CysRS recognizes the $tRNA^{cys}$ tertiary structure based on indirect and direct interaction with the discriminatory base (U73-in the $tRNA^{cys}$) [25-27], anticodon loop (GCA) [27, 28] and acceptor stem (3' CCA).[21, 27] The presence of the G15:G48, called the "Levitt pair", in the tertiary structure of $tRNA^{cys}$ is an important factor in the recognition and aminoacylation of cysteine specific tRNA. Studies have shown the need for G15:G48 for aminoacylation. If either base is mutated aminoacylation is abolished.[29, 30]

Studies have shown that a shape–selection mechanism between the $tRNA^{cys}$ and CysRS is important in aminoacylation.[28] However, the tertiary structure of cysteine specific tRNA plays the decisive role in the formation of $tRNA^{cys}$-CysRS complex, thus in cysteinylation.

1.3.1. Unnatural Aminoacyl-tRNA a new area in modern biochemistry

The aminoacyl-tRNA synthetases are a class of enzyme important in the fidelity of translation through the accurate matching the amino acid to their cognate tRNA. However, it is possible to alter amino acids with new functional groups. Johnson and his coworkers derivatized for the first time a lysyl-tRNA with N-acetoxysuccimide.[31] This was the beginning of a very interesting new technological area in biochemistry to use unnatural amino acids in the synthesis of proteins with new properties. The strategy engaged by Johnson and his coworkers was to attach N-acetoxysuccimide to the ε-amino group of lysyl-$tRNA^{lys}$ and then use this new N^{ε}- acetyl-lysyl-$tRNA^{lys}$ in a cell free rabbit reticulocyte system to translate hemoglobin.[31] The limiting factors for this method are the incorporation of modified lysine residues in all the sites which encode lysine. Mixed populations of proteins containing modified/unmodified lysine residues were present. The presence of different cross linkers attached to the ε-amine group of lysyl-tRNA, was described previously in the literature.[31-38] This technology is the basis for commercial kits using non-radioactive detection of chemiluminescent compounds attached to the modified lysyl-tRNA for easy visualization of the synthesized protein.[39-41] Kadat and his coworkers reported the

attachment of a sulfhydryl spin-label compound (*N*-(l-oxyl-2, 2, 5, 5-tetramethyl-3-Pyrrolidinyl) iodoacetamide) to cysteinyl-tRNA side chain.[42] Lysine and cysteine are very attractive amino acids for derivitization due to their chemically reactive side chains.

It would be more efficient to have the unnatural amino acid function as a substrate for the aaRS; however, aaRSs' are very precise enzymes which acylate only a specific tRNA with their cognate amino acid, thus misacylation of tRNA with unnatural amino acids is very difficult to achieve. To overcome this difficulty, it is necessary to chemically attach the amino acids to the tRNA [43-46], to "engineer" the synthetase to utilize a unnatural amino acid substrate [47, 48] or to create an "artificial" synthetase such as a ribozyme [49-54] to carryout the reaction.

The chemical attachment of an amino acid was first reported by Hecht and his coworkers[43]. A T4 RNA ligase was employed to condense an *E. coli* phenylalanine specific $tRNA^{Phe}$ missing the last two nucleotides (C75 and A76) with several 2' (3')-O-acylated pCpA derivatives. The α-amino group of to the amino acid must be protected by a chemical group before the chemical aminoacylation but the protective group must be removed prior to translation. Several years later, two independent groups took this method a step forward using the chemical acylation for site-specific incorporation of unnatural amino acids in proteins. The site-specific incorporation is possible using a suppressor tRNA. Suppressor tRNAs recognize the stop codons UAG (amber), UGA (opal), and UAA (ocher). Instead of terminating translation, suppressor tRNAs insert an amino acid and allow translation to continue past the termination codon. The use of suppressor tRNAs charged with unnatural amino acids would allow incorporation of the

unnatural amino acid at a specified site- using on the termination codons (amber, opal or ocher).

Based on this methodology Schultz's [46] and Chamberlin's [44, 45] groups, independently, chemically misacylated an amber suppressor yeast phenylalanine specific tRNA $_{CUA}$ with a phenylalanine, para-fluorophenylalanine, para-nitrophenylalanine [46] and an *E. coli* amber suppressor glycine specific tRNA $_{CUA}$ with a radiolabeled iodo-tyrosine [44], respectively, and showed site-specific incorporation of the modified amino acid in proteins and short peptides. Starting with these reports, in the last decade over 100 different unnatural aminoacyl-tRNAs were reported.[55-60] The applications for the site incorporation of the unnatural amino acids is vast and is closely related to the structure-function of a wide range of proteins in eukaryotic or prokaryotic systems. However, the chemical attachment and the *in vitro* site-specific incorporation of unnatural amino acids is limited by several important factors: (1) the suppressor tRNA has to be orthogonal (statistically independent) to the *in vitro* translation system; if the tRNA is not orthogonal the endogenous aminoacyl-tRNA synthetase present in the system, this will be acylated with its cognate natural amino acid and then incorporate into the protein as an unmodified amino acid residue, yielding the formation of a mixed population of proteins (modified/unmodified proteins); (2) the chemical attachment of unnatural amino acids is inefficient ; (3) the suppressor tRNA competes with the release factors present in the translation mixture and (4) apparently suppressor tRNAs charged with unnatural amino acids have very low suppression efficiency.[56, 57] To overcome some of these problems yeast suppressor tRNA was used in *in vitro E. coli* translation

systems [46, 61] or *E. coli* suppressor tRNA were used in eukaryotic translation systems.[44, 56] The breakthrough came, when an orthogonal tRNA/aaRS pair was developed for use in *in vivo* translation. The aaRS was evolved to recognize unnatural amino acids and aminoacylate the suppressor tRNA in vivo.[47] This methodology has been further developed in Schultz's group for a variety of non-natural amino acids.[55-60]

Another promising solution for aminoacylation of tRNA with unnatural amino acids was developed by Suga and his coworkers.[49-54] They showed that ribozymes can be used as an alternate method to aminoacylate a tRNA. An acyl-transferase ribozyme which was evolved i*n vitro* was demonstrated to specifically catalyze the aminoacylation reaction of an unnatural amino acid at the 3' end of their cognate tRNA. The tRNAs are recognized by the ribozymes through the CCA-3' end and also through the anticodon loop. Ribozyme specificity towards different substrates is programmed into the internal guide sequence, which is the complementary sequence to the last five nucleotides at the 3'end of the tRNA.[49] The possibility of using ribozymes as a catalyst for aminoacylation opens a new direction for the synthetic pathway of unnatural aminoacyl-tRNA.

Although a variety of amino acids modified with functional organic groups or single atoms (I or Hg) were described [62, 63], no modifications with nanoparticles or quantum dots (less or bigger than 10 nm) had been reported. Modifying proteins with nanoparticles of various properties could have many potential applications.

1.4. QUANTUM DOTS

Quantum dots are zero-dimensional systems in which the charge carriers and the excitations are confined in all three directions of space, thus leading to discrete levels of energy, similar to the ones found in a single atom. The energetic confinement of the electrons is translated in terms of the size of the atomic cluster by the fulfillment of certain conditions, *i.e.* the high symmetry (ideal case: spherical) and a particle size (<1-10 nm) comparable with the de Broglie wavelength of its charge carriers.[64] Nanoparticles obeying these two shape and size requirements have an icosahedral geometry consisting of layered shells of highly packed atoms, in which the total number of atoms is given by the Mackay formula for sphere-packed icosahedral structures:

$$N = 1 + \sum_{p=1}^{n} (10\,p^2 + 2)$$

where is p = the number of atom shells, N = total number of atoms

Quantum dots of relevant importance, usually metals and inorganic semiconductors thus have fixed numbers of atomic constituents; usually 13 for one-shell quantum dots and 55 for two-shell nanoparticles and this corresponds to high percentages in terms of surface atoms: 92% and 76%, respectively. The direct consequence of this unusually high ratio of surface atoms relative to the total number of constituent atoms is the high chemical reactivity of the quantum dots. In order to protect the nanoparticles against agglomeration and self-aggregation, the quantum dots are capped with ligands that are most commonly organic molecules of various type and nature, depending on the practical applications considered. The main feature of the quantum dots, the atom-like

discrete levels of energy is more significant for inorganic semiconductors, being more enhanced at the edges of the valence and conduction bands. The discrete levels of energy in a quantum dot can be calculated by applying the particle-in-a-box model, in which the charge carriers are confined in all 3 directions and the potential energy, is zero anywhere inside the box and infinite at the walls of the box. The allowed energy levels inside the box can be calculated applying the Schrumalaufedinger equation and if the shape of the box is spherical, the energy levels have the general form:

$$E = n^2h^2 / 2\,m\,d^2,$$

where n is the energy level, m is the mass of the charge carrier and d is the diameter of the sphere .[64]

Quantum dots of semiconductor materials display an energy gap greater than in the bulk form and this particularity has a great impact upon their optical properties.[65] The minimum energy needed to form an electron-hole pair (exciton) is defined by the value of the valence band-conduction band gap and this increases as the dimension of the quantum dot decreases.[66] Appropriate tailoring by specific chemical synthetic routes of the size of the semiconductor quantum dots results in particular, targeted values for the energy band gap and this important feature has important practical applications. Excitons in quantum dots poses a limited lifetime and their dissolution leads to fluorescence, which is defined as an emission of photons through a radioactive decay mechanism.[67] The energy emitted through fluorescence of the quantum dots is always red-shifted (smaller) when compared to the minimum of energy (band gap) absorbed for the formation of the exciton in the first place.[68] Metallic quantum dots

display optical absorption spectra similar to the semiconductor quantum dots but the nature of the energy transitions differ. The metal nanoparticles possess collective modes of motion for the free electron gas (surface plasmons) and these can be excited by absorbing appropriate amounts of energy. By contrast to their semiconductor counterparts, the metallic quantum dots do not have a significant dependence of the surface plasmons resonance frequency to the size of the nanoparticles.

Most of the important applications for the quantum dots involve the optical or electrical excitation which upon relaxation leads to generation of photons with a specific energy. Thus, quantum dots may be used as single photon sources, lasing media, and charge storage media or as fluorescent labels.[69, 70]

1.4.1. Nanotechnology tool for tagging biological substrates

During the last decade, developments from the newly emerging field of nanotechnology found biochemical applications and thus a new, promising area surfaced - nanobiotechnology. This new field evolved rapidly from a conceptual tool to a research tool and has now reached the stage of a devise tool.[71] The full potential of nanobiotechnology is still to be discovered but a few breakthroughs have already been reported in the scientific literature.[71-74] The use of nanocrystals for biopolymer labeling opens a new direction in labeling and detection techniques for the biological substrates. The need for radioactive isotopes or/and organic dyes may be minimized or potentially totally replaced by quantum dots.[73, 74] Nanocrystals of various size and

composition have been used to conjugate to biological substrates, i.e. zinc sulfide-capped cadmium selenide (CdSe/ZnS) for detection of proteins [73-76] and oligonucleotides.[77-80] Besides the semiconductor quantum dots, i.e. zinc sulfide-capped cadmium selenide CdSe/ZnS, cadmium telluride (CdTe) [81] and titanium oxides (TiO_2)[82], metal quantum dots, i.e. gold and silver nanoparticles, were used efficiently to visualize and detect biological substrates.[72, 83-85] In addition, during the last year the nanobiotechnology evolved to the stage where the cell can by visualized and tracked [86, 87] and DNA [88] and proteins [84] can be detected using bio-barcode oligonucleotides mo dified by a gold nanoparticle. The synthetic pathways to generate these quantum dots or nanoparticles modified biopolymers are various and implicate several strategies: (i) electrostatic adsorption-nanoparticles have negative charge ions on the surface and interact with the positive charges of proteins [89, 90] ; (ii) chemisorptions of nanoparticle and /or quantum dots to proteins through the amino acids residues side chains i.e. thiol group of cysteine [83] , or DNA modified with a cysteine residue [72, 91] ; (iii) covalent attachment of gold nanoparticles to DNA [72, 92, 93], RNA [94], and proteins [95]-the attachment it is possible through the single reactive group, i.e. sulfo-N-hydroxysuccinimide ester or monomaleimido groups, present on the surface of the nanoparticle which is reactive towards different reactive groups, i.e. ε-amino group belonging to lysine residues or sulfhydryl group from cysteine residues; (iv) through specific affinity interactions- nanoparticles conjugated with streptavidin interact with biotinylated proteins [96] or oligonucleotides [97] or interaction between antibody conjugated nanoparticles with their cognate antigens [98]. In addition, Sweeny and

coworkers (2004) reported for the first time the possibility of using an *E. coli* organism to synthesize cadmium sulfide nanocrystals (2-5 nm).[99]

Nanobiotechnology is a rapidly expanding field and many interesting discoveries are yet to come. The interactions between these two very different and complex fields have already brought many changes to classic material science. The complexity of biological substrates combined with the particular properties introduced by the quantum dot and/or nanoparticles will allow novel applications and has a virtually unlimited potential.

1.5. IS IT POSSIBLE TO USE THE RIBOSOME TO MANUFACTURE AN INORGANIC MODIFIED AMINO ACID?

The research described in this dissertation project was to determine if it was possible to use the ribosome to synthesize new bio-inorganic materials. Specifically, modify amino acids with quantum dots and have the ribosome assemble polypeptides containing the quantum dots at specific sites in the polypeptide. The major obstacles to be overcome were the stable attachment of the quantum dot to the amino acid and determining whether the ribosome would accept such a modified amino acid and use it for peptide bond formation.

The quantum dots must be linked to the chemically reactive side chain of an amino acid, i.e. lysine (epsilon amino group) or cysteine (sulfhydryl group), that has already been assembled on the carrier tRNA by aminoacylation. The integration of the quantum dot modified amino acid into polypeptide will be carried out by ribosomes in *in vitro* translation programmed with a messenger RNA (mRNA) template (see Figure 1.1).

If successful, this method will provide a method for the supramolecular assembly of new bioinorganic heterostructures, using ribosomes as natural molecular machines and an artificial coding template to regularly space the quantum dots.

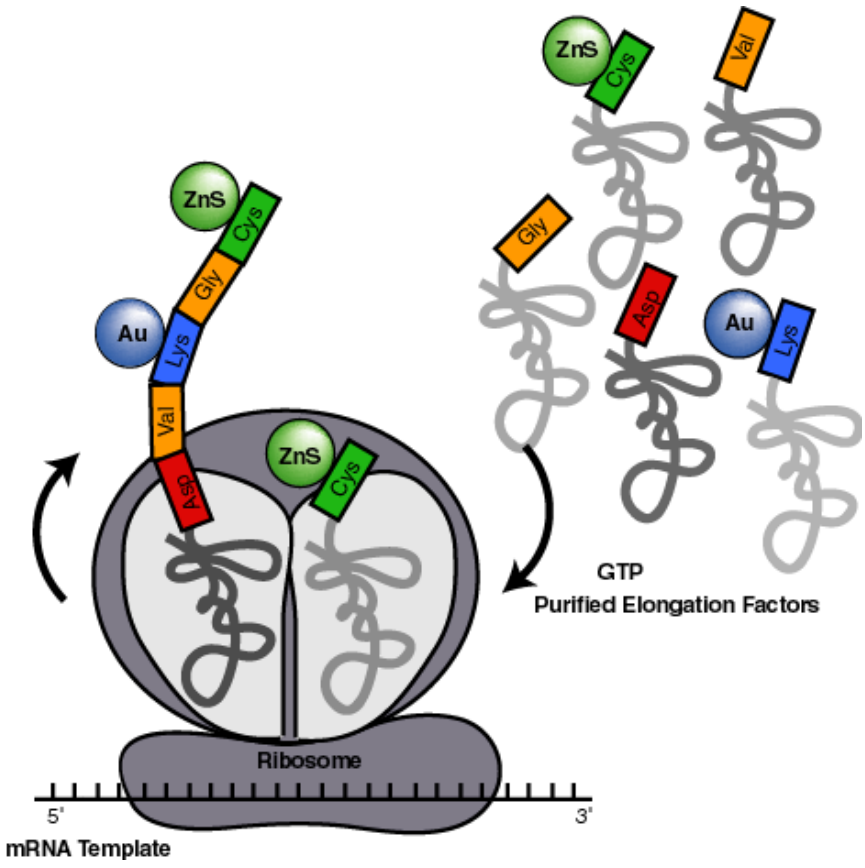

Figure 1.1. ***In vitro*** **assembly of polypeptides containing nanocrystals.**

1.5.1. My ideal nanodot.

To use the ribosome to assemble quantum dot modified amino acids, a very special quantum dot would be required. In the last few years several new types of nanodots have been synthesized that have a variety of different shapes [100], sizes (2-200 nm, some under 1.2 nm) [101, 102] and have monodistribution. One of the limitations of these quantum dots and/or nanoparticles is the multiple reaction sites present on the surface. In the last two years, two groups reported the synthesis of gold nanoparticles with a single reactive group on the surface.[103-105] These successful syntheses showed that the mono-functionalization of nanodots or nanoparticles is possible. Nanoprobes, Inc. makes 1.4 nm gold nanoparticles that have only one single reactive group on the surface. Other types of nanoparticles that are derivatized with streptavidin or fluorescent groups are also available commercially from Nanoprobes. The nanoparticle/quantum dot needs to have the following characteristics. The ideal quantum dot would be made from a semiconductor material which has fluorescent properties for ease of detection such as CdS, CdSe, ZnS, ZnSe, $CdSe_{core}/ZnS_{shell}$. The quantum dot should also have a size under 2 nm, due to potential physical limitations of the ribosome exit tunnel (average diameter ~1.5nm). The quantum dot should also have a single reactive group on the surface so it reacts with only one amino acid and be commercially available. The only available particle that satisfies most of these requirements was the 1.5 nm Nanogold particles from Nanoprobes, Inc. The only property missing was fluorescence.

If the idea of quantum dot assembly into polypeptides by ribosomes was possible,

the following questions would have to be answered:

1. Can large quantities of aminoacyl-tRNA modified by inorganic nano-materials be prepared?
2. Can a ribosome translate an inorganic modified aminoacyl-tRNA?
3. Will the inorganic modified amino acid residue be incorporated successfully into proteins?
4. Can we analyze and visualize the inorganic modified protein?

CHAPTER 2

LYSINE SYSTEM

2.1. INTRODUCTION

Ribosomes are molecular machines that catalyze the assembly of amino acids into polypeptides according to the information encoded in an mRNA template using aminoacylated transfer RNAs (aa-tRNA) as substrates.

The first system tested was modified lysyl-tRNA. The reason for this choice was the availability and the high reactivity of the primary ε-amine contains in the side chain of lysine.[31-41, 106] Lysine residues are often at the protein's surface, due to hydrophilic character, and allow a better visualization of quantum dots attached to its ε-amino group. The amino acylation and modification of lysyl-tRNA has been well developed.[107] The scheme in Figure 2.1 outlines two methods for modification of lysyl-tRNA. A heterobifunctional cross linker may be covalently attached to the ε-amino group and then the quantum dot covalently attached or the quantum dot may be directly linked to the side chain to yield the formation of a new unnatural aminoacyl-tRNA containing inorganic nanomaterials Inaa-tRNA). The inorganic nanoparticle labeled aminoacyl-tRNAs will be used in an *in vitro* translation system to arrange the quantum dots according to the mRNA template.

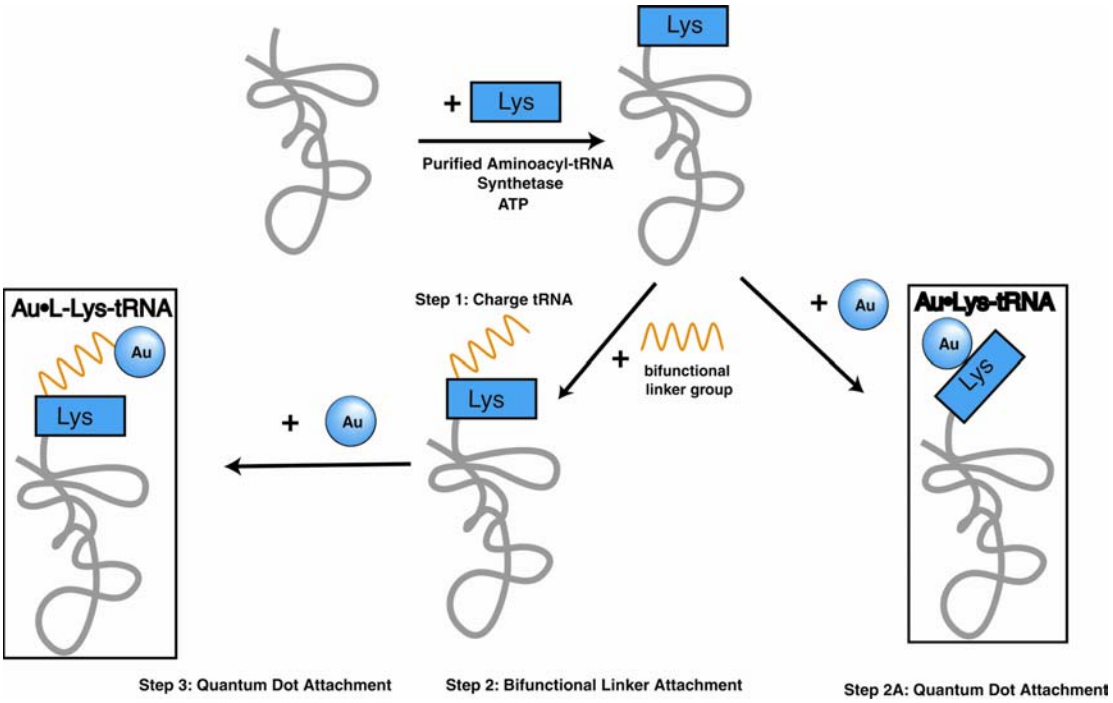

Figure 2.1. Two methods of preparation of gold nanoparticle •lysyl tRNA^{lys}.

A lysine specific tRNA^{lys} is aminoacylated with lysine to yield the formation of lysyl- tRNA^{lys} (see Figure 2, step 1), a heterobifunctional cross linker was covalently attached to the side chains of amino acid (see Figure 2, step 2). Ultimately, gold nanoparticles, 1.4 nm mono-*sulfo*-NHS nanogold, were attached to the linker molecule or directly to the side chains of the lysyl-tRNA^{lys} (see Figure 2, step 3 and 2A).

2.2. MATERIALS AND METHODS

2.2.1 Enzymes:

2.2.1.1. *E. coli* His^N-LysRS:

The ORF encoding the *E. coli* his^N-LysRS was amplified from genomic DNA template using gene specific primers designed with BamHI and NdeI restriction sites at the 5' and 3' ends respectively. The resulting amplified product was digested with BamHI and Nde I, separated by agarose gel electrophoresis and purified from the gel. The purified DNA product was ligated into a BamI/NdeI digested plasmid (pET19b) and transformed into DH5a cells. The resulting colonies were screened by PCR for the correct insert and sequenced to confirm the correct insert was obtained.

The resulting plasmid was used to transform expression cells (*E. coli* BL21Star strain cells (Invitrogen, Carlsbad, CA)). A single isolated colony was picked and grown overnight at 37^0C in a 4 x 50 mL LB [Luria -Bertani (LB) broth] medium and 100 μg/mL ampicillin. The overnight cultures (50 mL) were used for the inoculation of four liters (4 x 1L) of LB medium /ampicillin (AMP) (100 μg/mL). To each 1L of LB/AMP a 50 mL culture grown overnight was added. The incubation was continued at 37^0C with continuous shaking. The OD_{600} was read hourly and when it reached approximately 1.0, expression was induced with IPTG (isopropyl-1-thio-β-D-galactopyranoside). The final concentration of IPTG was 1.0 mM. The incubation was continued at 37^0C for 3 hours. The cells were harvested by centrifugation at 2500 x g for 20 minutes at 4^0C. The cell pellet was removed and resuspended in 15 mL of lysis buffer (50 mM NaH_2PO_4, 300 mM NaCl, 10 mM imidazole, pH 8). To the resuspended

mixture of the cells 100 mM PMSF (phenylmethylsulfonyl fluoride) and 22 mg of lysozyme were added. The cells were gentle stirred for 30 minutes, followed by lysis with gentle sonication. The lysed cells were centrifuged at 14,000 x g for 45 minutes and the supernatant was collected. The *E. coli* his^N-LysRS was purified using a nickel-nitrilotriacetic acid resin (Ni-NTA) (QIAGEN, Valencia, CA) according to the manufacturer's instructions. A 2 ml column was washed with 10 mL water and 20 ml equilibration buffer (50 mM NaH_2PO_4, 300 mM NaCl, 10 mM imidazole, pH 8). The extract (30mL) was loaded onto the column and the column was washed with 100 mL of wash buffer (50 mM NaH_2PO_4, 300 mM NaCl, 20 mM imidazole, pH 8). The lysyl synthetase was eluted with a step gradient from 50 mM to 400 mM imidazole. The 1 mL fractions (12-40) containing the largest amount of protein were pooled together and dialyzed against 20 mM NaH_2PO_4 pH 7.5, 100 mM NaCl, 1 mM EDTA, 1 mM DTT, 50% glycerol, and stored in 200 μL aliquots at -20°C. The yield was approximately 150 mg of protein and after dialysis the concentration of *E. coli* his^N-LysRS was ~20 mg/ml. The protein was soluble but was inactive.

2.2.1.2. E. coli His^C-LysRS:

The ORF encoding the *E. coli* his^C-LysRS was amplified from genomic DNA template using gene specific primers designed with XhoI and NdeI restriction sites at the 5' and 3' ends respectively. The resulting amplified product was digested with XhoI and Nde I, separated by agarose gel electrophoresis and purified from the gel. The purified DNA product was ligated into a XhoI/NdeI digested plasmid (pET22b) and transformed into DH5a cells. The resulting colonies were screened by PCR for the

correct insert and sequenced to confirm the correct insert was obtained.

The resulting plasmid was used to transform expression cells (*E. coli* BL21Star strain cells (Invitrogen, Carlsbad, CA)). A single isolated colony was picked and grown overnight at 37^0C in a 4 x 50 mL LB [Luria -Bertani (LB) broth] medium and 100μg/mL ampicillin. The overnight cultures (50 mL) were used for the inoculation of four liters (4 x 1L) of LB medium /ampicillin (AMP) (100 μg/mL). To each 1L of LB/AMP a 50 mL culture grown overnight was added. The incubation was continued at 37^0C with continuous shaking. The OD_{600} was read hourly and when it reached approximately 1.0, expression was induced with IPTG (isopropyl-1-thio-β-D-galactopyranoside). The final concentration of IPTG was 1.0 mM. The incubation was continued at 37^0C for 3 hours. The cells were harvested by centrifugation at 2500 x g for 20 minutes at 4^0C. The cell pellet was removed and resuspended in 15 mL of lysis buffer (50 mM NaH_2PO_4, 300 mM NaCl, 10 mM imidazole, pH 8). To the resuspended mixture of the cells 100 mM PMSF (phenylmethylsulfonyl fluoride) and 22 mg of lysozyme were added. The cells were gentle stirred for 30 minutes, followed by lysis with gentle sonication. The lysed cells were centrifuged at 14,000 x g for 45 minutes and the supernatant was collected. The *E. coli* his^N-LysRS was purified using a nickel-nitrilotriacetic acid resin (Ni-NTA) (QIAGEN, Valencia, CA) according to the manufacturer's instructions. A 2 ml column was 10 mL washed with water and 20 mL equilibration buffer (50 mM NaH_2PO_4, 300 mM NaCl, 10 mM imidazole, pH 8). The extract (30mL) was loaded onto the column and the column was washed with 100 mL of wash buffer (50mM NaH_2PO_4, 300mM NaCl, 20 mM imidazole, pH 8). The lysyl

synthetase was eluted with a step gradient from 50 mM to 400 mM imidazole. The 1 mL fractions (12-40) containing the largest amount of protein were pooled together and dialyzed against 20 mM NaH_2PO_4 pH 7.5, 100 mM NaCl, 1 mM EDTA, 1 mM DTT, 50% glycerol, and stored in 200 μL aliquots at -20°C. The yield was approximately 150 mg of protein and after dialysis the concentration of *E. coli* his^C-LysRS was ~25 mg/ml. The protein was soluble but was inactive. Also, a different method of purification of *E. coli* his^C-LysRS was performed and the protocol was reported by Ueda and his coworkers.[108]

2.2.1.3. Human His^N-LysRS*:*

Human lysyl-tRNA synthetase-histidine (pM368) tagged at the N terminus (Human His-LysRS) were generously provided by Prof. Dr. Karin Musier-Forsyth of the University of Minnesota. The preparation and purification were carried out as previously described.[107] The plasmid pM368 was transformed in expression cells, *E. coli* BL21 (DE3) (Novagen, Madison, WI) and a single isolated colony was grown overnight in a 4 x 50 mL LB medium and 100 μg/mL ampicillin. The overnight cultures (50 mL) were used for the inoculation of four liters (4 x 1L) of LB medium /ampicillin (AMP) (100 μg/mL). To each 1L of LB/AMP a 50 mL culture grown overnight was added. The inoculation was continued at 37^0C under continuous shaking. The OD_{600} was read hourly and when it reached approximately 0.15, upon which the temperature was changed to 20^0C, and IPTG was added. The final concentration of IPTG was 0.1 mM. The incubation was continued at 20^0C for approximately 6 hours.

The rest of the steps were performed at 4^0C. The cells were harvested by centrifugation at 2500 x g for 20 minutes. The cell pellet was removed and resuspended in 15 mL of lysis buffer (50 mM NaH_2PO_4, 300 mM NaCl, 10 mM imidazole, pH 8). The rest of the steps were identical with the ones performed for *E. coli* his^N-LysRS.

2.2.2. Transfer RNA

The $tRNA^{Lys}$ gene in pUC19 was a gift from Dr. Karin Musier-Forsyth (University of Minnesota). Large quantities of the plasmid were prepared by cesium chloride preps.

Digestion of the plasmid with BstNI generates a linear template with the appropriate –CCA end for the tRNA to be aminoacylated. The plasmid contains several BstNI sites; however, this does not interfere with in vitro transcription. The linearized template (0.36-0.5 mg/mL final concentration) was transcribed using a T7-Megashortscript^{TM} high yield transcription kit (Ambion, Austin, TX). Briefly, the reaction contains linearized template, NTPs, buffer provided by the manufacturer and a mixture of T7 RNA polymerase and placental RNAse inhibitors.

Initially, the $tRNA^{Lys}$ was purified using a Sephadex G-50 column (10 cc) and eluted with HE150 buffer (20 mM HEPES-KOH, pH 7.5, 10 mM EDTA, and 150 mM KCl). The recovered $tRNA^{Lys}$ was precipitated using cold ethanol and 200 mM NH_4OAc pH 7.5. The tRNA was then purified using denaturing 6% polyacrylamide-urea gel electrophoresis, and recovered by electroelution in sterile 1x TBE using a BioRad Electro-eluder apparatus(model 422). The gel slice was placed into a glass tube

modified with glass frits and filled with sterile buffer. A silicon adaptor with the membrane cap (which was pretreated by boiling for 1 hour at 60^0C in 1x TBE; the dialysis membrane is a 3,500 MW cut off) was fitted onto the bottom of the glass tube. The electro-elution was done at 10 mA for 3-5 hour. At the end of elution the polarity was reversed (1-2 minutes to remove the tRNA from the membrane). All the elution steps were done at room temperature. All components were autoclaved in 1x TBE buffer to have an RNAse free system, except the plastic case, to prevent nuclease contamination. The plastic case was treated with RnaseZap (Ambion). The $tRNA^{Lys}$ recovered in the electroelution buffer was precipitated with ethanol in the presence of 200mM ammonium acetate pH 7.5. All the steps were performed at 4^0C if not stated otherwise.

Lysine Specific $tRNA^{lys}$ sequence:

GGGTCGTTAGCTCAGTTGGTAGAGCAGTTGACTTTTAATCAATTGGTC GCAGGTTCGAATCCTGCACGACCCACCA

2.2.3. Aminoacyl-tRNA.

The reaction mixtures contained in 40 μL 100 mM Tris-HCl (pH 7.5), 5 mM magnesium acetate, 10 mM potassium chloride, 3.75 mM DTT, 3 mM ATP, 0.32 μM L-[^{14}C] lysine (309mCi/mmol) (NEN™ Life Science Products, Boston, MA) or 0.1 mM L-lysine (Aldrich), $tRNA^{Lys}$ (140pmol/reaction), and purified E. coli or human lysyl-tRNA synthetase (1 μg/μL). The reactions were incubated at 37^0C for 15 minutes. To

quantitate the incorporation of [^{14}C] lysine onto tRNA^{Lys}, cold 10% TCA was added, and the resulting precipitate was collected onto glass fiber filters (Schleicher & Schuler, Germany). The radioactivity on the filters was measured using a liquid scintillation counter. The reactions that show significant incorporation of [^{14}C] lysine were phenol extracted and precipitated with ethanol and 200mM ammonium acetate pH 7.5.

2.2.4. Coupled Transcription-Aminoacylation Reactions

Coupled transcription-aminoacylation reactions were carried out in 40 μL or 100 μL volumes. The Ambion T7 Mega Shortscript transcription kit was used and the reaction supplemented with 2-4 μL lysyl-tRNA synthetase (1 μg/μL) and 75 mM [^{32}P]-UTP (0.05 mCi/mmol, to monitor RNA synthesis**)** or 0.32 μM L-[^{14}C] lysine (309 mCi/mmol, to monitor aminoacylation). The reactions were incubated at 37^{0}C for 135 minutes. Aliquots of 10 μL were collected at different times (0, 60, 90,120,135 minutes), and precipitated with cold 10% TCA to determine the incorporation of radioactivity.

The lysyl-tRNA (100 μL) was purified using ethanol precipitation in the presence of 200 mM ammonium acetate pH 7.5.

2.2.5. Attachment of Cross-Linker [6-aminohexanoic acid (L_2)] to lysyl-tRNA

The attachment of 6-aminohexanoic acid to lysyl-$tRNA^{lys}$ was performed following the protocol from the manufacturer (Pierce Chemical, Co).[31, 109] The only change to the procedure was that the reaction between EDC (1-ethyl-3- (3-dimethylaminopropyl) carboiimide), NHS (N-hydroxysuccinimide), and 6-aminohexanoic acid (L_2) was performed in a higher concentration (2 M EDC, 5 M NHS and 2 M L_2) than the one suggested (2 mM EDC, 5 mM NHS and 2 mM L_2). The reaction was stirred overnight at room temperature instead of the suggested 1 hour to increase the final product yield. The final product, N-hydroxysuccinimidyl-6-aminohexanoate, was reacted with lysyl-tRNA. The modified lysyl-tRNA (N^{ε}-NHS-L_2-lys-tRNA) was precipitated as described above (cold ethanol and 200 mM NH_4OAc pH 7.5). All the steps were performed at 4^0C if not stated otherwise. A duplicate set of reactions using L- [^{14}C] lysine (309 mCi/mmol) were run as controls to be able to monitor the aminoacylation state during the modification steps.

2.2.6. Attachment of nanogold to lysyl-tRNA or linker- lysyl-tRNA

The attachment of the 1.4-nm mono-*sulfo*- succinimido-nanogold (Nanoprobes, Yaphank, NY) to tRNA was performed using methods modified from the manufacturer's instructions. The lysyl-tRNA (1.5 nmoles) or N^{ε}-NHS-L_2-lysyl-tRNA (1 nmoles) were ethanol precipitated overnight and collected by centrifugation at 10,000 x g for 15 minutes. The pellets were resuspended in 20 mM HEPES-KOH (pH 7.5), and 5 nmoles

of gold particles resuspended in water were added. The reaction was stirred for one hour and left overnight on ice. The gold-lysyl-tRNA and gold-L_2-lysyl-tRNA were then ethanol precipitated in the presence of 200 mM ammonium acetate pH 7.5, and the gold-tRNA complexes were purified from unreacted gold particles using a Micro Bio-Spin 6 column (BioRad, Hercules, CA). A duplicate set of reactions using L-[^{14}C] lysine (309 mCi/mmol) were run as controls to monitor the aminoacylation state.

2.2.7. Coupled Transcription/Translation

The translation reactions were performed, as was previously described.[110] An E. coli S30 fraction and reagents was generously provided by Dr. Gisela Kramer, The University of Texas at Austin. The translation reaction contained in 30 μL; 5 μL of the *E. coli* S30 fraction, 55 mM Tris-acetate (pH 7.8), 2 mM DTT, 1 mM ATP, 0.8 mM each GTP, CTP,and UTP, 2% poly(ethy1ene glycol)-6000, 25 mM phosphoenol pyruvate, 0.4 mM CAMP, 3 6 mM NH_3OAC7, 2 mM KOAc, 16 mM $Mg(OAc)_2$, 0.5 mM EDTA, 1 μg of the pGEM-3z plasmid as template (contains the infC gene, the *E. coli* gene for initiation factor 3 (IF3) and has 21 lysines), 0.33 μM of leucine, 0.83μM all the amno acids(minus-leucine and lysine) and 0.069 μM of the Au•[^{14}C] lysyl-tRNA or L-[^{14}C] lysyl-tRNA ([^{14}C]lysyl-tRNA). The reactions were incubated at 37^{0}C for 30 minutes, stopped by the addition of 100 μL of 1M NaOH, and incubated for an extra 5 minutes at 37^{0}C to degrade the tRNA. Aliquots of 5 μL were precipitated with 5% TCA and the incorporation of radiolabled lysine was determined by scintillation counting.

2.3 RESULTS AND DISCUSSIONS:

The *E. coli* lysyl-tRNA synthetase is encoded in two different genes *LysS* (constitutive) and *LysU* (thermoinducible) which yield the formation of two isoforms of the enzyme.[111] Brick and his coworkers reported in 1995 the structure of *E. coli* LysRS-*LysU*.[112] They found that the protein is a dimer and the N-terminal domains are involved in the binding of the tRNA anticodon domain and the C-terminal domain is the catalytic domain characteristic for all the enzymes from class II synthetases.[112] The lysyl-tRNA synthetase is recognized by the $tRNA^{Lys}$ through the anticodon triplet (UUU) [111, 113], the "discriminator" base A73 [107, 114] and through the acceptor stem.[115]

Preparation of E. coli $tRNA^{lys}$. The *E. coli* lysine specific tRNA ($tRNA^{lys}$) was encoded on plasmids, containing a T7 promoter and generously provided by Dr. Karin Musier-Forsyth of the University of Minnesota. The $tRNA^{lys}$ gene was constructed to have the restriction enzyme site for BstN I (5'…CCAGG…3'). Linearization of the plasmid with BstN I yielded the required ...GGT 3' end template to generate the CCA3" end of the tRNA required for aminoacylation of the tRNA by the lysine synthetase. Large amounts of purified plasmid are easily prepared and used as template for *in vitro* transcription by T7 polymerase. A typical 0.5-1.0 ml transcription reaction yielded 1-3 mg of $tRNAs^{lys}$ (see Figure 2.2). The $tRNAs^{lys}$ was purified using column chromatography; gel electrophoresis and electroelution (see materials and methods).

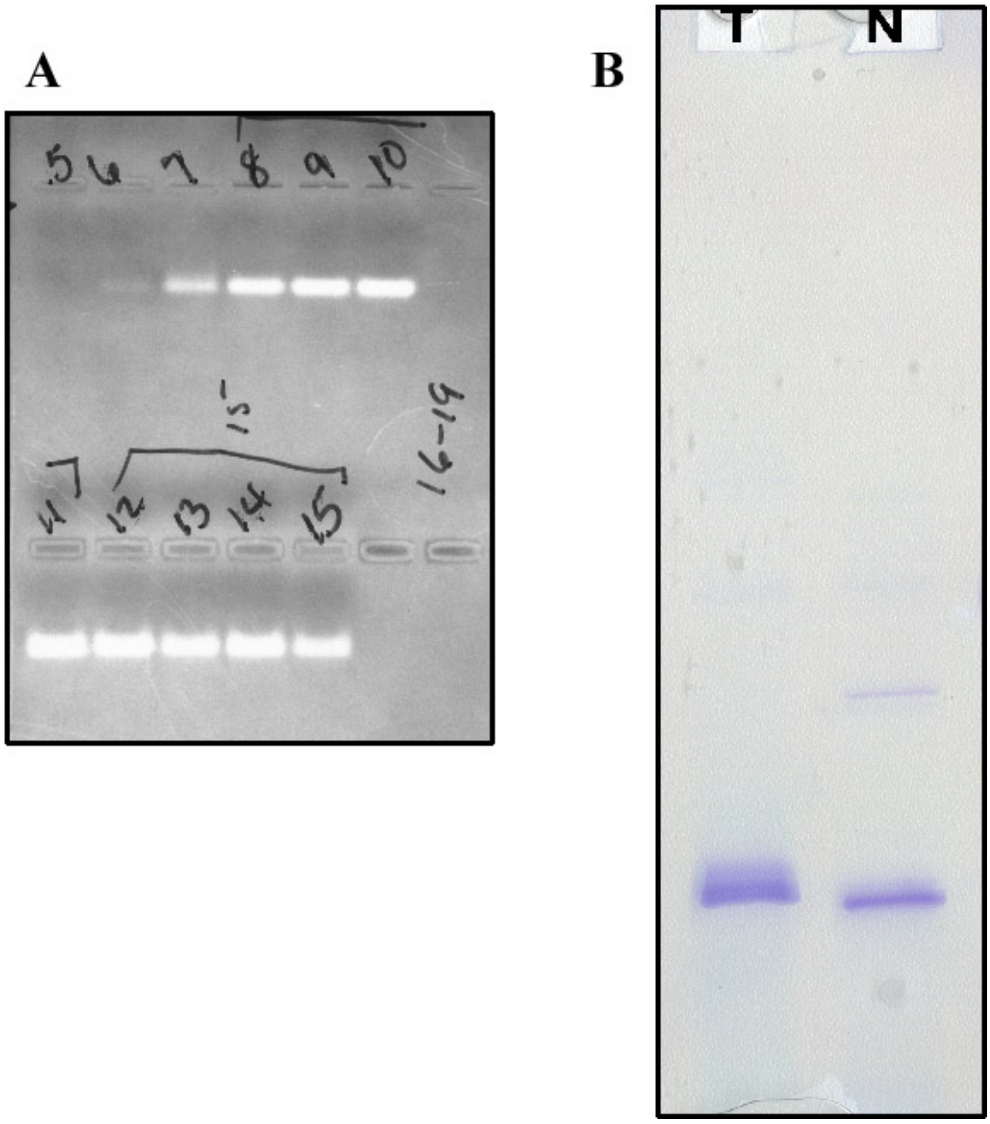

Figure 2.2. Purification of *in vitro* synthesized *E. coli* lysine specific tRNA^{lys}.

A. The *in vitro* synthesized tRNA^{lys} was purified using a G-50 Sephadex column. Fractions of 1 ml were collected and aliquots of 10 µL were run on a 2% agarose gel in TBE. **B.** Urea Gel Analysis of tRNA. Aliquots of 9µg of *in vitro* synthesized lysine specific tRNA^{lys} (T) and native *E. coli* lysine specific tRNA^{lys} (N) (Sigma) were mixed with an equal amount of 10X urea-gel dye. The samples were separated on a 6% urea acrylamide gel. The tRNA was visualized with 0.1% Stains-All (Sigma) and the gel dried.

Preparation of E. coli lysyl-tRNA synthetase. The plasmid which encodes *E. coli* lysyl-tRNA synthetase was a gift from Dr. Karin Musier-Forsyth (University of Minnesota). The *E. coli* lysyl-tRNA synthetase, that was histidine tagged at the N-terminal or C- terminal were prepared and purified as described in materials and methods.

Aminoacylation of E. coli $tRNA^{lys}$ by E. coli lysyl-tRNA synthetase. The established method of amino acylation of tRNA is to use purified tRNA and aminoacylate the tRNA with the respective synthetase in the presence of the cognate amino acid and ATP.[114, 116] However, the yields for the charging of *E. coli* $tRNA^{lys}$ with *E. coli* synthetase were quite low (aminoacylation yields were approximately 10-20 %). All the assays conducted with *E. coli* His^{N}-LysRS, showed that the synthetase is not active and failed to charge. A C-terminal histidine tagged *E. coli* HisC-LysRS, was prepared and purified.[108] The aminoacylation assay carried out using *E. coli* HisC-LysRS, also failed to aminoacylate the *in vitro* synthesized $tRNA^{Lys}$ to a satisfactory level. To prove the poor activity of the *E. coli* lysyl synthetases was due to the unmodified transcribed tRNA and not the activity of the expressed protein, native yeast and/or *E. coli* total tRNA mixture were used as substrates. Using the *E. coli* lysyl-synthetases with the yeast total tRNA gave an estimated yield of 45% aminoacylation assuming that the $tRNA^{lys}$ is at least 1/20 of the tRNA population. One can conclude that the modified nucleotides [107] are essential for charging *E. coli* $tRNA^{lys}$ efficiently and that the *E. coli* synthetases are unsatisfactory for preparing large amounts of aminoacylated tRNA(prepared by *in vitro* transcription) for labeling with nanoparticles and/or quantum dots. However, human lysyl-tRNA synthetase (Human LysRS) does not have the requirement for post

transcriptional modification of the tRNA.

Preparation of the Human lysyl-tRNA synthease. The plasmid which encodes human lysyl-tRNA synthetase was a gift from Dr. Karin Musier-Forsyth (University of Minnesota) and was prepared and purified as described in Materials and Methods. The expression of the human enzyme in *E. coli* was very low and the yield of enzyme was very low compared to the *E. coli* lysyl-synthetase.

Aminoacylation of *E. coli* $tRNA^{lys}$ by human lysyl-tRNA synthetase. The aminoacylation of the *in vitro* transcribed *E. coli* $tRNA^{lys}$ was considerably better with the human synthetase than with the *E. coli*. The yield of the aminoacylation reaction for human LysRS was approximately 35 to 50%. As shown in Table 2.1 the yields of aminoacylation depend on the amount of human LysRS and on the source of lysine specific $tRNA^{Lys}$. The native lysine specific tRNA was not aminoacylated in presence of human LysRS showing that the synthetase recognizes only the *in vitro* synthesized $tRNA^{lys}$.

Table 2.1. Comparison of aminoacylation between the native and *in vitro* synthesized lysine specific $tRNA^{lys}$.

Type of *E. coli* $tRNA^{lys}$	Pmols of tRNA in reaction	Amount of the *Human* LysRS μg/μL	pmols of lys-$tRNA^{lys}$	% aminoacylation
In vitro	112	3	51	45
In vitro	112	6	60	53
In vitro	112	12	81	72
Native	112	3	1	0.93
Native	112	6	1.34	1.26
Native	112	12	0.5	0.5

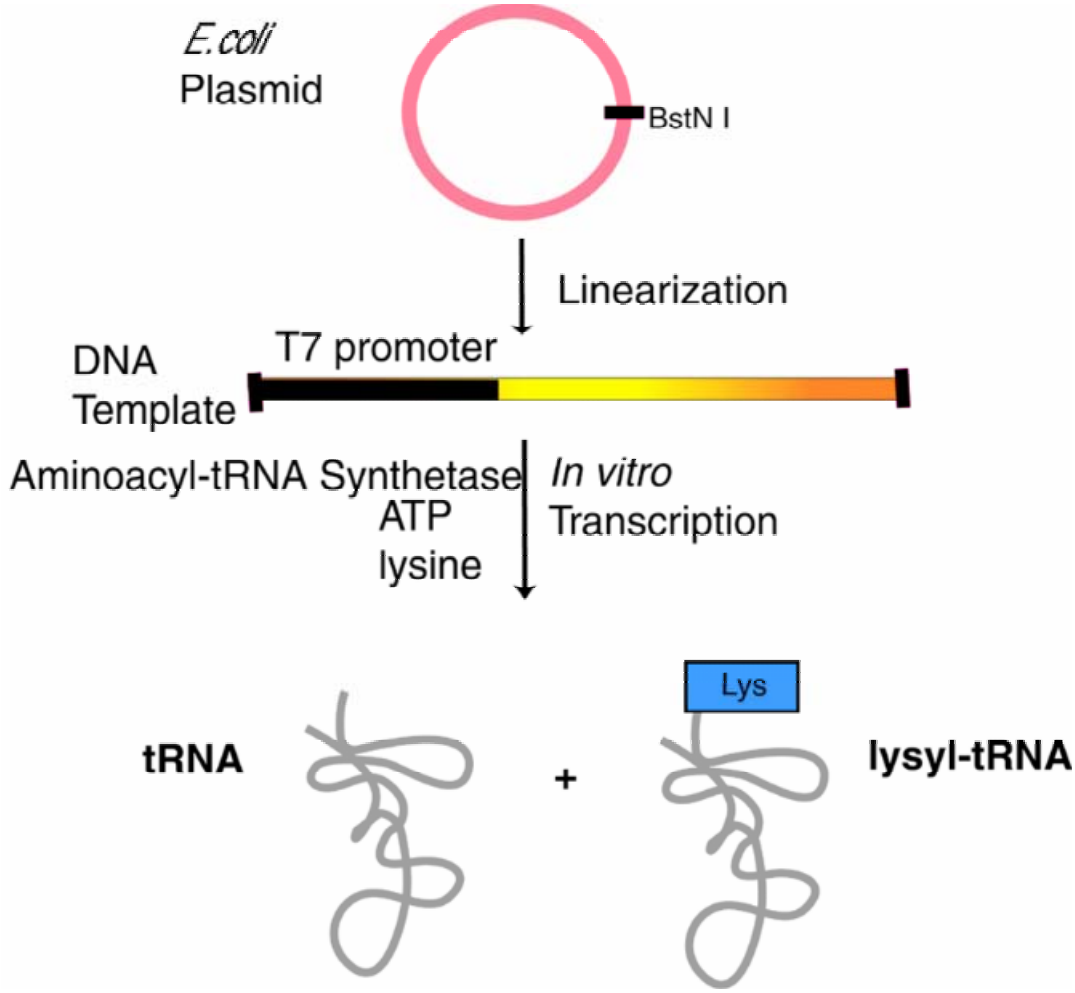

Figure 2.3. Coupled Transcription-Aminoacylation for lysine specific tRNA^{lys}

Development of a new method for preparation of aminoacylated tRNA. One of the goals set forth was to prepare large amounts of nanoparticles and/or quantum dots labeled tRNA. The established method of in *vitro* preparation of tRNA involved gel purification, elution from the gel, phenol extraction and ethanol precipitation prior to aminoacylation. All of these steps caused losses of the tRNA, presented opportunities

for RNAase contamination and degradation and required renaturation of the RNA by heating/cooling.

To improve the efficiency of the process, the human lysyl synthetase was added directly to the *in vitro* transcription assay. Thus, the tRNA would be aminoacylated as soon as it was transcribed and folded correctly. This novel method was called "coupled transcription aminoacylation" or CTA. For the monitoring of the coupled transcription–aminoacylation reactions, radiolabeled α-[^{32}P] UTP and the L-[^{14}C] lysine were used, and their incorporation was monitored over a time course shown in Figure 2.4 and summarized in Table 2.2 and Figure 2.4.

Table 2.2. Quantitative incorporation of radiolabeled UTP and lysine in tRNA at different time frames

Time (min)	pmols of tRNA synthesized [^{32}P] UTP	pmols of [^{14}C]lys -tRNA	% aminoacylation
0	0	0	0
30	102	74	72.5
60	110	87	79
120	161	91	57

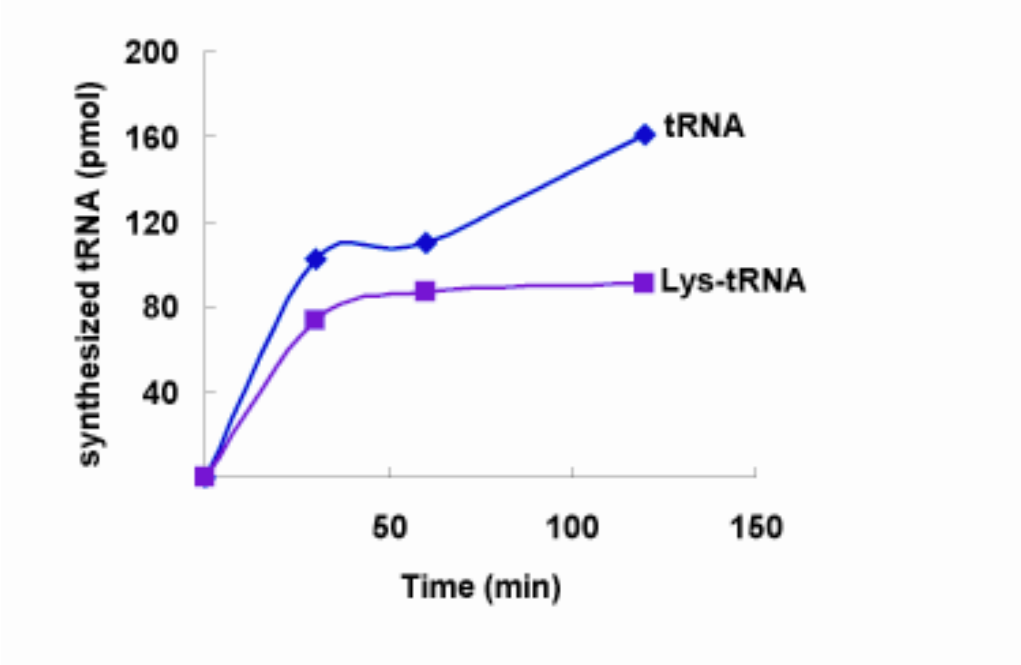

Figure 2.4. Incorporation of radiolabeled [^{32}P] UTP and [^{14}C] lysine in tRNA^{lys} within the two-hour period .

Time course of incorporation of α-[^{32}P] UTP (54 dpm/pmol) into lysine specific tRNA^{lys} (♦) and [^{14}C] lysine into [^{14}C]lys-tRNA^{lys} (■)(682 dpm/pmol). Aliquots of 10 µL were removed at indicated times and precipitated with cold 10% trichloroacetic acid and collected on glass fiber filters by vacuum filtration.[117] The filters were dried and counted in a scintillation counter (Beckman) and the amount of tRNA synthesized or aminoacylated was calculated.

The increase in both [^{32}P] UTP and [^{14}C] lysine shows the efficiency of both the tRNA^{Lys} synthesis and the aminoacylation reaction. It appears that the aminoacylation of tRNA^{Lys} occurs rapidly after the tRNA is transcribed and presumably folds correctly. The yields of aminoacylation in these reactions were around 50 - 60%. The CTA method was used later for the cysteine system and it generated large amounts of

aminoacylated tRNA.[118]

Electrospray ionization mass spectroscopy (ESI-MS) was used to verify that lysyl-tRNA is formed (Figure 2.5). In the ESI-MS spectrum two peaks were expected, one for $tRNA^{Lys}$ (MW=24630) and the other one for lysyl-tRNA (MW=24754).

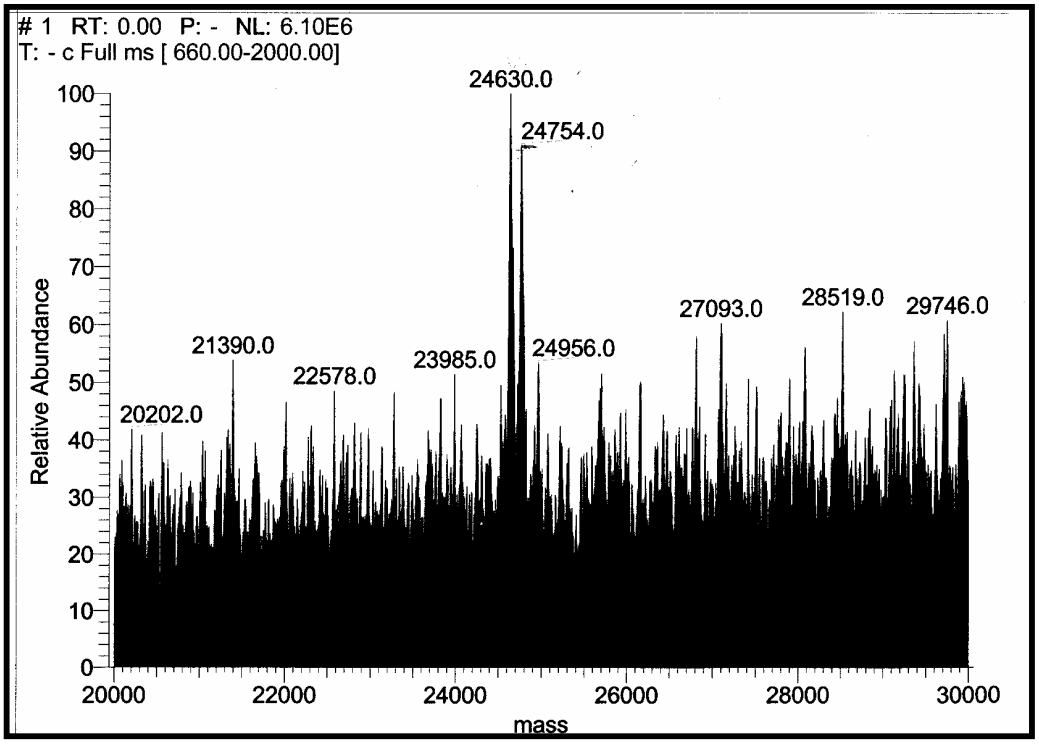

Figure 2.5. ESI-MS of a mixture of lysine specific tRNA (24630) and lysyl-tRNA (24754).

An aliquot of 3 nmols of a mixture of lysine specific $tRNA^{lys}$ and lysyl-$tRNA^{lys}$ was purified using phenol extraction and ethanol precipitation. The salt used in ethanol precipitation was 200 mM NH_4OAc pH 7.5.

Attachment of Nanogold to lysyl-tRNA^{lys}. The next step was the attachment of a heterobifunctional cross linker to the aminoacylated tRNA and then to the Nanogold (see Figure 1.2, step 2). A heterobifunctional cross linker is a reagent which has two different functional groups, each reactive towards two different functional target. The chosen heterobifunctional linkers for the lysine system have one functional group (i.e. -COOH) reactive towards an amine group and the other functional group (i.e. -NH_2) is reactive towards a carboxylic group. The heterobifunctional linkers used are the 11-aminoundecanoic acids (L_1) and the 6-aminohexanoic acid (L_2). The 6-aminohexanoic acid reacted with N-hydroxysuccinimide in the presence of EDC to yield the NHS ester of the target linker. The NHS ester reacted with the lysyl-tRNA and the linker is covalently attached to the ε-amine group. The ε-amine group is more reactive than the α-amine group (the ratio is approximately 97:1) most likely due to steric impediments (the size and folding of the tRNA plays an important role).[31, 33-36, 106] However, it has been reported that the NHS ester of the linker may react with the α-amino group which would prevent the incorporation of modified lysine residues into proteins.[31]

The remaining free reactive group of the linker was reacted with gold nanoparticles to yield a novel gold nanoparticle-conjugated-L-aa-tRNA (See Figure 1.2, step3). For the lysine system 1.4 nm mono-*sulfo*-NHS nanogold was used and it was purchased from Nanoprobes, Inc. The nanogold compound has a single reactive group on the surface, a *sulfo*-N-hydroxysuccinimide ester (*sulfo*-NHS), which is very reactive towards primary amines under mild conditions (pH 7.5). A covalent attachment of the nanogold to the free epsilon amino group on the linker was obtained. An alternative

approach was to eliminate the bifunctional linker and to attach the gold nanoparticle directly to the side chain of the lysine, (see Figure 2.1, step 2'). The conditions used for direct linkage were the same as the ones used in the presence of a linker and in both experiments a unique nanogold-tRNA complex was obtained. The successful attachment of nanogold to lysyl-tRNA in the absence or presence of a linker was verified by mass spectroscopy (Figures 2.6 and 2.7, respectively; Table 2.3) and TEM.

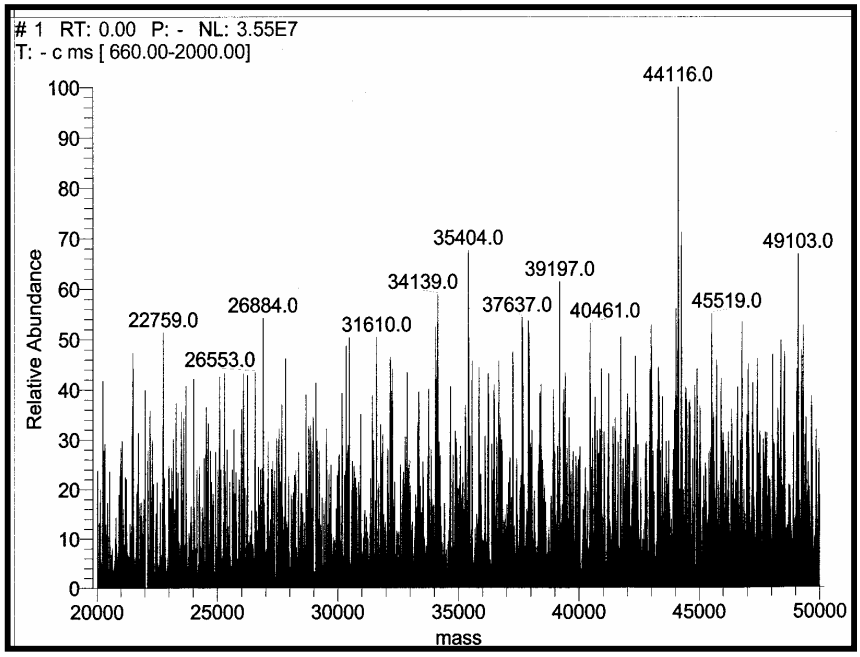

Figure 2.6. ESI-MS on nanocrystal tRNA complex (Au•Lys-tRNA).

An aliquot of 1 nmols of lysyl-tRNA^{lys} modified with 1.4 nm mono-*sulfo*-NHS nanogold was ethanol precipitation. The salt used in ethanol precipitation was 200 mM NH_4OAc pH 7.5.

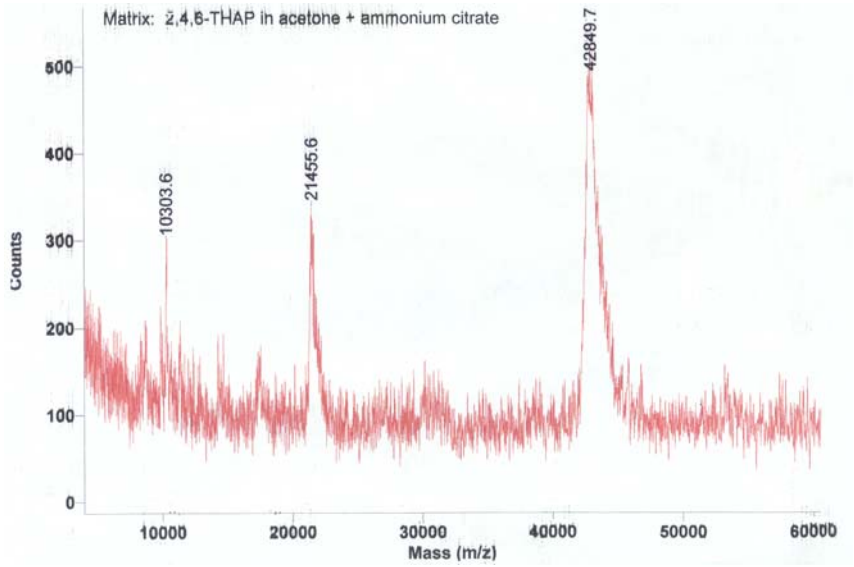

Figure 2.7. MALDI-MS on nanocrystal tRNA complex (Au•L_2Lys-tRNA^{lys}).

An aliquot of 300 pmol of gold modified L_2lysyl-tRNA^{lys} was mixed with 2, 4, 5-Trihydroxyacetophenone monohydrate (THAP) in acetone and ammonium citrate. The mixture was crystallized on a MALDI grid. The Lysyl-tRNA^{lys} was modified with 6-aminohexanoic acid (L_2) and subsequently modified with 1.4 nm mono-*sulfo*-NHS nanogold to yield the formation of Au•L_2Lys-tRNA^{lys}. The Au•L_2Lys-tRNA^{lys} was ethanol precipitation. The salt used in ethanol precipitation was 200 mM NH_4OAc pH 7.5.

Table 2.3. Mass spectroscopy theoretical and experimental data for lysine specific tRNA^{lys}, lysyl-tRNA^{lys} and its complexes.

	Theoretical Data Base[119]	Data MW as calculated	Experimental ESI	Data MALDI
tRNA^{Lys}	24659.2	24693.7	24647 24631(mix)	24687.4
Lys-tRNA		24822	24751	
Au Lys-tRNA			44116	
AuL_2 Lys-tRNA				42849.7
mono-*sulfo*-NHS nanogold	15 000 (manufacturer)			Particles do not fly

The molecular weight difference presented in the spectra for the gold nanoparticle modified lysyl-tRNA in the absence or presence of a linker (see figure 2.4 and 2.5) is due to variations in the molecular weight of the gold nanoparticles (approximately 15, 000Da as indicated by the manufacturer) and is dependent on the number of gold atoms present in the nanoparticle clusters (76-100 gold atoms/nanoparticle).

Further analysis of the Au-modified tRNA by TEM (see Figure 2.8) showed that the dimension of the gold nanocluster was in good agreement (~1.7 nm) with the reported size (1.4 nm).

These results were very encouraging and suggested that a gold nanoparticle could be successfully attached to an aminoacyl-tRNA.

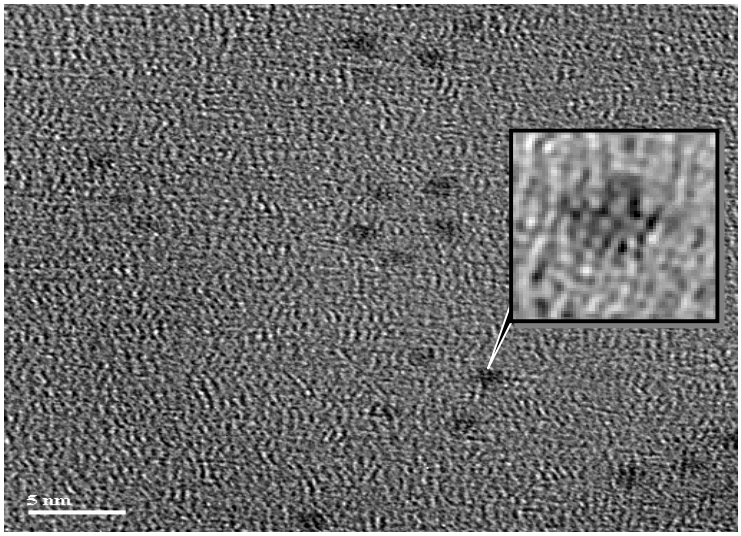

Figure 2.8. TEM image of nanogold particles attach to ε-amine of a lysyl-tRNA. An aliquot of 500 pmols of nanogold modified lysyl-tRNA^{lys} purified on a G-25 Sephadex column to remove unbound gold nanoparticles, were spotted on a cooper grid coated with a continuous carbon thin film.

***In vitro* translation with Au•Lys-tRNA.** The ability of the novel quantum dot-conjugated-L-aa-tRNA to be incorporated into a polypeptide was measured using an *E. coli* cell-free coupled transcription-translation system.[110] The translation system consists of an extract from *E. coli* (S30) that contains ribosomes, all the enzymes necessary for translation, the tRNAs with their respective synthetases, but is depleted of endogenous mRNA and small molecules (e.g. amino acids, NTP). The reaction mixture containing the *E. coli* extract is supplemented with T7 RNA polymerase to transcribe the desired mRNA from a plasmid. Dr.Gisela Kramer (The University of Texas at Austin) kindly provided the *E. coli* extract and T7 polymerase for these experiments. The *E. coli* extract is depleted of amino acids and small molecules during preparation. When the translation is performed, the amino acids and NTPs must be added to the reaction mixture. The amino acid corresponding to the radioactive label, in this case lysine, is omitted and the remaining 19 amino acids are added to the reaction mixture.

To test the ability of the Au•[^{14}C]lys-tRNA to function in translation was measured. The DNA plasmid used for the template for a mRNA encodes *E. coli* translation initiation factor (IF3) and the protein product has 21 lysine residues. The amount of radioactivity incorporated into protein was measured by precipitation using trichloroacetic acid (TCA). The amount of [^{14}C] lysine incorporated was similar (10-15 pmols) for [^{14}C] lysyl-tRNA or Au•[^{14}C] lysyl-tRNA. In the absence of added template the amount of [^{14}C] lysine incorporated was about 5 pmols. This result suggested that the gold nanoparticles do not inhibit the translation but the amount of translation was very low.

The incorporation of quantum dots into the polypeptides was analyzed by electrophoresis (SDS-PAGE), and electron microscopy (TEM). In the SDS-PAGE gels no full length product was observed; however, the TCA analysis suggests that small peptides may have been synthesized. The transmission electron microscopy (TEM) analysis was unsuccessful due to the high organic background present in the samples. We did not have the means to purify the full length protein or the small peptides from the *E. coli* extract.

2.4. CONCLUSION:

The binding of gold nanoparticle to the lysyl-tRNA (in presence or absence of the linker) demonstrates the viability of interaction between two very different and complex systems, and opens new opportunities for the interactions of similar systems.

Despite initial promising results with the lysine system, it was abandoned for multiple reasons. The detection of the L-[^{14}C] lysine required long exposure times to a phosphorimager screen and the [^{14}C] lysine is very expensive. The second reason was the poor expression and stability of human lysyl-tRNA synthetase (human LysRS). From 14 batches only two of them were active and the yield of protein expressed was very low. The third reason was the aminoacylation of the *in vitro* synthesizes lysine specific tRNA failed when C- and/or N-terminal histidine tagged *E. coli* tRNA-synthetases were used. The presence of the modified nucleotides in tRNA is necessary for enhanced aminoacylation.

Another tRNA/synthetase pair was sought that would have a more robust synthetase and not require modification of the tRNA for aminoacylation. The amino acid would need to have a reactive side chain. The best candidate for additional studies was the *E. coli* cysteinyl-tRNA and synthetase.

CHAPTER 3

CYSTEINE SYSTEM

3.1. WHY WE CHOOSE THIS SYSTEM *VERSUS* LYSINE OR OTHER AMINO ACIDS SYSTEMS

The cysteine system was chosen for several reasons:

(1) The *E. coli* cysteinyl-tRNA synthetase/tRNA pair does not require the base modification for an efficient aminoacylation and has been extensively studied by Dr. Ya-Ming Hou's group.[19-21, 23-29, 120-122]

(2) L-[^{35}S] cysteine would allow for faster visualization of the products (aminoacylated tRNA, translated proteins) and is considerably less expensive. One of the conclusions from the work on the lysine system was necessary to quickly visualize the products from the intermediate steps. All the intermediate steps in the preparation of the gold nanoparticle modified tRNA are labile and light sensitive.

(3) The cysteine has only one reactive site (SH-) compared to lysine (two amino groups).

(4) Cysteine also has a relatively low distribution in proteins (an average of 1-6 cysteine residues per protein) which implies that a high concentration of modified cys-tRNA would not be as critical in the *in vitro* translation reactions compared to the lysine system.

(5) The sulfhydryl group in the beta position of the cysteine side chain presents the possibility of modifying proteins with a variety of cross–linked labels and nanoparticles. In particular the gold nanoparticles available in the <2 nm range are modified with a

single monomaleimido group. The chemistry between sulfhydryl group and monomaleimido group is well known and intensively studied.[72, 123, 124]

For the reasons mentioned above, the cysteine system was chosen for demonstrating the concept that a molecular machine (ribosome) could accommodate an inorganic material without terminating translation and would incorporate inorganically modified cysteine into a protein to create novel nanoscale inorganic/biological materials. This would show that the ribosome could function to assemble novel inorganically modified peptide based materials (see Figure 3.1). This method makes it possible to imagine supramolecular assembly of novel bioinorganic heterostructures using the ribosome.

The research described in this chapter is: (1) *in vitro* synthesis and aminoacylation of the cysteine specific $tRNA^{cys}$ (see Figure 3.2, step 1); (2) attachment of gold nanoparticle (monomaleimido nanogold) to the sulfhydryl group present on the side chain of cysteine (see Figure 3.2, step 2); (3) incorporation of this new inorganically modified cysteinyl-tRNA in a coupled transcription-translation reaction to generate protein containing inorganic materials (see Figure 3.1).

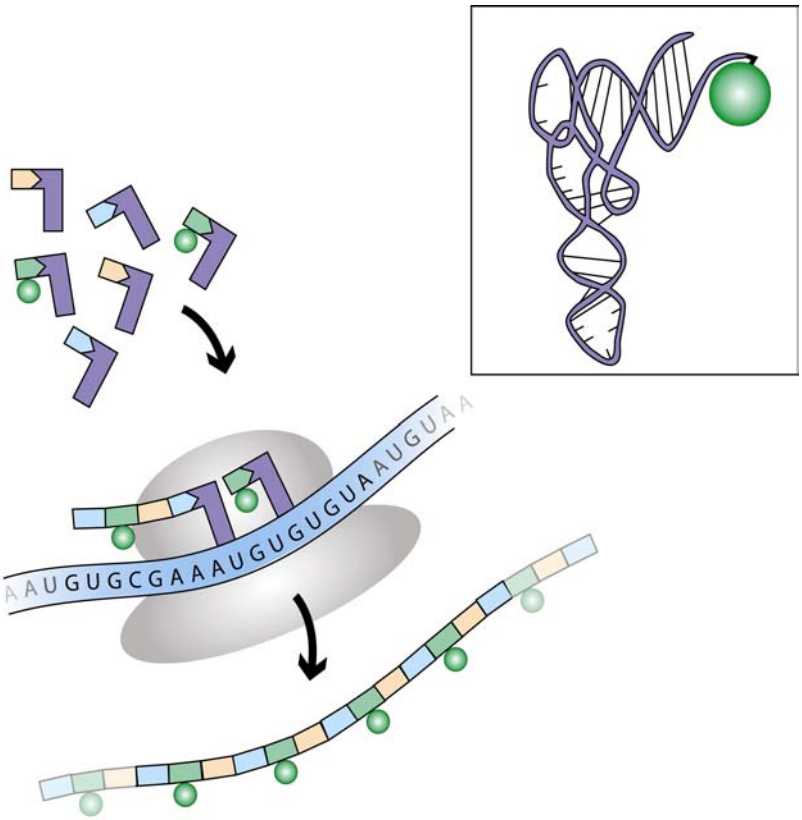

Figure 3.1. Model for the assembly of nanoparticles into proteins by molecular machines.

Ribosomes are molecular machines that catalyze the assembly of amino acids into polypeptides according to the information encoded in an mRNA template using aminoacylated transfer RNAs (aa-tRNA) as substrates. The tRNA molecules are specific to their cognate amino acids and deliver amino acids to the ribosome. An aminoacylated $tRNA^{cys}$ (cys-$tRNA^{cys}$) may be modified by attaching a nanogold particle to the sulfhydryl group of the amino acid. This inorganically modified aminoacylated $tRNA^{cys}$ (Au·cys-$tRNA^{cys}$) delivers the nanogold modified amino acid to the molecular assembly machine (ribosome). The molecular machine uses the inorganically modified tRNA to assemble a hybrid protein containing nanogold wherever cysteine is specified by the mRNA. Ultimately, this pioneering method may be used to assemble novel bio-inorganic materials such as peptide nanowires.

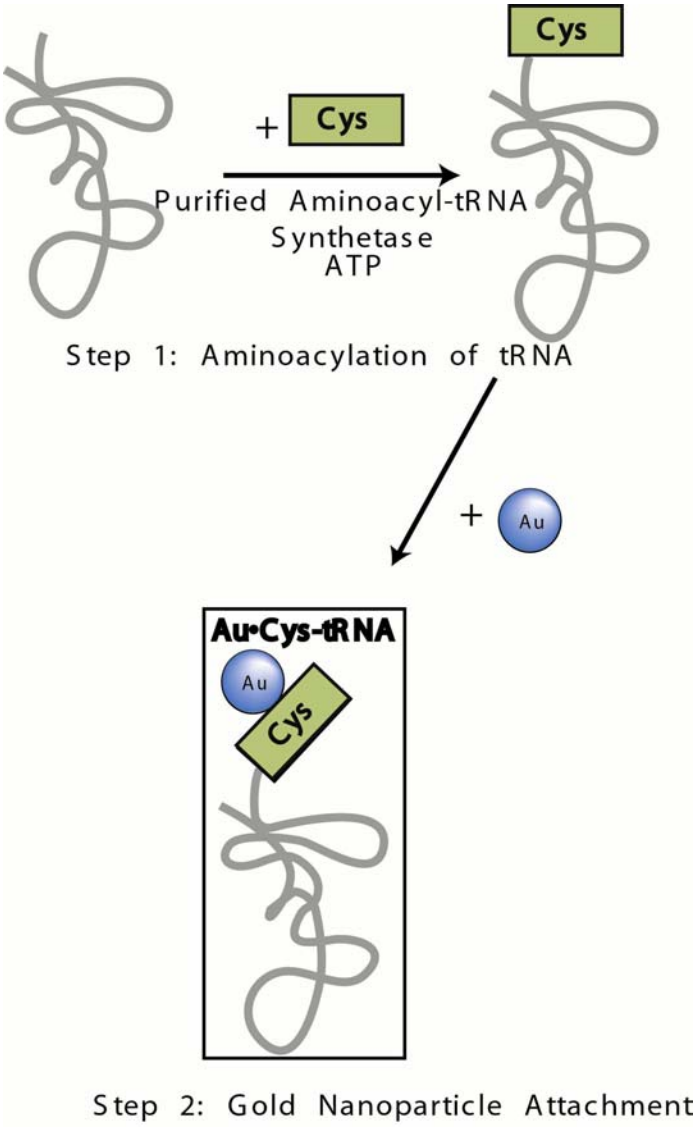

Figure 3.2. Method of preparing gold nanoparticles•cysteinyl-tRNA (InAA-tRNA)

3.2. MATERIALS AND METHODS

3.2.1. *E. coli* His^C-CysRS:

The plasmid pCysRS09 which encodes the gene for *E. coli* His^C-CysRS was a generous gift from Dr. Y-M Hou (Thomas Jefferson University, Philadelphia, PA).[122] The recombinant DNA was used to transform the expression cells *E. coli* BL21Star (Invitrogen, Carlsbad, CA). Single colonies were picked and grown overnight at 37^0C in a 4 x 50 mL LB [Luria -Bertani (LB) broth] medium and 100 μg/mL ampicillin. Four flasks (4 x 1L) of LB medium /ampicillin (AMP) (100 μg/mL) were each inoculated with a 50 mL culture grown overnight. The cultures were incubated at 37^0C under continuous shaking. The OD_{600} was read hourly until it reached approximately 0.5-0.9, when it was induced with IPTG (isopropyl-1-thio-β-D-galactopyranoside) at a final concentration of 0.1 mM. The incubation was continued at 37^0C for an additional 4 hours. The cells were harvested by centrifugation at 2500 x g for 20 minutes at 4^0C. The cell pellet was resuspended in 25 mL of lysis buffer (50 mM HEPES–KOH, pH 7.6, 1 M NH_4Cl, 10 mM $MgCl_2$, 10 mM $MgCl_2$, 0.3 mg/ml lysozyme, 0.1% Triton X-100, 0.2 mM phenylmethylsulfonyl fluoride (PMSF), and 7 mM β-mercaptoethanol) and lysed by sonication. The lysed cells were centrifuged at 100,000 x g for one hour and the supernatant was collected. The *E. coli* His^C-CysRS was purified using a nickel-nitrilotriacetic acid resin (Ni-NTA) (QIAGEN, Valencia, CA).

3.2.2. Coupled Transcription-Aminoacylation (CTA)

The plasmid containing the $tRNA^{cys}$ gene with a T7 promoter (250 μg) was digested with BstNI to linearize the template for transcription. Plasmid pTFMa containing the $tRNA^{cys}$ gene was a generous gift from Dr. Y-M Hou (Thomas Jefferson University, Philadelphia, PA).[29] The linearization reactions were performed at 37^0C for 18 hours. Digestion with BstNI leaves a template for the 3' CCA end of the transcribed tRNA. T7-Megashortscript™ transcription kits (Ambion, Austin, TX) were used according to the manufacturer's instructions. The digested template (0.36-0.5 mg/mL the final concentration in the reaction) was transcribed in a 100 μL reaction mixture volume. To couple the transcription and charging reactions, the mixture was supplemented with 6-12 μg purified *E. coli* cys-$tRNA^{cys}$ synthetase and either 75 mM [^{32}P]-UTP (444 cpm/pmol), Perkin-Elmer Life and Analytical Sciences, Inc, Boston, MA to monitor tRNA formation or 1.2 mM L- [^{35}S] cysteine (1000 cpm/pmol) (Perkin-Elmer Life and Analytical Sciences, Inc, Boston, MA) to monitor tRNA aminoacylation. The reaction was incubated at 37^0C for 2 hours, and aliquots were taken at various time points and analyzed by electrophoresis on a 6% urea-acrylamide gel.

Large scale synthesis of cys-$tRNA^{cys}$ (0.5 mL) was carried out as described above and supplemented with either [^{35}S]-cysteine or unlabeled cysteine. *E. coli* His^C-CysRS was removed batchwise from the charged tRNA with nickel-nitrilotriacetic acid resin (Ni-NTA, QIAGEN, Valencia, CA). The Ni-NTA matrix (200 μL) was washed twice in a 1.5 mL microcentrifuge tube with 500 μL of 20 mM HEPES-KOH pH=7.6.

The resin was allowed to settle and the supernatant removed. The cys-tRNA^{cys} was added to the matrix, gently mixed by rotation for 1 hour at 4^0C. The mixture was then centrifuged for 1 minute to pellet the resin, and the supernatant containing the cys-tRNA^{cys} was removed. This process was repeated as necessary to remove any remaining synthetase. The cys-tRNA^{cys} was purified by gel filtration on a Sephadex G-25 column as previously described.[36] The fractions containing the highest amount of cys-tRNA^{cys} were pooled (~0.5 mL), lyophilized, and dissolved in 75 μL of H_2O. The yield from a 0.5 mL reaction was approximately 1-1.5 mg. No phenol extraction, ethanol precipitation, gel filtration, or heating and reannealing were performed.

Cysteine Specific tRNA^{cys} sequence:

GGCGCGTTAACAAAGCGGTTATGTAGCGGATTGCAAATCCGTCTAGT CCGGTTCGACTCCGGAACGCGCCTCCA

3.2.3. Attachment of biotin [N-iodoacetyl-N-biotinhexylenediamine] to cysteinyl-tRNA

The attachment of biotin [N -iodoacetyl-N-biotinhexylenediamine] (ILCB) to [^{35}S]-cysteinyl-tRNA was carried out according to the manufacturer's instructions (Pierce Biotechnology, Rockford, Il.). Briefly, [^{35}S] cysteinyl-tRNA^{cys} (21 nmols) was incubated in the dark with ILCB (37.5 nmols) (2 mM ILCB resuspended in DMSO) for 2 hours at room temperature and 2 hours at 4^0C. The biotinylated cys-tRNA^{cys} was

purified by Sephadex G-25 column chromatography as described above and lyophilized.

3.2.4. Attachment of Monomaleimido Nanogold (MMA-Au) to cysteinyl-tRNA

The attachment of the 1.4nm monomaleido nanogold (Nanoprobes, Yaphank, NY) particle to [^{35}S] cysteinyl-tRNA and/or cysteinyl-tRNA was carried out accordingly to the manufacturer instructions with slight modifications. The purified cysteinyl-tRNA (30nmol) was resuspended in 20 mM sodium phosphate, 150 mM NaCl, 1mM EDTA, pH 6.5 and added to monomaleimido nanogold (MMA-Au), 60 nmol in water. The mixture was incubated at room temperature with rotation for 2 hours and for another 2 hours at 4^0C. The gold modified cysteinyl-tRNA was purified by Sephadex G-25 spin column chromatography and lyophilized. The 1 cc. Sephadex G-25 spin columns are equilibrated with 2 column volumes of water and collected by centrifugation at 900rpm for two minutes. The reaction mixtures (from 50 μL to no more then 125 μL per column) are added to the column and collected by centrifugation again at 900 rpm for 3-4 minutes.

3.2.5. *In vitro* Coupled Transcription-Translation reactions

The *E. coli* T7 S30 Extract System (Promega, Madison, WI) was used for coupled transcription/translation assays. Plasmid pIVEX 2.1 encoding green fluorescent protein (GFP, Roche Applied Science, Indianapolis, In) was used as the template in the coupled transcription-translation reaction. The reaction mixture was supplemented with 2 mM L-[^{35}S] cysteine, 2 mM L-[^{35}S]cys-tRNA^{cys}, 2 mM ILCB-

[^{35}S]cys-tRNA^{cys}, or 4 mM Au•[^{35}S]cys-tRNA. The biosynthesis of [^{35}S]-GFP or modified [^{35}S]-GFP was confirmed by SDS-PAGE and autoradiography. The biosynthesis of biotinylated GFP was confirmed by SDS-PAGE, western blotting to a PVDF membrane, and detection using streptavidin-horseradish peroxidase conjugate (Pierce Biotechnology, Inc., Rockford, IL) and a chemiluminescent or colorimetric substrate (TMB) (Pierce Biotechnology, Inc., Rockford, IL). The biosynthesis of Au-GFP was confirmed by SDS-PAGE, western blotting to a PVDF membrane, and detection using laser ablation ICP-mass spectrometry (see below),

An alternative method for detection of the protein products that eliminated the need for [^{35}S]-cysteine was to include [^{14}C]-leucine in the reaction mixture. An amino acid mix (18 amino acids minus cysteine and minus leucine) was used for these reactions. The reaction mixture was supplemented with 2 mM cys-tRNA^{cys}, 2 mM ILCB-cys-tRNA^{cys}, or 4-8 mM Au•Cys- tRNA^{cys} (the higher concentration improves translation and provides excess Au to scavenge up excess DTT (~1-2 mM)) and 2 mM L-[^{14}C]-leucine. The biosynthesis of [^{14}C]-GFP or gold modified [^{14}C]-GFP was confirmed by electrophoresis, autoradiography and LA-ICP MS. The reactions containing gold modified [^{14}C]-GFP and the no template control were further purified batchwise on a Strep-tactin matrix (IBA, Goettingen, Germany) according to the manufacturer's instructions. Strep –tactin matrix 10% v/v (5 μL matrix per 50 μL reaction) was washed tree times with the 50 μL washed buffer (100 mM Tris-HCl, 150 mM NaCl, 1 mM EDTA, pH 8). After the wash buffer was removed completely the transcription-

translation reaction was added to the matrix and rotated overnight at 4^0C. Next day the supernatant was removed and the matrix was washed tree times with the 100 μL wash buffer. The protein was eluted with 25 μL elution buffer (100 mM Tris-HCl, 150 mM NaCl, 1 mM EDTA, 2.5 mM desthiobiotin, pH 8). The fractions containing the purified protein were analyzed by electrophoresis, autoradiography, LA-ICP MS and HAADF.

3.2.5.1. Laser Ablation Inductively Coupled Plasma Mass Spectrometry-LA-ICP MS

The $tRNA^{cys}$ samples were separated by electrophoresis on a 6% urea/acrylamide gel. The gel was dried between two sheets of cellophane and cut in 3.00 cm strips. The strips were applied with double sided tape to 4.6 cm glass slides. The protein samples were run on Novex 10-20% Tris –Glycine gel (Invitrogen) and transferred to a PVDF membrane. The membrane was cut in strips (4.3 cm long and 1.2 cm wide) and similarly applied to a glass slide using a double sided sticky tape. The glass slide and gel or membrane were placed in the ablation chamber and purged with helium. Gold was monitored by the ICP-MS as the laser traversed down the center of the lane. All the measuring conditions and the instrument settings used for LA-ICP MS are detailed in Table 3.1.

Table 3.1. LA-ICP MS Measurement Conditions

ICP-MS	GVI Platform quadrupole ICP-MS
RF power	1380 W
Ar flow rates	
Cool	13.5 L min^{-1}
Auxilliary	1.20 L min^{-1}
Make-up gas	0.50 L min^{-1}
Hexapole collision/reaction cell	
He	5.5 mL min^{-1}
H_2	5.0 mL min^{-1}
Data acquisition	
Scanning mode	Peak hopping
Dwell time	20 to 100 msec
Inter Channel Delay	20 msec
Laser ablation system	New Wave LUV213 213 nm output, NdYAG laser source
Spot diameter	400 μm
Scan rate over transect	30 to 80 μm sec^{-1}
Run time	16 min-Au•cystRNA; 8.5 min-Au•GFP
Repetition rate	10 sec^{-1}
Power setting	80 to 100%
Energy	2.65 millijoules
Fluence	2.11 j cm^{-2}
He flow rate through sample ablation cell	0.80 to 0.90 liters min^{-1}

3.2.5.2. High Angle Annular Dark Field -HAADF.

The samples for HAADF were prepared on a copper grid coated with a continuous carbon thin film (Ted Pella, Inc, Redding, CA.). Samples of 3μL were added on top of the grid and dried at room temperature. The HAADF images were collected with a JEOL 2010F transmission electron microscope in STEM mode, using a HAADF detector equipped with an Oxford energy dispersive spectroscopy unit. The TEM was operated at an acceleration voltage of 200 kV using a 0.5 nm high resolution probe size.

3.3. RESULTS AND DISCUSSION:

Preparation of Cysteinyl-tRNA. The preparation of the cysteinyl tRNA was similar to the lysine system. The coupled transcription and aminoacylation reaction was used to by-pass all the intermediate purification steps. Similar results were obtained with the cysteine system as obtained in the lysine system.

The time course of cysteine-specific $tRNA^{cys}$ synthesis in an *in vitro* transcription and a CTA reaction is shown in Figure 3.3. To quantify the amount of synthesized $tRNA^{cys}$, radiolabeled α- [^{32}P] UTP was added to the reaction mixture (see Figure 3.3.B). Transcription products in both reaction mixtures increased over the time course; however, transcription in the CTA reaction mixture was reduced ~25% at later time points (see Figure 3.3.C). This may be due to consumption of ATP during aminoacylation, reducing transcription efficiency. An additional experiment was performed where an excess of ATP was added to the reaction mixture. An increase in the yield of $tRNA^{cys}$ was observed but not an increase in the aminoacylation (data not shown).

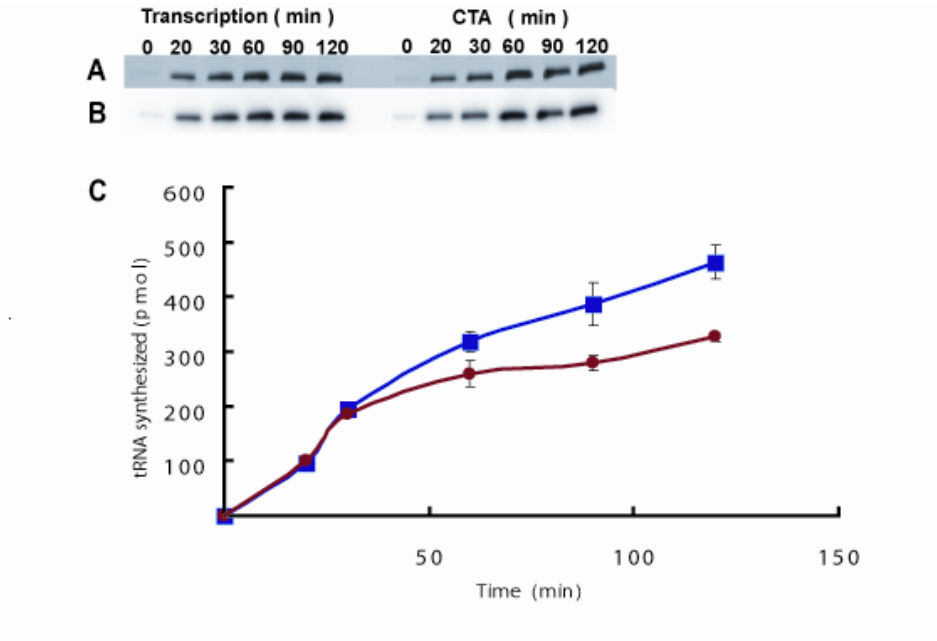

Figure 3.3. Time course of *in vitro* synthesis of [^{32}P] tRNA^{cys} (transcription) and cys-[^{32}P] tRNA^{cys} (CTA).

A. Aliquots of 2.5 µL were removed at indicated times and mixed with an equal amount of 10X urea-gel dye. The samples were loaded on a 6% urea acrylamide gel. The gel was stained with 0.1% Stains-All (Sigma) and dried. **B.** The gel shown in panel A. was exposed to a phosphorimager screen to visualize the incorporation of α-[^{32}P] UTP (54 dpm) in cysteine specific tRNA^{cys} (transcription) and cys-tRNA^{cys} (CTA). **C.** Time course of incorporation of α-[^{32}P] UTP (54 dpm) into cysteine specific tRNA^{cys} (■) and cys-tRNA^{cys} (●). Aliquots of 5 µL were removed at indicated times and precipitated with cold 10% trichloroacetic acid and collected on glass fiber filters by vacuum filtration.[117] The filters were dried and counted in a scintillation counter (Beckman) and the amount of tRNA synthesized calculated. The ratio of transcript (7500 pmol) to template (5.5 pmol) was approximately 1300:1.

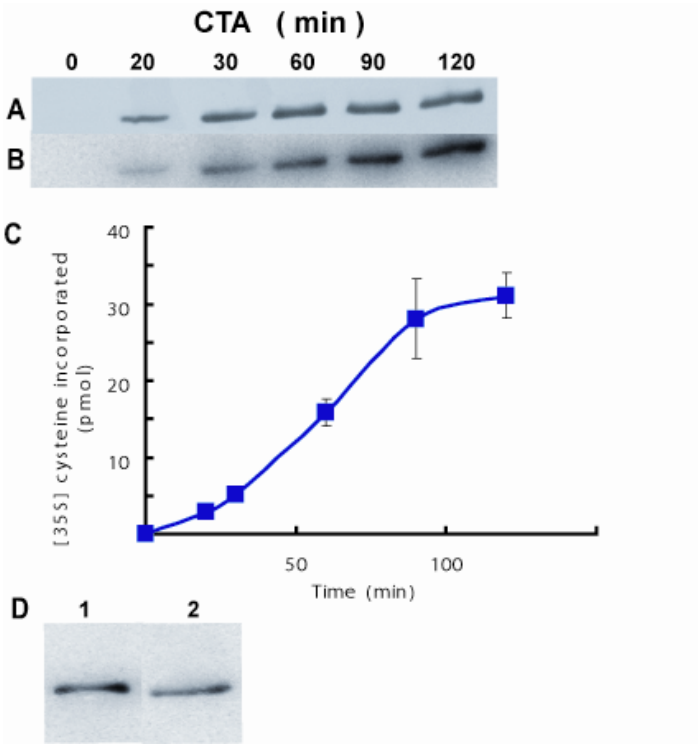

Figure 3.4. Time course of *in vitro* synthesis of [^{35}S]cys-tRNA^{cys}.

A. Aliquots of 2.5 µL were removed at indicated times and mixed with an equal amount of 10 X urea-gel dye. The samples were loaded on a 6% urea acrylamide gel. The gel was stained with 0.1% Stains-All (Sigma) and dried. **B**. The gel in panel A was exposed to a phosphorimager screen (Amersham Biosciences, Piscataway, NJ) to visualize the [^{35}S] cysteine (1538 dpm) incorporation at indicated times. **C.** Aliquots of 5 µL were removed at indicated times and incubated for 30 minutes with 24 µL CAM [5]. The aliquots were precipitated with cold 10% trichloroacetic acid and collected on glass fiber filter by vacuum filtration. The filters were dried and counted in a Multi-Purpose Scintillation Counter (Beckman). **D.** Phosphorimage of [^{35}S]cys-tRNA^{cys} (300pmol and 1000 cpm/pmol) and ILCB·[^{35}S]cys-tRNA^{cys}; Lane 1, 300 pmol [^{35}S]cys-tRNA^{cys} before reaction with biotin; Lane 2**,** 300 pmol [^{35}S]cys-tRNA^{cys} after reaction with biotin [N-iodoacetyl-N-biotinhexylenediamine] (ILCB). An aliquot of 2.5 µL were mixed with an equal amount of 10X urea-gel dye. The samples were loaded on a 6% urea acrylamide gel.

The aminoacylation of transcribed $tRNA^{cys}$ was monitored by the incorporation of [^{35}S] cysteine. The cys-$tRNA^{cys}$ synthesized was visualized by gel electrophoresis and staining (Figure 3.4A). The reaction contained [^{35}S] cysteine, and the amount of [^{35}S] cysteine incorporated into the $tRNA^{cys}$ is shown in the autoradiogram (Figure 3.4B). The amount of [^{35}S] cysteine incorporated in cys-$tRNA^{cys}$ increases with time as shown in Figure 3.4C. The data shows that the $tRNA^{cys}$ is being aminoacylated over the course of the transcription reaction (see Figures 3.3C and 3.4C). This suggests that the $tRNA^{cys}$ transcript is folded in the correct form and is immediately recognized by the synthetase in order to be aminoacylated. Note that no denaturation or annealing was required for the tRNA to be properly folded and recognized by the synthetase.

The assay for the quantification of the amount of [^{35}S] cysteine incorporated is complicated by the behavior of cysteine with TCA precipitation.[29] The free cysteine tends to precipitate and/or bind to nitrocellulose or glass fiber filters resulting in a very high background. Modifications have been developed to circumvent this problem. One method developed by Hou et al [29] modifies the cysteine with CAM solution (see materials and methods) prior to TCA precipitation. Although this procedure eliminates the background issues, it is probably not 100% efficient in the detection of [^{35}S] cysteine incorporated into protein. A comparison between Figure 3.4A (actual stain) and Figure 3.4B (autoradiogram) suggests the aminoacylation is reasonably efficient compared to the ~10% aminoacylation obtained from the TCA assay. In separate CTA experiments the efficiency was as high as 36% (data not shown). This data is comparable with the data from personal communications with Dr. Y-M Hou where the efficiency of

aminoacylation is reported to be around 20-36%.

These results suggest that the transcription reaction does not generate 100% full-length $tRNA^{cys}$ or some portion is not folded correctly. In addition, T7 polymerase is known to prematurely terminate transcription or to add untemplated nucleotides to the 3' end of the transcript [125] which would adversely affect the aminoacylation of the transcribed tRNA by damaging the CCA end critical for aminoacylation. Methods to improve fidelity of the 3' end formation may increase the efficiency of aminoacylation.

Purification of cysteinyl-$tRNA^{cys}$. The CTA reaction is a convenient method for preparation of aminoacylated tRNA. However, the unincorporated nucleotides, cysteine and cysteinyl tRNA synthetase need to be removed prior to attachment of any reactive groups to the cys-$tRNA^{cys}$. It is particularly important to remove the unincorporated cysteine and cysteinyl-tRNA synthetase (CysRS), (contains five cysteine residues) to prevent labeling of the synthetase or free cysteine by the modifying agents (biotin or gold nanoparticles) which will reduce the yield of labeled tRNA.

The cysteinyl synthetase has a 6X histidine tag for purification, issued to remove the synthetase, and is removed batchwise from the CTA reaction by incubation with Ni-resin. The supernatant from the Ni resin is applied to Sephadex G25 spin-columns to remove unincorporated nucleotides and cysteine. The flow through is collected, pooled and lyophilized.

Modification of the cysteinyl-tRNA with biotin. The next step is to demonstrate that the tRNA prepared using the CTA method may be further modified and functionalized in translation reactions. The cys-$tRNA^{cys}$ was coupled to a biotinylated linker [N-

iodoacetyl-N-biotinhexylenediamine] (ILCB) to make a biotin modified cys-tRNA^{cys} (ILCB·[^{35}S]cys-tRNA^{cys}). The iodoacetyl linkage was chosen for its reactivity to the SH group of cysteine, which yields a thioether that is stable in the reducing environment of the translation reaction. Excess ILCB reagent was removed by Sephadex G25 spin-columns and the flow through lyophilized.

Degradation or loss of [^{35}S] cysteine from the tRNA during the coupling process was not detected (compare lanes 1 and 2 in Figure 3.4D). These results suggest that the modified cysteinyl-tRNA^{cys} is stable over a reasonable time frame for purification.

In Vitro **Translation with [^{35}S]cys-tRNA^{cys} and ILCB·[^{35}S]cys-tRNA^{cys}.** To determine if [^{35}S]cys-tRNA^{cys} and ILCB·[^{35}S]cys-tRNA^{cys} were able to function in protein synthesis, a template for green fluorescent protein (GFP- containing 2 cysteine residues) was used in a commercial coupled transcription-translation reaction (see Figure 3.5). This system omits exogenous cysteine and should be dependent upon the addition of cysteine to the system in the form of cysteine, [^{35}S]cys-tRNA^{cys} or ILCB·[^{35}S]cys-tRNA^{cys}. Any incorporation of [^{35}S] cysteine into GFP should have been provided by the [^{35}S]cys-tRNA^{cys} and ILCB·[^{35}S]cys-tRNA^{cys}. However, it is expected that some free cysteine will arise from degradation of proteins in the S-30 extract. The incorporation was monitored by SDS-PAGE and autoradiography. As shown in Figure 3.5A [^{35}S] cysteine was incorporated into GFP from the [^{35}S]cys-tRNA^{cys} and depended upon the addition of the DNA template. Similar experiments with the ILCB·[^{35}S]cys-tRNA^{cys} are shown in Figure 3.5B. [^{35}S] cysteine was incorporated into GFP from the ILCP·[^{35}S]cys-tRNA^{cys} and depended upon the addition of DNA template. Lastly, the

incorporation of ILCB·cysteine into GFP was monitored by detection of the biotin with streptavidin HRP (Figure 3.5B, second panel, lane 3).

These results show that the tRNAs synthesized by the CTA method are functional in *in vitro* translation assays and as expected, biotinylation did not affect the ability of the tRNA to function.

Modification of the cysteinyl-tRNA^{cys} with gold nanoparticles.

The tRNA synthesized using the CTA method was functional in a translation mixture and could be modified with ICLB (biotin) that also functions in *in vitro* translation. The next step was to modify the cysteinyl-tRNA^{cys} produced in CTA with an inorganic nanomaterial and determining if can function in translation.

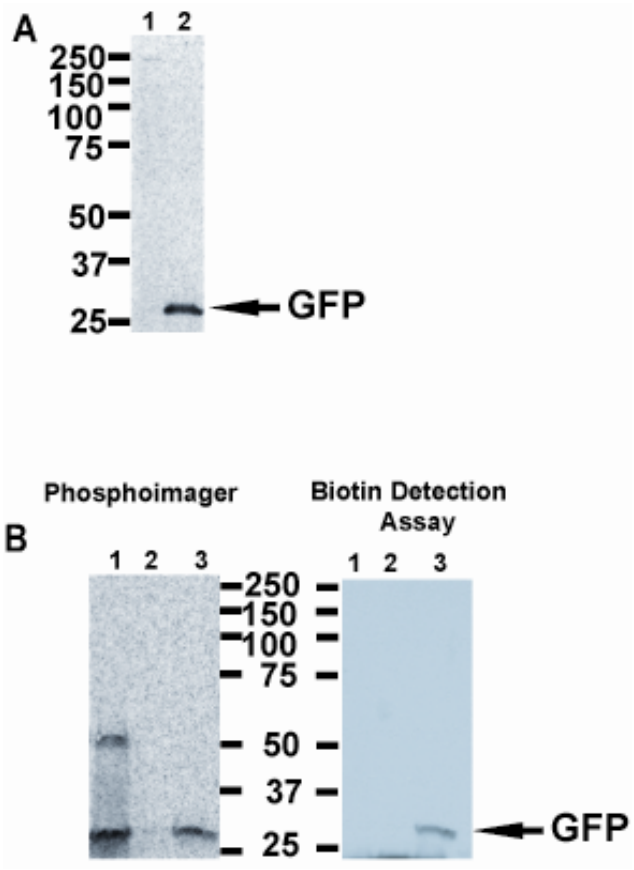

Figure 3.5. ***In vitro*** **translation using tRNAs synthesized by CTA.**

A. Lane 1, translation mixture containing [^{35}S]cys-tRNA^{cys} minus GFP plasmid template; Lane 2, translation mixture containing [^{35}S]cys-tRNA^{cys} containing GFP plasmid template (4 μg); [^{35}S]cysteine incorporation into GFP was visualized with a phosphorimager. **B.** In both panels: Lane 1, translation mixture containing [^{35}S]cys-tRNA^{cys} and GFP plasmid template (4 μg); Lane 2, translation mixture containing ILCB·[^{35}S]cys-tRNA^{cys} minus GFP plasmid template; Lane 3, translation mixture containing ILCB·[^{35}S]cys-tRNA^{cys} and GFP plasmid template (4 μg). The phosphorimager shows the [^{35}S] cysteine incorporated into GFP. The biotin detection assay shows incorporation of ILCB·[^{35}S]cysteine into GFP.

.

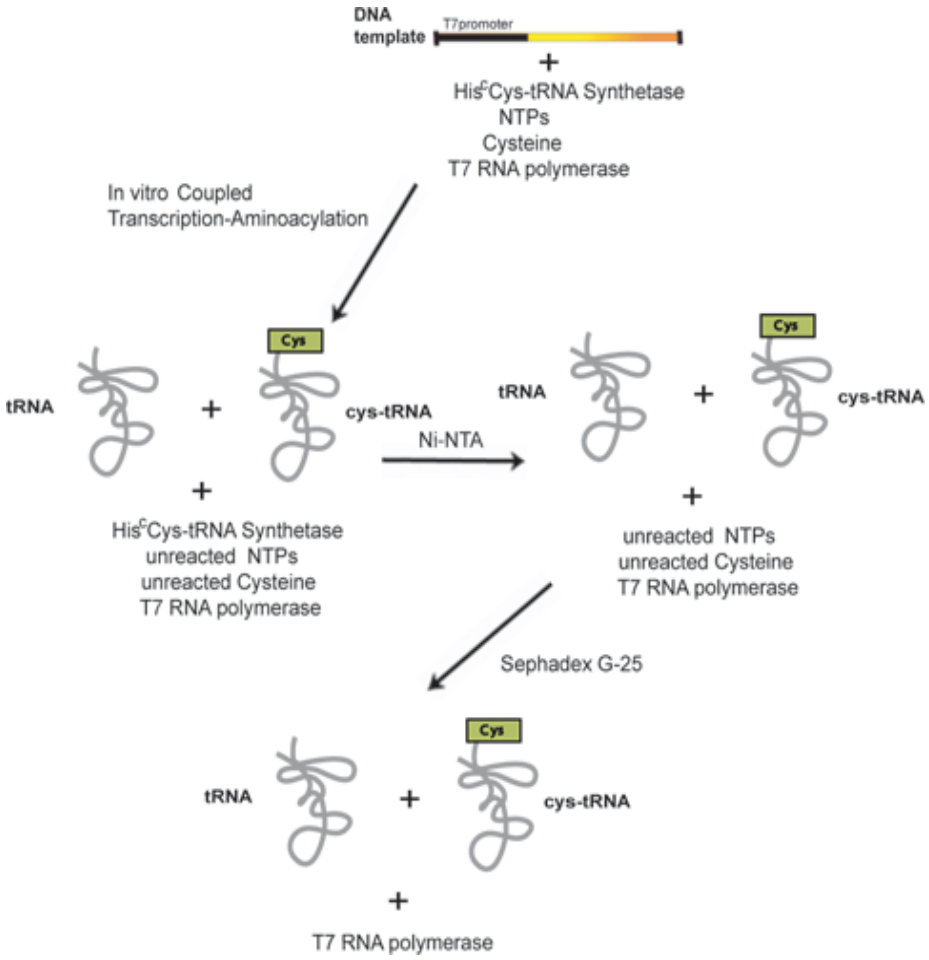

Figure 3.6. Scheme for purifying the cys-tRNA^{cys}.

The ideal nanoparticle for attachment to the cysteinyl-tRNA^{cys} must have two key features. 1) It is very important to have just one possible reactive site on the surface of nanoparticle in order to limit the number of tRNA molecules reacting with the nanoparticle and 2) the nanoparticles must fit within the size parameters of what is

estimated the ribosome will tolerate (~2 nm). A gold nanoparticle that has a single reactive monomaleimido group on the surface that will react with sulfhydryl groups is commercially available from Nanoprobes. This type of gold monomaleimido nanoparticle, have been used extensively for labeling different biological substrates.[72, 113, 123, 124] These nanoparticles have a narrow size distribution, with an average diameter of 1.4 nm and are capped with triphenyl phosphines or halide ions and yet remain uncharged. This nanoparticle has the appropriate properties to test the idea of ribosome assembly of a nanoparticle attached to an amino acid.

The cys-tRNA^{cys} prepared by CTA was modified with 1.4 nm gold monomaleimido nanoparticle. To determine if the attachment of the gold nanoparticles to cysteinyl-tRNA was successful, several analytical methods were employed including electrophoresis, Laser Ablation-Inductively Coupled Plasma-Mass Spectrometry (LA-ICP-MS) and High Angle Annular Dark Field (HAADF) techniques.

Electrophoresis of Au•cys-tRNA^{cys}. Surprisingly, electrophoresis results show no apparent change in mobility for the gold nanoparticle modified cys-tRNA^{cys} (Au•cys-tRNA^{cys}) compared to unmodified cys-tRNA^{cys} (see Figure 3.7A). The gold nanoparticles used are uncharged (manufacturer specifications) and the average size of the gold nanoparticles (1.4 nm) is relatively small compared to the length of a tRNA (~7.5 nm, see inset in Figure 3.1). The lack of charge and the small size of the gold nanoparticle compared to the negative charge of the tRNA could account for the lack of change in mobility.

To test the charge of the gold nanoparticles, different amounts of un-reacted

nanoparticles (gold nanoparticles were dissolved in water and loading dye) were loaded on SDS-PAGE or denaturing urea/acrylamide gels and subjected to electrophoretic current. No mobility of the nanoparticles was observed, regardless of the polarity of current applied (data not shown).

Laser Ablation-Inductively Coupled Plasma-Mass Spectrometry (LA-ICP-MS). La-ICP-MS introduced in the late '80, is one of the most commonly used techniques for sensitive multi- and/or single-element determination at trace levels. Starting as a tool for determination of trace elements in geology, LA-ICP-MS (for solid samples) and ICP-MS (for liquid samples) are now used as an analytical technique in biology, for example for medical sampling of trace elements in blood, urine and tissues.[126, 127] LA-ICP-MS is also used in material science, nuclear and radioactive waste monitoring.[126, 127] The laser (Light Amplification by Stimulated Emission of Radiation) used for ablation of the gold containing solid sample is a New wave Research LUV 213 which has a neodymium-doped yttrium aluminium garnet (Nd:YAG) laser source that produces a 200 mJ beam of Infra Red (IR) laser light at 1064 nm. The laser beam is polarized and then passes through a series of harmonic resonators resulting in a final beam of up to 5 mJ of 213 nm ultraviolet (UV) light. The spot size (5-400 μm range) used for all these experiment was 400 μm. When the laser ablates the samples several process take place on the sample surface including melting, vaporization or ablation (which can be varied by adjusting the power density), followed by atomization and ionization, and the formation of a plasma near the sample surface which contains sample components. The laser-generated plasma interacts with the sample and causes further ionization.

The helium or argon carrier gas transports the atoms, ions, molecules and particles to the ICP-MS, where they are ionized in the plasma. Once drawn inside the ICP-MS, the beam of ions is carried into a hexapole collision cell (containing hydrogen and helium gases). Collisions with gas molecules in the hexapole thermalize the ion beam generating a beam with a smaller spread in kinetic energies. The quadrupole mass filter rapidly switches setting to allow selected elements into the detector based on their mass to charge ratio and the detector records the number of ions entering per time period acquiring data in counts per second (CPS) of each element.[126-129]

Laser Ablation ICP-MS of Au•cys-tRNA^{cys}. The Laser Ablation-Inductively Coupled Plasma-Mass Spectrometry (LA-ICP-MS) method may be used to detect gold and other elements. This method is largely used for analysis of geological samples to detect various elements, but has been used in the analysis of selenium modified proteins.[130-136]

The Au•cys-tRNA^{cys} was separated on a urea gel, stained and dried between thin sheets of cellulose. The region corresponding to the Au•cys-tRNA^{cys} was cut out and placed on a glass slide for the LA-ICP-MS analysis. Briefly, the laser beam moves in a straight line (transects) through the region of the gel containing the Au•cys-tRNA^{cys}. The gel material containing the Au•cys-tRNA^{cys} is vaporized and any Au released is detected and recorded by the instrument. Using this method, the LA-ICP-MS analysis confirms that ^{197}Au is present in the Au•cys-tRNA^{cys} (see Figure 3.7B, panel a). A series of control experiments shows that Au was not present in any area except that corresponding to the Au•cys-tRNA^{cys} (see Figure 3.7B, p anels b-e).

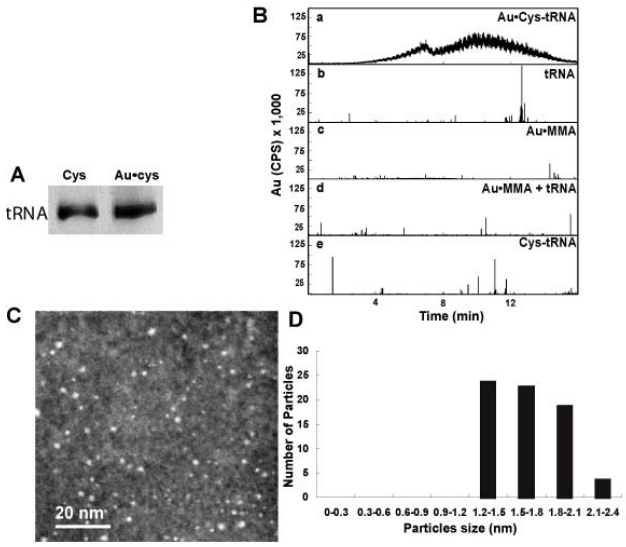

Figure 3.7. Attachment of Monomaleimido gold nanoparticles (Au-MMA) to cysteinyl-tRNA^{cys}. Urea Gel Analysis of tRNA.

Aliquots of 9 µg of cys-tRNA^{cys} (cys) and Au•cys-tRNA^{cys} (Au•cys) were mixed with an equal amount of 10X urea-gel dye. The samples were separated on a 6% urea acrylamide gel. The tRNA was visualized with 0.1% Stains-All (Sigma) and the gel dried. **B**. LA-ICP-MS detection of ^{197}Au in tRNA. The presence of ^{197}Au in the modified tRNA and control samples was measured by laser ablation-ICP-MS (LA-ICP-MS) of a dried urea gel. Each lane was cut in strips of 3.0 cm from the dried gel and mounted on a glass slide. The glass slide and gel were placed in the ablation chamber and purged with He. Gold was monitored by the ICP-MS as the laser traversed down the center of the lane. Panel a, 9 µg of gold nanoparticle modified cysteinyl-tRNA^{cys} (Au•cys-tRNA); Panel b, 9µg tRNA^{cys} (not aminoacylated); Panel c, 9µg monomaleimido gold nanoparticles (Au-MMA); Panel d, 18 µg monomaleimido gold nanoparticles (Au-MMA) and 9 µg tRNA^{cys} (not aminoacylated); Panel e, 9 cysteinyl-tRNA^{cys} (cys-tRNA). Panels b-e, are controls to demonstrate that the gold counts observed in panel a are from Au•cys-tRNA^{cys} (see broad peak at 10 min). The very narrow areas of elevated counts ("spikes") in the control traces (panels b-e) do not represent gold from a band in the gel but rather represent single particles entrained in the He carrier flow that were displaced from the wall of the ablation cell or tubing. Similar spikes were seen in blanks of Helium passed through the ablation cell and tubing with the laser turned off. In the tRNA^{cys} (panel b) and cysteinyl-tRNA^{cys} (panel e) samples, no gold peaks were observed as expected. The Au-MMA nanoparticles alone do not give any counts for ^{197}Au in the area of the tRNA (panel c). A reaction between the Au-MMA nanoparticles and the non-aminoacylated tRNA^{cys} (panel d) also gave a flat background demonstrating that the Au-MMA cannot label the tRNA in absence of cysteine aminoacylation. **C.** High Angle Annular Dark Field image of Au•cys-tRNA^{cys}. 3 µL of Au•cysRNA^{cys} was placed on a copper grid coated with a thin, continuous carbon film. **D.** Particle size distribution histogram. The size distribution was calculated for 70 particles picked randomly from the HAADF image shown in Panel C. (See appendix for larger image.)

These results demonstrate that the gold nanoparticles are chemically attached to the side chain of the cysteine, and non-specific binding between the gold nanoparticles and the $tRNA^{cys}$ did not occur.

Transmission electron microscopy of Au•cys-$tRNA^{cys}$. To visualize the gold nanoparticle modified cys-$tRNA^{cys}$, a transmission electron microscope (TEM) in scanning mode using the HAADF detector was employed. The HAADF technique, also known as Z-contrast, is a straightforward approach to visualize nanoparticles in biological systems.[83, 137-140] In this dark field technique, the images are formed using electrons scattered at high angles due to Rutherford-like scattering. As a result, the image contrast depends on the atomic number (Z) of the visualized elements while the intensity varies as $\sim Z^2$. In this case, the difference in atomic number between the gold nanoparticles and the protein (which is mainly composed of carbon), is high enough to produce an excellent contrast.[83] Based on the HAADF images, the particles were shown to have a narrow size distribution (see Figure 3.7C) and from the profile data they were spherical (not shown). The size distribution was between 1.2 nm and 2.1 nm (standard deviation 0.2 nm) for the 70 particles randomly picked (see Figure 3.7D). From all the data collected one can conclude, that the gold nanoparticle was successfully attached to SH-group of cysteinyl-tRNA and inorganic nanomaterial modified aminoacyl-tRNA (InAA-tRNA) was synthesized.

Optimization of *In vitro* translation using Au•cys-$tRNA^{cys}$. The ability of the Au•cys-$tRNA^{cys}$ to be used in polypeptide synthesis was measured using an *E. coli* S30 coupled transcription-translation system (Promega) with a template for green fluorescent

protein (GFP).

Previous experiments with the lysine system indicated that *E. coli S30* translation system was not inhibited by gold nanoparticles. However, the presence of dithiothreitol (DTT) in the translation mixture is a problem for the stability of the gold nanoparticles. The DTT exchanges the tri-(aryl) phosphine capping agent present on the surface of the gold nanoparticles. Thus, the gold is cleaved off and the tRNAs remain unmodified in the presence of DTT/BME. The DTT is required to be present in the *in vitro* translation reactions, because it keeps the proteins from the S30 mixture active by preventing oxidation and/or the formation of disulphide bonds. It was necessary to develop a method to scavenge the excess DTT which was detrimental to the gold modified cys-$tRNA^{cys}$. These steps were generally omitted to prevent any untoward damage to the gold nanoparticles. Comparison of the LA-ICP-MS of lanes 2 and 3, in Figure 3.8C shows that DTT and heating are detrimental to the gold nanoparticle.

One solution tried, was to incubate the S-30 translation mixture containing 1 mM DTT with an excess of hydrolyzed gold nanoparticles. The gold nanoparticles were kept in water for one week, the manufacturer specification indicate that the maleimide groups are hydrolyzed in few hours aqueous solution. The coupled transcription-translation reactions included an incubation of reaction mixture with the hydrolyzed gold nanoparticles for 15 minutes before the template was added to start the coupled transcription-translation reaction. The reactions were analyzed by SDS-PAGE gels and LA-ICP-MS. The LA-ICP-MS on dried 10-20% Tri-Glycine SDS-PAGE gels were inconclusive. The presence of a shoulder of ^{197}Au in the area of GFP suggested that

the gold modified GFP was synthesized but the signal was sufficiently low to be inconclusive.

The gold detection was hindered by the excessive amount of organic matter ablated and carried to the plasma. The acrylamide gels containing the gold modified GFP was dried between layers of cellophane. To reduce the amount of organic material, the proteins in the gel were transferred electrophoretically to a PVDF (polyvinylidene fluoride) membrane to improve ^{197}Au detection (see Figure 3.8). PVDF is a thin material that when ablated by the laser creates less organic matter to be burned in the ICP-MS torch and creates less interference in the gold detection by the ICP-MS.

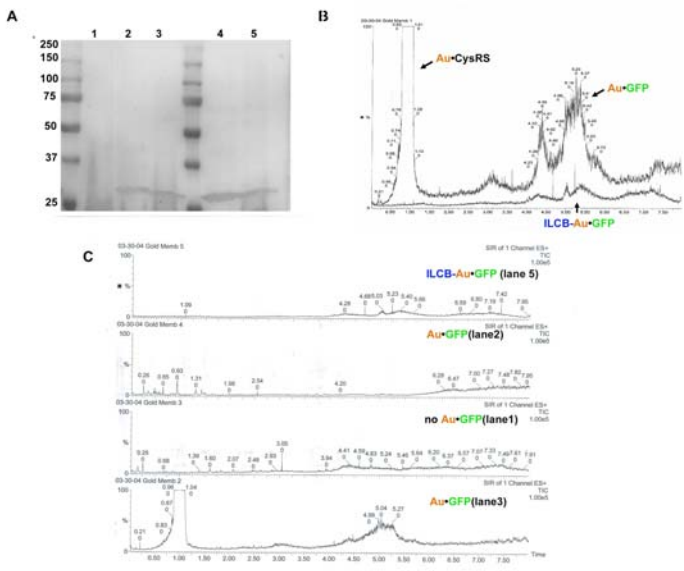

Figure 3.8. ***In vitro*** **translation using gold nanoparticle modified cys-tRNA^{cys} (Au•cys-tRNA^{cys}) and an excess of hydrolyzed Au nanoparticles.**

A. Detection of green fluorescent protein (GFP) in an *E. coli* coupled transcription-translation system (Promega) using a plasmid template encoding the gene for GFP. The GFP template used contained a strep tag at the C-terminus which is detected by streptavidin -HRP. TMB colorimetric substrate was used to visualize the GFP. **Lane 1**, 7.5 µL of the translation mixture containing Au•cys-tRNA^{cys} minus template; **Lane 2**, 7.5 µL of the translation mixture containing Au•cys-tRNA^{cys} plus template (4 µg); **Lane 3**, 7.5 µL of the translation mixture containing Au•cys-tRNA^{cys} plus template (4 µg), but no DTT was added to the loading buffer and the sample was not heated prior to loading on the gel; **Lane 4**, 7.5 µL of the translation mixture containing ILCB-cys-tRNA^{cys} and Au•cys-tRNA^{cys} plus template (4 µg); **Lane 5**, 7.5 µL of the translation mixture containing ILCB-cys-tRNA^{cys} and Au•cys-tRNA^{cys} plus template (4 µg), but no DTT was added to the loading buffer and the sample was not heated previously to be loaded on the gel. The samples were separated on a Novex 10-20% Tris–Glycine gel (Invitrogen) and transferred to a PVDF membrane. **B.** Detection of incorporation of ^{197}Au into protein. LA-ICP-MS was used to detect Au in the region of the PVDF membrane where GFP was detected (Lanes 3 and 5). Lanes 3 and 5 from the membrane shown in panel A were cut in strips (4 cm long and 0.9 cm width) and mounted on a glass slide. The glass slide and gel were placed in the ablation chamber and purged with He. Gold was monitored by the ICP-MS as the laser traversed down the center of the lane. Lane 3 shows significant gold counts in the region where the GFP was detected meanwhile in Lane 5 shows less detection of Au in the same region. **C.** Detection of incorporation of ^{197}Au into protein. LA-ICP-MS was used to detect Au in the region of the PVDF membrane where GFP was detected (Lanes 1, 2, 3 and 5). Lanes from the membrane shown in panel A were cut in strips (4 cm long and 0.9 cm width) and mounted on a glass slide. Lanes 1 and 2 shows significant less gold counts in the region where the GFP compared to Lane 3 or 5. (See appendix for larger image.)

The *in vitro* translation experiment shown in Fig. 2.16 was carried out with excess hydrolyzed gold particles to scavenge up any excess DTT and prevent degradation of the Au•cys-tRNA^{cys}. The reactions were separated by gel electrophoresis and transferred to PVDF membrane for LA-ICP-MS analysis. The LA-ICP-MS data clearly shows that Au•cysteine residues were incorporated into the GFP protein (see Figure 3.8B). The laser was traversed down the center of the lanes (3 or 5) generating a ^{197}Au peak only in the region where GFP (~30 kDA) would migrate.

An "isotope dilution" effect is seen in the difference in the amount of Au•cysteine detected in lanes 3 and lane 5. For lane 3, the only source for cysteine in the translation mixture is Au•cys-tRNA^{cys} (3 nmols) whereas, in lane 5 equal amounts of Au•Cys-tRNA^{cys} (1.5 nmols) and ILCB-cys-tRNA^{cys} (1.5 nmols) were added. The amount of Au•cysteine residues incorporated into GFP was reduced considerably if non-gold modified tRNA is included in the translation mixture. This experiment showed that an excess of gold particles could protect from degradation of DTT in the reaction mixture and that using PVDF for LA-ICP-MS analysis of the proteins vastly improved the detection of gold.

Further refinement of the *in vitro* translation was necessary to insure that the gold modified cysteine residues visualized in the LA-ICP-MS were present due to the fact the Au•cys-tRNA^{cys} was incorporated through the ribosome and not because the gold was attached post-translationally. The excess hydrolyzed gold nanoparticles could have been a source of post-translational labeling; however, this possibility is very unlikely since gold was only detected in the region of the GFP. The position of the GFP was

estimated from knowledge of the length and width of the PVDF membrane strips relative to the position of GFP on the PVDF based on visualization of the ^{14}C-leucine incorporated. Using the scanning rate of the laser the position of the ^{197}Au-GFP peak was predicted. The PVDF strips (40 mm long and 9 mm width) were scanned by the laser at approximately 4.8 mm/min. The GFP is present approximately 25mm from the top of the strip which correlates to the 5 minute mark in the scan. From Figure 3.8B, we can conclude that the ^{197}Au peak appears in the region where the GFP is present (~5.25 min).

Had post-translational labeling by the excess gold taken place, the gold would have been present throughout the gel since the translation mixture is an extract of *E. coli* proteins. The concentration of the gold at the point in the gel where GFP should migrate strongly suggests the gold was incorporated by the ribosome. The only other ^{197}Au peak present in the LA-ICP-MS spectrum was from the traces of cysteinyl–tRNA synthetase, which was not completely removed from the system using a Ni-NTA affinity matrix (see Figure 3.8). The CysRS has five cysteine residues that are labeled with gold nanoparticles if no completely removed from the CTA reaction (Figure 3.8).

To improve the efficiency of incorporation of Au•cys and to remove the need for hydrolyzed gold nanoparticles to scavenge excess DTT (1 mM), a large excess of Au•cys-tRNA^{cys} (4-8 nM) was added to the reaction mixture. Even if some of the Au•cys-tRNA^{cys} was degraded by the excess DTT, a sufficient molar excess of the Au•cys-tRNA^{cys} was still present for translation

These reactions were analyzed by SDS-PAGE and transferred to a PVDF

membrane for LA-ICP-MS analysis[135] (see Figure 3.9A). The LA-ICP-MS data shows that Au•cysteine residues were incorporated into the protein, producing a peak in the region where GFP migrates (see Figure 3.9B, lane 4, ~3 minutes). The control reaction contained Au•cys-tRNA^{cys} and omitted plasmid template. The absence of the gold peak (see Figure 3.9B, lane 3) in the control reaction demonstrates that the template is required for the assembly of Au•cys into the protein and cannot be added post-translationally, otherwise gold would be detected throughout the gel attached to other proteins.

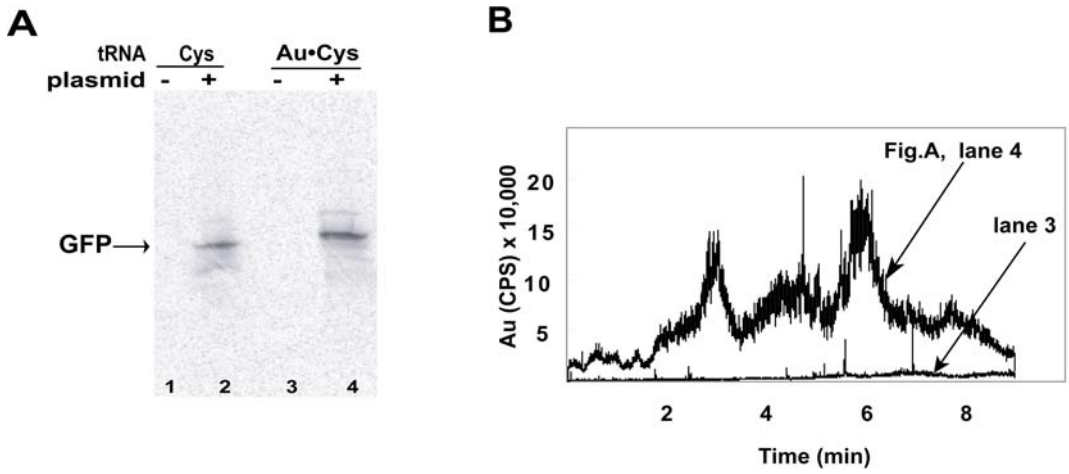

Figure 3.9. ***In vitro*** **translation using gold nanoparticle modified cys-tRNA^{cys} (Au•cys-tRNA^{cys}).**

A. Incorporation of [^{14}C]-leucine into green fluorescent protein (GFP) in an *E. coli* coupled transcription-translation system (Promega) using a plasmid template encoding the gene for GFP. **Lane 1**, 7.5 μL of the translation mixture containing cys-tRNA^{cys} (cys) minus template; **Lane 2**, 7.5 μL of the translation mixture containing cys-tRNA^{cys} (cys) plus template (4 μg); **Lane 3**, 7.5 μL of the translation mixture containing Au•cys-tRNA^{cys} minus template; **Lane 4**, 7.5 μL of the translation mixture containing Au•cys-tRNA^{cys} plus template (4 μg). The samples were separated on a Novex 10-20% Tris–Glycine gel (Invitrogen) and transferred to a PVDF membrane.[^{14}C]-leucine incorporation into GFP was visualized by a phosphorimager. The incorporation of [^{14}C]-leucine into trichloroacetic acid precipitable material was used to estimate the amount of protein synthesized (~78 pmol/μL). **B.** Detection of incorporation of ^{197}Au into protein. LA-ICP-MS was used to detect Au in the region of the PVDF membrane where [^{14}C]-labeled GFP was detected (Lane 4). Lanes 3 and 4 from the membrane shown in panel A were cut into strips (4.3 cm long and 1.2 cm width) and mounted on a glass slide. The glass slide and gel were placed in the ablation chamber and purged with He. Goldwas monitored by the ICP-MS as the laser traversed down the center of the lane.Lane 4 shows significant gold counts in the region where the [^{14}C]-labeled GFP was detected. Lane 3 shows little detection of Au in the same region.

These data strongly suggest that the Au•cys-tRNA^{cys} must enter and be used by the ribosome to assemble the polypeptide.

Fluorescence Analysis of Au•GFP. The presence of functional GFP was detected by fluorescence spectroscopy. As shown in Figure 3.10 emission spectra depend on the addition of the GFP encoding template (see spectra **1** and **3**) and cysteine (see spectra **1** and **2**). Comparing the spectra **1** and **2,** free cysteine is clearly present at some level in the S30 translation mixture which is incorporated into the GFP. The free cysteine present in the system is generated from protein degradation in the S-30 extract. However, these results suggest that the amount of GFP obtained increased in the presence of the Au•cys-tRNA^{cys} and therefore at least one of the cysteine residues in the GFP most likely contains a gold nanoparticle. Improving the dependence of the translation system on exogenous cysteine would insure complete incorporation of the Au•cysteine at all the cysteine sites.

At this point, no definitive statement can be made about the fluorescence of Au-GFP. The problem is the presence of a mixed population of GFP (unlabeled from the free cysteine) and gold modified GFP in the final translation mixture. The only way to know if the Au-GFP is fluorescent is to incorporate the gold modified cysteine residue using a suppressor tRNA as the only source of gold.

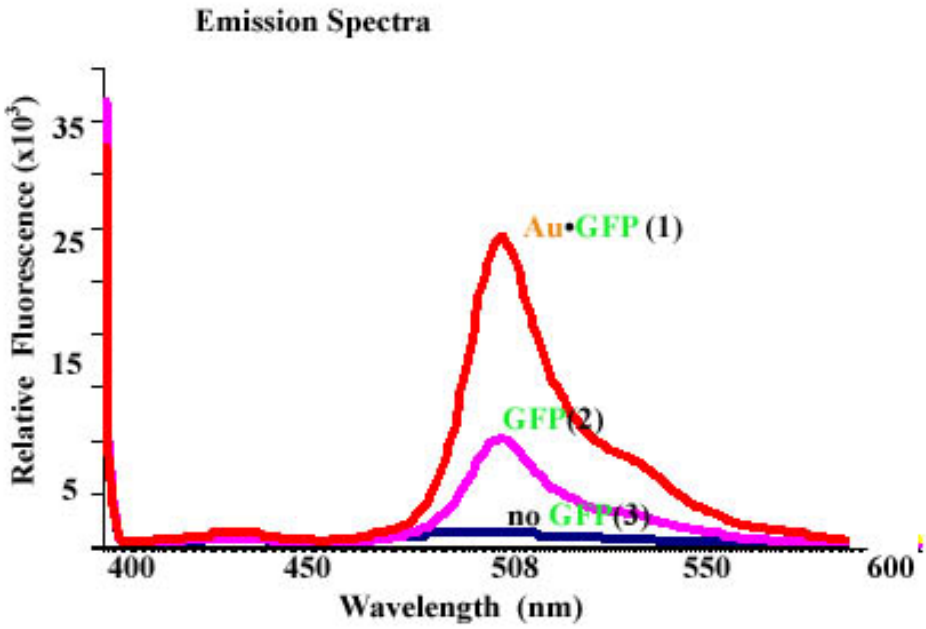

Figure 3.10. GFP emission spectra. Fluorescent data were collected for 50 µL aliquots of: **(1)** the translation mixture containing Au•cys-tRNA^{cys} plus template (4 µg); **(2)** the translation mixture containing the GFP encoding template but no cysteine was added to the reaction mixture; **(3)** the translation mixture containing Au•cys-tRNA^{cys} minus template.

Transmission Electron Microscopy of Au-GFP. The High Angle Annular Dark Field (HAADF) technique was used to visualize the gold nanoparticles and determine if they were in the same region as the protein. To obtain better results with the TEM, it was necessary to remove excess organic material (*i.e*, protein from the S30 extract). The GFP template used encodes a Strep-tag (Trp-Ser-His-Pro-Gln-Phe-Glu-Lys) on the C-terminus that binds biotin. The Strep-tag provided a method to affinity purify the Au•GFP using Strep-Tactin beads (IBA).

Translation reactions containing Au•cys-tRNA^{cys} and [^{14}C]-leucine. The [^{14}C]-leucine was used to monitor translation and the affinity purification process. The protein eluted from the Strep-Tactin beads (see protocol in Materials and Methods) was analyzed by SDS PAGE (see Figure 3.11). As shown in Figure 3.11B, [^{14}C] leucine was incorporated into GFP and depended upon the addition of the GFP encoding template. The [^{14}C] leucine incorporation also shows that the Step-Tactin bead can be used successfully to purify the gold modified GFP but some degradation was detected in the elution fraction (see Figure 3.11B lane 8).

The HAADF image and Energy Dispersive Spectroscopy (EDS) analysis showed that gold nanoparticles were present in the same region as protein aggregates (see Figure 3.9A). A processed HAADF image, masking the noise caused by the organic background, visualizes the nanoparticles more distinctly (see Figure 3.9B).

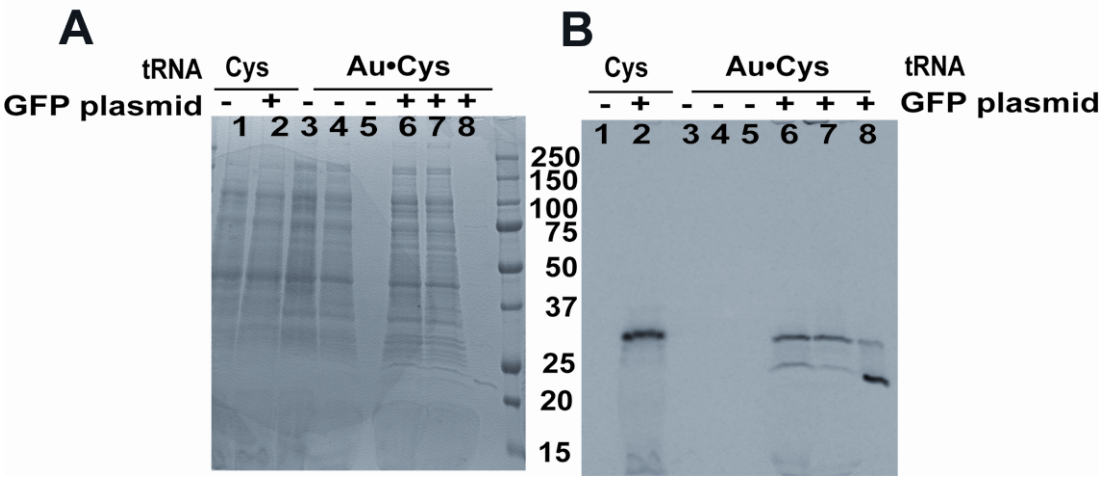

Figure 3.11. ***In vitro*** **translation using gold nanoparticle modified cys-tRNA^{cys} (Au•cys-tRNA^{cys}) which was affinity purified Step-Tactin beads.**

A. The Coomassie stain of *E. coli* S30 coupled transcription-translation system (Promega) using a plasmid template encoding the gene for GFP. **Lane 1**, 7.5 μL of the translation mixture containing cys-tRNA^{cys} (cys) minus template; **Lane 2**, 7.5 μL of the translation mixture containing cys-tRNA^{cys} (cys) plus template (4 μg); **Lane 3**, 7.5 μL of the translation mixture containing Au•cys-tRNA^{cys} minus template-supernatant ; **Lane 4**, 7.5 μL of the translation mixture containing Au•cys-tRNA^{cys} minus template-wash ; **Lane 5**, 7.5 μL of the translation mixture containing Au•cys-tRNA^{cys} minus template-elution; **Lane 6**, 7.5 μL of the translation mixture containing Au•cys-tRNA^{cys} plus template (4 μg)-supernatant; **Lane 7**, 7.5 μL of the translation mixture containing Au•cys-tRNA^{cys} plus template (4 μg)-wash; **Lane 8**, 7.5 μL of the translation mixture containing Au•cys-tRNA^{cys} plus template (4 μg)-elution . **B**. Incorporation of [^{14}C]-leucine into green fluorescent protein (GFP) for the gel from panel A.[^{14}C]-leucine incorporation into GFP was visualized by a phosphorimager.

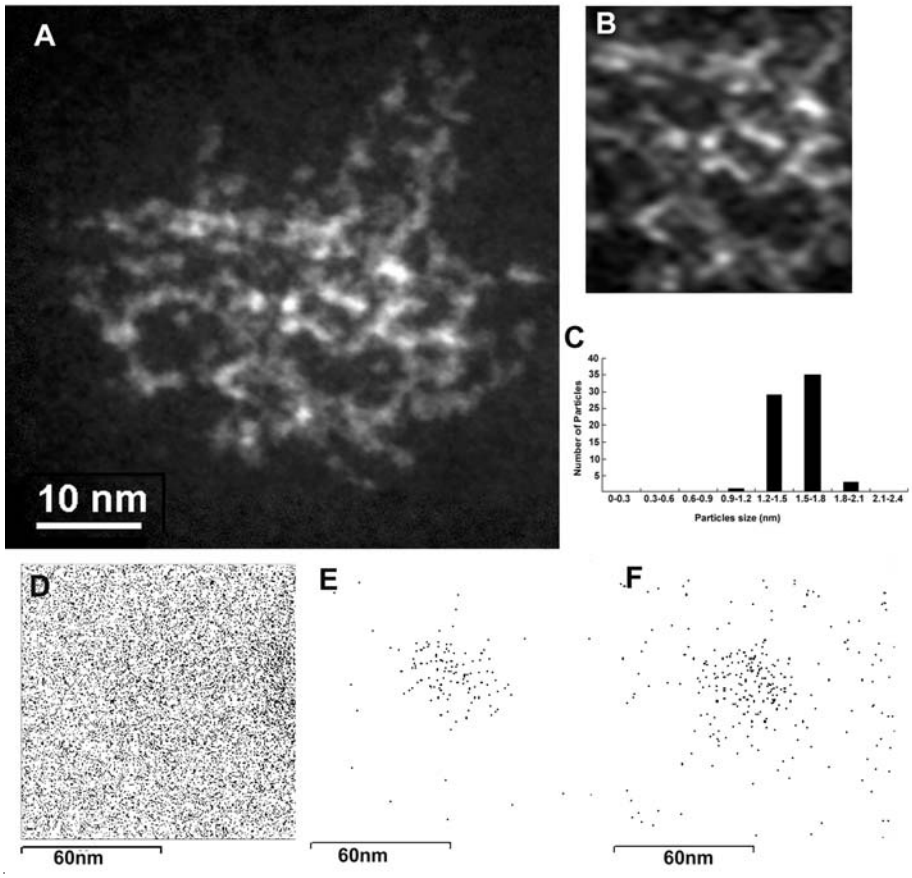

Figure 3.12. Visualization of Au-labeled protein synthesized by *in vitro* translation.

The GFP template used contained a strep tag at the C-terminus. The strep tag was used to affinity purify (Strep-tactin, IBA) the *in vitro* translated Au-labeled GFP from the *E. coli* extract. The affinity purified protein (5 μL) was placed on a copper grid coated with a continuous carbon film. **A.** HAADF image of Au·GFP. **B.** HAADF image from panel A was processed by masking the noise produced by the organic background in the Fourier Transform of the image in Panel A. **C.** Particle size distribution histogram for Au•GFP in panel A. The size distribution was calculated for 70 particles picked randomly from the HAADF image. **D.** Energy Dispersive Spectroscopy (EDS) mapping for carbon. **E.** EDS mapping for Au. **F.** EDS mapping for S.

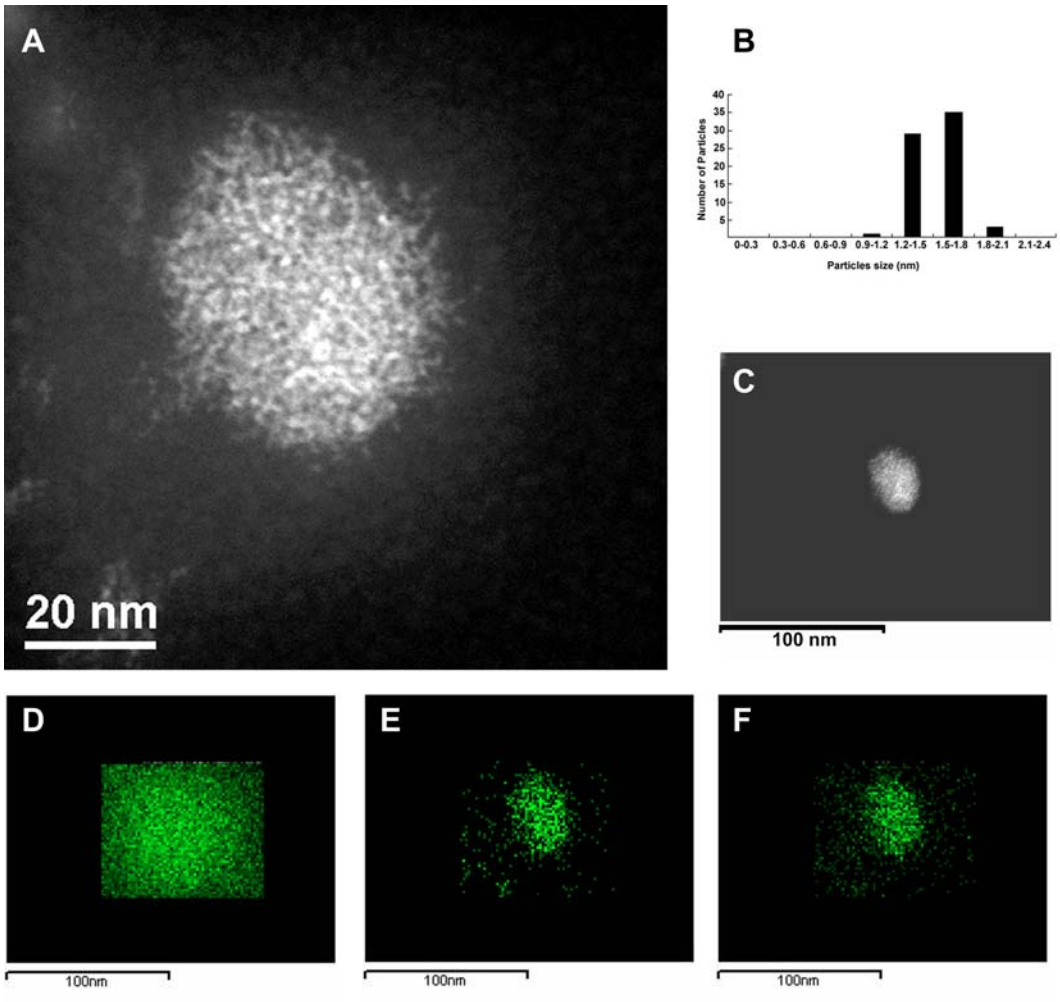

Figure 3.13. Visualization of Au-labeled protein synthesized by *in vitro* translation.

The same affinity purified sample from Figure 3.9 but placed on a grid after 2 months of storage at -80^{0}C. The affinity purified protein (5 μL) was placed on a copper grid coated with a continuous carbon film. **A.** HAADF image of Au•GFP. **B.** Particle size distribution histogram for Au•GFP in panel A. The size distribution was calculated for 70 particles picked randomly from the HAADF imagE. c **.** HAADF image from panel A at higher magnification. **D.** Energy Dispersive Spectroscopy (EDS) mapping for carbon. **E.** EDS mapping for Au. **F.** EDS mapping for S.
From the size distribution histogram, one can conclude that particles with diameters

within the range 1.2 -1.8 nm (standard deviation 0.2 nm), were incorporated into the polypeptide (see Figure 3.12. panel C). If the size distribution histograms from Figure 3.7D and Figure 3.12C are compared, it appears that the ribosome acts as a size exclusion machine, only particles less than 1.8 nm are present in the protein in contrast to the size range seen in the tRNA sample (see Figure 3.7).

Overlaying of the carbon (Figure 3.12D and 3.13D), gold (Figure 3.12E and 3.13E) and sulfur (Figure 3.12F and 3.13F) signals strongly suggests that the gold nanoparticles were present in the same region as the protein, entirely consistent with the gold nanoparticles being associated with the cysteine residues on the protein. The HAADF image (see Figure 3.13) suggests that the gold modified protein is stable in elution buffer (100 mM Tris-HCl, 150 mM NaCl, 1mM EDTA, 2.5 mM desthiobiotin, pH 8) in time at -80^0C. These results (LA-ICP-MS and HAADF analyses) confirm that the gold nanoparticles attached to cys-tRNA^{cys} were incorporated into the protein by the ribosome and the intact gold nanoparticles were subsequently observed with GFP after affinity purification to remove exogenous protein.

3.4. CONCLUSIONS:

The coupled transcription-aminoacylation (CTA) method was developed as a single step reaction, in which the tRNA is transcribed and aminoacylated in the same *in vitro* reaction mixture. This method is efficient and eliminates the need to purify the tRNA prior to aminoacylation. The ability of the tRNA to be aminoacylated by the synthetase suggest it must be correctly folded as it is transcribed to be recognized. Furthermore, the cys-tRNA^{cys} may be modified with easily detectable functional groups (*e.g.,* biotin) and still remain functional. Both [^{35}S]cys-tRNA^{cys} and ILCB-·[^{35}S]cys-tRNA^{cys} were successfully used to synthesize green fluorescent protein (GFP) in a coupled transcription-translation reaction (see Figure 3.5). No phenol extraction, ethanol precipitation, or reannealing steps were performed on the tRNA, allowing for an efficient "single pot" synthesis of aminoacylated tRNA.

Taking a step further, the *E. coli* cysteinyl-tRNA^{cys} prepared using the CTA method was modified with an inorganic nanomaterial to form a new class of unnatural cysteinyl-tRNA^{cys}. The inorganic nanomaterial used was monomaleimido nanogold which has a single maleimido group on the surface and is very reactive towards the sulfhydryl group present on the side chain of cysteine. This new class of gold nanoparticle modified cysteinyl-tRNA^{cys} was used successfully in a coupled transcription-translation reaction to synthesize gold modified green fluorescent proteins. To prove that the Au-cysteine residues were incorporated into proteins electrophoresis, LA-ICP-MS and HAADF techniques were used.

CHAPTER 4

CONCLUSION AND FUTURE WORK

4.1. CONCLUSIONS:

To address the question of whether nanoparticles attached to amino acids would be assembled by ribosomes into polypeptides, several experimental difficulties had to be overcome.

Can large quantities of aminoacyl-tRNA modified by inorganic nanomaterials be prepared?

One unexpected result of this work was the development of the coupled transcription-aminoacylation (CTA) method.[118] This method is a single step reaction, in which the tRNA is transcribed and aminoacylated in the same *in vitro* reaction mixture. This method is efficient and eliminates the need to purify the tRNA prior to aminoacylation. This method worked with both the lysine and cysteine systems. Recently CTA has been applied to Tyr-tRNA^{tyr} from *Methanococcus jannaschii* and the Trp-tRNA^{trp} from *Bacillus stearothermophilus* (Randy Hughes, personal communication). An interesting conclusion that may be drawn from the coupled system is that tRNA transcribed *in vitro* is folded correctly following transcription and does not require denaturation or reannealing prior to aminoacylation. This new method of preparation of aminoacyl-tRNA was published in Analytical Biochemistry.[118]

What is the best amino acid/synthetase pair to use? The lysyl-tRNA was initially chosen for its reactive epsilon amino group; however, problems with the activity

of the lysyl synthetase, the requirement for post-transcriptional modification of the tRNA for maximal activity, and the need for more detection of the amino acid required another amino acid system. The cysteinyl-tRNA system had the advantages of a robust synthetase, the tRNA did not require post-transcription modification and [^{35}S]-cysteine is easily detected. Further the reactive thiol group of cysteine may be modified with easily detectable functional groups (*e.g.,* biotin) and still remain functional. This system proved to be a robust method for the preparation of large amounts of cysteinyl-tRNA^{cys} that was modified with a biotin group (ILCB). Both [^{35}S]cys-tRNA^{cys} and ILCB-·[^{35}S]cys-tRNA^{cys} were successfully used to synthesize green fluorescent protein (GFP) in a coupled transcription-translation reaction (see Figure 3.5).

Can the aminoacylated tRNA be modified with a nanoparticle? The *E. coli* cysteinyl-tRNA^{cys} prepared using the CTA method was modified with an inorganic nanomaterial to form a new class of unnatural cysteinyl-tRNA^{cys}. The monomaleimido nanogold (~1.4 nm) has a single maleimido group on the surface and is very reactive towards the sulfhydryl group of cysteine. This new class of inorganically modified Au•cys-tRNA^{cys} is the first functional nanoparticle modified tRNA reported.

Can the Au modification be monitored? It was necessary to utilize new methods to detect the presence of the Au-nanoparticle on tRNA and incorporated into protein. A method for detection of metals in geological samples, laser ablation inductively coupled plasma mass spectrometry (LA-ICP-MS) was utilized to detect the presence of gold in tRNA and protein. The LA-ICP-MS method was very successful in proving the presence of gold in the modified tRNA and in *in vitro* translated protein. HAADF

was also utilized to visualize the gold particles in tRNA and protein samples and confirm their size distribution.

Can the ribosome use an inorganic modified aminoacyl-tRNA? The Au•cys-tRNA^{cys} was used in a coupled transcription-translation reaction to synthesize green fluorescent protein. Incorporation of the gold nanoparticle into protein was demonstrated using LA-ICP-MS and HAADF. The inorganic nanoparticles (1.4 nm) do not appear to block the protein exit tunnel (~ 1.5 nm). A comparison between the nanoparticles size distribution histograms for the tRNA (see Figure 3.7D) and synthesized protein (Figure 3.12B) suggests that the ribosome appears to size select the nanoparticles. The size distribution for gold nanoparticle modified cys-tRNA^{cys} was 1.2 to 2.1 nm meanwhile the size distribution of gold nanoparticle incorporated into the proteins was 1.2 to 1.8 nm. No particle bigger then 2 nm was translated through the ribosome.

This research proves that it is possible for the ribosome to be used as a nanomachine to assemble hybrid inorganic-polypeptide material. This will open the way for the creation of unique inorganic-biological materials that will have new properties, such as peptides that are conductive nanowires.

4.2. FUTURE DIRECTIONS:

The conclusion that the ribosome can translate inorganic modified aminoacyl-tRNAs opens up several areas of interest and new directions for this research to explore. One area of prime interest is placing the nanoparticle in a precise location even if there are other cysteine residues encoded in a particular protein. The technology for doing this with non-natural amino acids is already established using suppressor tRNAs.[60] Collaboration is underway with Randy Hughes in the Ellington laboratory for site-specific incorporation of the nanoparticles to study potential applications, such as protein-protein interactions, structure–function relations and protein folding. Two categories of suppressor cysteinyl-$tRNA^{cys}$, opal (UGA) and amber (UAG) have been prepared and modified with gold nanoparticles. This novel gold modified suppressor cysteinyl-$tRNA^{cys}$ will be used in coupled transcription-translation reactions to biosynthesize bacteriophage MS2 coat protein or GFP with a termination codon placed in a specific location. If this method is successful, an *in vitro* continuous cell flow system to biosynthesize large quantities of a desired protein (milligrams amounts have been reported) and used study the behavior of these new inorganic/organic protein complexes

Producing proteins with inorganic modified amino acids will have benefits in monitoring assembly of viral particles, e.g., a "gold studded" viral particle or a protein that has a single nanoparticles that may facilitate structural studies. There applications are only limited by the success of optimization and preparation of large amounts of the suppressor tRNA.

One area that needs to be optimized is the yield of aminoacylation. The low

level of amino acylation (10-30%) is typical for *in vitro* transcribed tRNAs. This is probably due to several factors, but most specifically to the incomplete formation of the tRNA-CCA 3' end. The –CCA 3' end is crucial for amino acylation. A method using primers with 2'-O methyl sugars to generate the transcription template by PCR[27, 141] improves the amount of full length tRNA with the correct –CCA at the 3' end of the transcript. By improving the fidelity of the 3' end, the amount of aminoacylated tRNA will be increased significantly. Preliminary date suggests aminoacylation of up to 80-90% may be possible by the CTA method with the 2'-O methyl sugars modified template. Improving the percentage of aminoacylated tRNA will improve the amount of synthesized protein.

The possibility of the nanoparticle-amino acids systems to be used for translation of a polypeptide opens new opportunities in the elucidation of the tRNA dynamics when binding to ribosomes, peptide bond formation and protein folding. The binding of gold nanoparticle to the aminoacyl-tRNA (in presence or absence of the linker) demonstrates the viability of interaction between two very different and complex systems, and opens new opportunities for the interactions of similar systems. Besides the nanogold systems that are employed, other nanoparticle systems may be used when they become available with the appropriate single reactive groups and sizes. Semiconductor-type systems like cadmium sulfide (CdS) and cadmium selenide (CdSe) could be used in addition to the other metal-type nanoparticles, such as cobalt.

If all the optimization problems can be overcome (generating large amounts of tRNA, finding less expensive, fluorescent nanoparticles, trouble shooting continuous flow protein synthesis to name a few). This technology may be used to generate new types of inorganic/biological molecules and may also be used to study mechanistic aspects of protein synthesis such as using cryo-electron microscopy to localize the exit of the modified nascent peptide from the ribosome through the exit tunnel or the cleft. At the very least this technology may be used to generate new types of inorganic/biological molecules with novel properties, such as conductive nanowire peptides that have nanoparticles spaced at regular intervals.

Appendix

PROTEIN SEQUENCE:

***E. coli* His^{N}-LysRS protein sequence:**

MetGlyHisHisHisHisHisHisHisHisHisHisHisSerSerGlyHisIleAspAspAspAspLysHisMet
SerGluGlnHisAlaGlnGlyAlaAspAlaValValAspLeuAsnAsnGluLeuLysThrArgArgGluLy
sLeuAlaAsnLeuArgGluGlnGlyIleAlaPheProAsnAspPheArgArgAspHisThrSerAspGlnLe
uHisAlaGluPheAspGlyLysGluAsnGluGluLeuGluAlaLeuAsnIleGluValAlaValAlaGlyAr
gMetMetThrArgArgIleMetGlyLysAlaSerPheValThrLeuGlnAspValGlyGlyArgIleGlnLeu
TyrValAlaArgAspAspLeuProGluGlyValTyrAsnGluGlnPheLysLysTrpAspLeuGlyAspIle
LeuGlyAlaLysGlyLysLeuPheLysThrLysThrGlyGluLeuSerIleHisCysThrGluLeuArgLeu
LeuThrLysAlaLeuArgProLeuProAspLysPheHisGlyLeuGlnAspGlnGluAlaArgTyrArgGl
nArgTyrLeuAspLeuIleSerAsnAspGluSerArgAsnThrPheLysValArgSerGlnIleLeuSerGlyI
leArgGlnPheMetValAsnArgGlyPheMetGluValGluThrProMetMetGlnValIleProGlyGlyAl
aAlaAlaArgProPheIleThrHisHisAsnAlaLeuAspLeuAspMetTyrLeuArgIleAlaProGluLeu
TyrLeuLysArgLeuValValGlyGlyPheGluArgValPheGluIleAsnArgAsnPheArgAsnGluGly
IleSerValArgHisAsnProGluPheThrMetMetGluLeuTyrMetAlaTyrAlaAspTyrLysAspLeuI
leGluLeuThrGluSerLeuPheArgThrLeuAlaGlnAspIleLeuGlyLysThrGluValThrTyrGlyAs
pValThrLeuAspPheGlyLysProPheGluLysLeuThrMetArgGluAlaIleLysLysTyrArgProGlu
ThrAspMetAlaAspLeuAspAsnPheAspSerAlaLysAlaIleAlaGluSerIleGlyIleHisValGluLy
sSerTrpGlyLeuGlyArgIleValThrGluIlePheGluGluValAlaGluAlaHisLeuIleGlnProThrPhe
IleThrGluTyrProAlaGluValSerProLeuAlaArgArgAsnAspValAsnProGluIleThrAspArgPh
eGluPhePheIleGlyGlyArgGluIleGlyAsnGlyPheSerGluLeuAsnAspAlaGluAspGlnAlaGln
ArgPheLeuAspGlnValAlaAlaLysAspAlaGlyAspAspGluAlaMetPheTyrAspGluAspTyrV

alThrAlaLeuGluHisGlyLeuProProThrAlaGlyLeuGlyIleGlyIleAspArgMetValMetLeuPhe
ThrAsnSerHisThrIleArgAspValIleLeuPheProAlaMetArgProValLysOchOchGlyProAlaAl
aAla

DNA sequence of *E. coli* His^{N}-LysRS in pET19b:

CCATGGGCCATCATCATCATCATCATCATCATCATCACAGCAGCGGCCAT
ATCGACGACGACGACAAGCATATGTCTGAACAACACGCACAGGGCGCTGAC
GCGGTAGTCGATCTTAACAATGAACTGAAAACGCGTCGTGAGAAGCTGGCGA
ACCTGCGTGAGCAGGGGATTGCCTTCCCGAACGATTTCCGTCGCGATCATACC
TCTGACCAATTGCACGCAGAATTCGACGGTAAAGAGAACGAAGAACTGGAA
GCGCTGAACATCGAAGTCGCCGTTGCTGGCCGCATGATGACCCGTCGTATTAT
GGGTAAAGCGTCTTTCGTTACCCTGCAGGACGTTGGCGGTCGCATTCAGTTGT
ACGTTGCCCGTGACGATCTGCCGGAAGGCGTTTACAACGAGCAGTTCAAAAA
ATGGGACCTCGGCGATATCCTCGGCGCGAAAGGTAAACTGTTCAAAACCAAA
ACCGGCGAACTGTCTATCCACTGTACCGAGCTGCGTCTGCTGACCAAAGCAC
TGCGTCCGCTGCCGGATAAATTCCACGGCTTGCAGGATCAGGAAGCGCGCTA
TCGTCAGCGTTATCTGGATCTCATCTCTAACGATGAATCCCGCAACACCTTTA
AAGTGCGCTCGCAGATCCTCTCTGGTATTCGCCAGTTCATGGTGAACCGCGGC
TTTATGGAAGTTGAAACGCCGATGATGCAGGTGATCCCTGGCGGTGCCGCTG
CGCGTCCGTTTATCACTCACCATAACGCGCTGGATCTCGACATGTACCTGCGT
ATCGCGCCGGAACTGTACCTCAAGCGTCTGGTGGTCGGTGGCTTCGAGCGTG
TATTCGAAATCAACCGTAACTTCCGTAACGAAGGTATTTCCGTACGTCATAAC
CCAGAGTTCACCATGATGGAACTCTATATGGCTTACGCAGATTACAAAGATC
TTATCGAGCTGACCGAATCGCTGTTCCGTACTCTGGCACAGGATATTCTCGGT
AAGACGGAAGTGACCTACGGCGACGTAACGCTGGACTTCGGTAAACCGTTCG

AAAAACTGACCATGCGTGAAGCGATCAAGAAATATCGCCCGGAAACTGACAT
GGCGGATCTGGACAACTTCGACTCTGCGAAAGCGATTGCTGAATCTATCGGC
ATCCACGTTGAGAAAAGCTGGGGTCTGGGCCGTATCGTTACCGAGATCTTCG
AAGAAGTGGCAGAAGCACATCTGATCCAGCCGACCTTCATTACTGAATATCC
GGCAGAAGTTTCTCCTCTGGCGCGTCGTAACGACGTTAACCCGGAAATCACA
GACCGCTTTGAGTTCTTCATTGGTGGGCGTGAAATCGGTAACGGCTTTAGCGA
ACTGAATGACGCGGAAGATCAGGCGCAGCGCTTCCTGGATCAGGTTGCCGCG
AAAGATGCAGGTGACGACGAAGCGATGTTCTACGACGAAGATTATGTCACCG
CACTGGAACATGGCTTACCACCGACAGCCGGTCTGGGAATTGGTATCGACCG
TATGGTAATGCTGTTCACCAACAGCCATACCATCCGCGACGTTATTCTGTTCC
CGGCGATGCGTCCGGTGAAATAATAAGGACCGGCTGCTGCTAA

***E. coli* His^{C}-LysRS protein sequence:**

MetSerGluGlnHisAlaGlnGlyAlaAspAlaValValAspLeuAsnAsnGluLeuLysThrArgArgGl
uLysLeuAlaAsnLeuArgGluGlnGlyIleAlaPheProAsnAspPheArgArgAspHisThrSerAspGl
nLeuHisAlaGluPheAspGlyLysGluAsnGluGluLeuGluAlaLeuAsnIleGluValAlaValAlaGl
yArgMetMetThrArgArgIleMetGlyLysAlaSerPheValThrLeuGlnAspValGlyGlyArgIleGln
LeuTyrValAlaArgAspAspLeuProGluGlyValTyrAsnGluGlnPheLysLysTrpAspLeuGlyAs
pIleLeuGlyAlaLysGlyLysLeuPheLysThrLysThrGlyGluLeuSerIleHisCysThrGluLeuArg
LeuLeuThrLysAlaLeuArgProLeuProAspLysPheHisGlyLeuGlnAspGlnGluAlaArgTyrAr
gGlnArgTyrLeuAspLeuIleSerAsnAspGluSerArgAsnThrPheLysValArgSerGlnIleLeuSer
GlyIleArgGlnPheMetValAsnArgGlyPheMetGluValGluThrProMetMetGlnValIleProGly
GlyAlaAlaAlaArgProPheIleThrHisHisAsnAlaLeuAspLeuAspMetTyrLeuArgIleAlaProGl
uLeuTyrLeuLysArgLeuValValGlyGlyPheGluArgValPheGluIleAsnArgAsnPheArgAsnG
luGlyIleSerValArgHisAsnProGluPheThrMetMetGluLeuTyrMetAlaTyrAlaAspTyrLysAs
pLeuIleGluLeuThrGluSerLeuPheArgThrLeuAlaGlnAspIleLeuGlyLysThrGluValThrTyr
GlyAspValThrLeuAspPheGlyLysProPheGluLysLeuThrMetArgGluAlaIleLysLysTyrArg

ProGluThrAspMetAlaAspLeuAspAsnPheAspSerAlaLysAlaIleAlaGluSerIleGlyIleHisVal
GluLysSerTrpGlyLeuGlyArgIleValThrGluIlePheGluGluValAlaGluAlaHisLeuIleGlnPro
ThrPheIleThrGluTyrProAlaGluValSerProLeuAlaArgArgAsnAspValAsnProGluIleThrAs
pArgPheGluPhePheIleGlyGlyArgGluIleGlyAsnGlyPheSerGluLeuAsnAspAlaGluAspGln
AlaGlnArgPheLeuAspGlnValAlaAlaLysAspAlaGlyAspAspGluAlaMetPheTyrAspGluAs
pTyrValThrAlaLeuGluHisGlyLeuProProThrAlaGlyLeuGlyIleGlyIleAspArgMetValMet
LeuPheThrAsnSerHisThrIleArgAspValIleLeuPheProAlaMetValMetLeuPheThrAsnSerHi
sThrIleArgAspValIleLeuPheProAlaMetArgProValLysLeuGluHisHisHisHisHisHis

DNA sequence of *E. coli* His^{C}-LysRS in pET22b:

ATGTCTGAACAACACGCACAGGGCGCTGACGCGGTAGTCGATCTTAAC
AATGAACTGAAAACGCGTCGTGAGAAGCTGGCGAACCTGCGTGAGCAGGGG
ATTGCCTTCCCGAACGATTTCCGTCGCGATCATACCTCTGACCAATTGCACGC
AGAATTCGACGGTAAAGAGAACGAAGAACTGGAAGCGCTGAACATCGAAGT
CGCCGTTGCTGGCCGCATGATGACCCGTCGTATTATGGGTAAAGCGTCTTTCG
TTACCCTGCAGGACGTTGGCGGTCGCATTCAGTTGTACGTTGCCCGTGACGAT
CTGCCGGAAGGCGTTTACAACGAGCAGTTCAAAAAATGGGACCTCGGCGATA
TCCTCGGCGCGAAAGGTAAACTGTTCAAAACCAAAACCGGCGAACTGTCTAT
CCACTGTACCGAGCTGCGTCTGCTGACCAAAGCACTGCGTCCGCTGCCGGAT
AAATTCCACGGCTTGCAGGATCAGGAAGCGCGCTATCGTCAGCGTTATCTGG
ATCTCATCTCTAACGATGAATCCCGCAACACCTTTAAAGTGCGCTCGCAGATC
CTCTCTGGTATTCGCCAGTTCATGGTGAACCGCGGCTTTATGGAAGTTGAAAC
GCCGATGATGCAGGTGATCCCTGGCGGTGCCGCTGCGCGTCCGTTTATCACTC
ACCATAACGCGCTGGATCTCGACATGTACCTGCGTATCGCGCCGGAACTGTA
CCTCAAGCGTCTGGTGGTCGGTGGCTTCGAGCGTGTATTCGAAATCAACCGTA
ACTTCCGTAACGAAGGTATTTCCGTACGTCATAACCCAGAGTTCACCATGATG
GAACTCTATATGGCTTACGCAGATTACAAAGATCTTATCGAGCTGACCGAAT
CGCTGTTCCGTACTCTGGCACAGGATATTCTCGGTAAGACGGAAGTGACCTA
CGGCGACGTAACGCTGGACTTCGGTAAACCGTTCGAAAAACTGACCATGCGT

GAAGCGATCAAGAAATATCGCCCGGAAACTGACATGGCGGATCTGGACAACT
TCGACTCTGCGAAAGCGATTGCTGAATCTATCGGCATCCACGTTGAGAAAAG
CTGGGGTCTGGGCCGTATCGTTACCGAGATCTTCGAAGAAGTGGCAGAAGCA
CATCTGATCCAGCCGACCTTCATTACTGAATATCCGGCAGAAGTTTCTCCTCT
GGCGCGTCGTAACGACGTTAACCCGGAAATCACAGACCGCTTTGAGTTCTTC
ATTGGTGGGCGTGAAATCGGTAACGGCTTTAGCGAACTGAATGACGCGGAAG
ATCAGGCGCAGCGCTTCCTGGATCAGGTTGCCGCGAAAGATGCAGGTGACGA
CGAAGCGATGTTCTACGACGAAGATTATGTCACCGCACTGGAACATGGCTTA
CCACCGACAGCCGGTCTGGGAATTGGTATCGACCGTATGGTAATGCTGTTCA
CCAACAGCCATACCATCCGCGACGTTATTCTGTTCCCGGCGATGGTAATGCTG
TTCACCAACAGCCATACCATCCGCGACGTTATTCTGTTCCCGGCGATGCGTCC
GGTAAAACTCGAGCACCACCACCACCACCACTGAGATCCGGNTGCTAACAAA
AAACGAAAGGAAG

Human His^{N}-LysRS protein sequence:

MetArgGlySerHisHisHisHisHisHisSerSerGlyTrpValAspGlySerGluProLysLeuSerLysAs
nGluLeuLysArgArgLeuLysAlaGluLysLysValAlaGluLysGluAlaLysGlnLysGluLeuSerGl
uLysGlnLeuSerGlnAlaThrAlaAlaAlaThrAsnHisThrThrAspAsnGlyValGlyProGluGluGlu
SerValAspProAsnGlnTyrTyrLysIleArgSerGlnAlaIleHisGlnLeuLysValAsnGlyGluAspPr
oTyrProHisLysPheHisValAspIleSerLeuThrAspPheIleGlnLysTyrSerHisLeuGlnProGlyAs
pHisLeuThrAspIleThrLeuLysValAlaGlyArgIleHisAlaLysArgAlaSerGlyGlyLysLeuIlePh
eTyrAspLeuArgGlyGluGlyValLysLeuGlnValMetAlaAsnSerArgAsnTyrLysSerGluGluGl
uPheIleHisIleAsnAsnLysLeuArgArgGlyAspIleIleGlyValGlnGlyAsnProGlyLysThrLysL
ysGlyGluLeuSerIleIleProTyrGluIleThrLeuLeuSerProCysLeuHisMetLeuProHisLeuHisPh
eGlyLeuLysAspLysGluThrArgTyrArgGlnArgTyrLeuAspLeuIleLeuAsnAspPheValArgG
lnLysPheIleIleArgSerLysIleIleThrTyrIleArgSerPheLeuAspGluLeuGlyPheLeuGluIleGlu
ThrProMetMetAsnIleIleProGlyGlyAlaValAlaLysProPheIleThrTyrHisAsnGluLeuAspMe
tAsnLeuTyrMetArgIleAlaProGluLeuTyrHisLysMetLeuValValGlyGlyIleAspArgValTyr
GluIleGlyArgGlnPheArgAsnGluGlyIleAspLeuThrHisAsnProGluPheThrThrCysGluPheT
yrMetAlaTyrAlaAspTyrHisAspLeuMetGluIleThrGluLysMetValSerGlyMetValLysHisIle

ThrGlySerTyrLysValThrTyrHisProAspGlyProGluGlyGlnAlaTyrAspValAspPheThrProP
roPheArgArgIleAsnMetValGluGluLeuGluLysAlaLeuGlyMetLysLeuProGluThrAsnLeuP
heGluThrGluGluThrArgLysIleLeuAspAspIleCysValAlaLysAlaValGluCysProProProArg
ThrThrAlaArgLeuLeuAspLysLeuValGlyGluPheLeuGluValThrCysIleAsnProThrPheIleC
ysAspHisProGlnIleMetSerProLeuAlaLysTrpHisArgSerLysGluGlyLeuThrGluArgPheGlu
LeuPheValMetLysLysGluIleCysAsnAlaTyrThrGluLeuAsnAspProMetArgGlnArgGlnLe
uPheGluGluGlnAlaLysAlaLysAlaAlaGlyAspAspGluAlaMetPheIleAspGluAsnPheCysTh
rAlaLeuGluTyrGlyLeuProProThrAlaGlyTrpGlyMetGlyIleAspArgValAlaMetPheLeuThr
AspSerAsnAsnIleLysGluValLeuLeuPheProAlaMetLysProGluAspLysLysGluAsnValAla
ThrThrAspThrLeuGluSerThrThrValGlyThrSerVal

DNA Sequence of Human His^{N}-LysRS in pM368:

ATGAGAGGAAGTCATCATCATCATCATCATAGTAGTGGCTGGGTGGAT
GGCAGCGAGCCGAAACTGAGCAAGAATGAGCTGAAGAGACGCCTGAAAGCT
GAGAAGAAAGTAGCAGAGAAGGAGGCCAAACAGAAAGAGCTCAGTGAGAA
ACAGCTAAGCCAAGCCACTGCTGCTGCCACCAACCACACCACTGATAATGGT
GTGGGTCCTGAGGAAGAGAGCGTGGACCCAAATCAATACTACAAAATCCGCA
GTCAAGCAATTCATCAGCTGAAGGTCAATGGGGAAGACCCATACCCACACAA
GTTCCATGTAGACATCTCACTCACTGACTTCATCCAAAAATATAGTCACCTGC
AGCCTGGGGATCACCTGACTGACATCACCTTAAAGGTGGCAGGTAGGATCCA
TGCCAAAAGAGCTTCTGGGGGAAAGCTCATCTTCTATGATCTTCGAGGAGAG
GGGGTGAAGTTGCAAGTCATGGCCAATTCCAGAAATTATAAATCAGAAGAAG
AATTTATTATGAGAGGAAGTCATCATCATCATCATCATAGTAGTGGCTGGCAT
ATTAATAACAAACTGCGTCGGGGAGACATAATTGGAGTTCAGGGGAATCCTG
GTAAAACCAAGAAGGGTGAGCTGAGCATCATTCCGTATGAGATCACACTGCT
GTCTCCCTGTTTGCATATGTTACCTCATCTTCACTTTGGGCTCAAAGACAAGG
AAACAAGGTATCGCCAGAGATACTTGGACTTGATCCTGAATGACTTTGTGAG
GCAGAAATTTATCATCCGCTCTAAGATCATCACATATATAAGAAGTTTCTTAG
ATGAGCTGGGATTCCTAGAGATTGAAACTCCCATGATGAACATCATCCCAGG

GGGAGCCGTGGCCAAGCCTTTCATCACTTATCACAACGAGCTGGACATGAAC
TTATATATGAGAATTGCTCCAGAACTCTATCATAAGATGCTTGTGGTTGGTGG
CATCGACCGGGTTTATGAAATTGGACGCCAGTTCCGGAATGAGGGGATTGAT
TTGACGCACAATCCTGAGTTCACCACCTGTGAGTTCTACATGGCCTATGCAGA
CTATCACGATCTCATGGAAATCACGGAGAAGATGGTTTCAGGGATGGTGAAG
CATATTACAGGCAGTTACAAGGTCACCTACCACCCAGATGGCCCAGAGGGCC
AAGCCTACGATGTTGACTTCACCCCACCCTTCCGGCGAATCAACATGGTAGA
AGAGCTTGAGAAAGCCCTGGGGATGAAGCTGCCAGAAACGAACCTCTTTGAA
ACTGAAGAAACTCGCAAAATTCTTGATGATATCTGTGTGGCAAAAGCTGTTG
AATGCCCTCCACCTCGGACCACAGCCAGGCTCCTTGACAAGCTTGTTGGGGA
GTTCCTGGAAGTGACTTGCATCAATCCTACATTCATCTGTGATCACCCACAGA
TAATGAGCCCTTTGGCTAAATGGCACCGCTCTAAAGAGGGTCTGACTGAGCG
CTTTGAGCTGTTTGTCATGAAGAAAGAGATATGCAATGCGTATACTGAGCTG
AATGATCCCATGCGGCAGCGGCAGCTTTTTGAAGAACAGGCCAAGGCCAAGG
CTGCAGGTGATGATGAGGCCATGTTCATAGATGAAAACTTCTGTACTGCCCTG
GAATATGGGCTGCCCCCCACAGCTGGCTGGGGCATGGGCATTGATCGAGTCG
CCATGTTTCTCACGGACTCCAACAACATCAAGGAAGTACTTCTGTTTCCTGCC
ATGAAACCCGAAGACAAGAAGGAGAATGTAGCAACCACTGATACACTGGAA
AGCACAACAGTTGGCACTTCTGTCTAGAAAATAATAATTGCAAGTTGTATAA
CTCAGGCGTCTTTGCATTTCTGCGAAAGATCAAGGTCTGCAAGGGAATTCTTG
TGTGCTGCTTTCCATTTGACACCGCAGTTCTGTTCAGCCATCAGAAGAGAGAC
AAGGAATTAAAAATTTCTTTTTAATCCTGTTA

***E. coli* His^{C}-CysRS protein sequence:**

MetLeuLysIlePheAsnThrLeuThrArgGlnLysGluGluPheLysProIleHisAlaGlyGluValGlyM
etTyrValCysGlyIleThrValTyrAspLeuCysHisIleGlyHisGlyArgThrPheValAlaPheAspVal
ValAlaArgTyrLeuArgPheLeuGlyTyrLysLeuLysTyrValArgAsnIleThrAspIleAspAspLysI
leIleLysArgAlaAsnGluAsnGlyGluSerPheValAlaLeuValAspArgMetIleAlaGluMetHisLys
AspPheAspAlaLeuAsnIleLeuArgProAspMetGluProArgAlaThrHisHisIleAlaGluIleIleGlu
LeuThrGluGlnLeuIleAlaLysGlyHisAlaTyrValAlaAspAsnGlyAspValMetPheAspValPro
ThrAspProThrTyrGlyValLeuSerArgGlnAspLeuAspGlnLeuGlnAlaGlyAlaArgValAspVal
ValAspAspLysArgAsnProMetAspPheValLeuTrpLysMetSerLysGluGlyGluProSerTrpPro
SerProTrpGlyAlaGlyArgProGlyTrpHisIleGluCysSerAlaMetAsnCysLysGlnLeuGlyAsnH
isPheAspIleHisGlyGlyGlySerAspLeuMetPheProHisHisGluAsnGluIleAlaGlnSerThrCys
AlaHisAspGlyGlnTyrValAsnTyrTrpMetHisSerGlyMetValMetValAspArgGluLysMetSer
LysSerLeuGlyAsnPhePheThrValArgAspValLeuLysTyrTyrAspAlaGluThrValArgTyrPhe
LeuMetSerGlyHisTyrArgSerGlnLeuAsnTyrSerGluGluAsnLeuLysGlnAlaArgAlaAlaLeu
GluArgLeuTyrThrAlaLeuArgGlyThrAspLysThrValAlaProAlaGlyGlyGluAlaPheGluAla
ArgPheIleGluAlaMetAspAspAspPheAsnThrProGluAlaTyrSerValLeuPheAspMetAlaArg
GluValAsnArgLeuLysValGluAspMetAlaAlaAlaAsnAlaMetAlaSerHisLeuArgLysLeuSer
AlaValLeuGlyLeuLeuGluGlnGluProGluAlaPheLeuGlnSerGlyAlaGlnAlaAspAspSerGlu
ValAlaGluIleGluAlaLeuIleGlnGlnArgLeuAspAlaArgLysAlaLysAspTrpAlaAlaAlaAspA
laAlaArgAspArgLeuAsnGluMetGlyIleValLeuGluAspGlyProGlnGlyThrThrTrpArgArgL
ysLysProGlyAspProAsnSerSerSerValAspLysLeuAlaAlaAlaLeuGluHisHisHisHisHisHis

DNA Sequence of *E. coli* His^{C}-CysRS in pCysRS09:

AAGAAGGAGATATACAATGCTAAAAATCTTCAATACTCTGACACGCCAAAAA
GAGGAATTTAAGCCTATTCACGCCGGGGAAGTCGGCATGTACGTGTGTGGAA
TCACCGTTTACGATCTCTGTCATATCGGTCACGGGCGTACCTTTGTTGCTTTTG
ACGTGGTTGCGCGCTATCTGCGTTTCCTCGGCTATAAGCTGAAGTATGTGCGC

AACATTACCGATATCGACGACAAAATCATCAAACGCGCCAATGAAAATGGCG
AAAGCTTTGTGGCGCTGGTGGATCGCATGATCGCCGAAATGCACAAAGATTT
TGATGCGTTGAACATTCTGCGCCCGGATATGGAGCCGCGCGCGACGCACCAT
ATCGCAGAAATTATTGAACTCACTGAACAACTGATCGCCAAAGGTCACGCTT
ATGTGGCGGACAACGGCGACGTGATGTTCGACGTCCCGACCGATCCAACTTA
TGGCGTGCTGTCGCGTCAGGATCTCGACCAGCTGCAGGCAGGCGCGCGCGTT
GACGTGGTCGACGACAAACGCAACCCAATGGACTTCGTTCTGTGGAAGATGT
CGAAAGAGGGCGAACCGAGCTGGCCGTCTCCGTGGGGCGCGGGTCGTCCTGG
CTGGCACATTGAATGTTCGGCAATGAACTGCAAGCAGCTGGGTAACCACTTT
GATATCCACGGCGGCGGTTCAGACCTGATGTTCCCGCACCACGAAAACGAAA
TCGCGCAGTCCACCTGTGCCCATGATGGTCAGTATGTGAACTACTGGATGCAC
TCGGGGATGGTGATGGTTGACCGCGAGAAGATGTCCAAATCGCTGGGTAACT
TCTTTACCGTGCGCGATGTGCTGAAATACTACGACGCGGAAACCGTGCGTTA
CTTCCTGATGTCGGGCCACTATCGCAGCCAGCTGAACTATAGCGAAGAGAAC
CTGAAGCAGGCGCGTGCGGCGCTGGAGCGTCTCTACACTGCGCTGCGCGGCA
CAGATAAAACCGTTGCGCCTGCCGGTGGCGAAGCGTTTGAAGCGCGCTTTAT
TGAAGCGATGGACGACGATTTCAACACCCCGGAAGCCTATTCCGTGCTGTTT
GATATGGCGCGTGAAGTAAACCGTCTGAAAGTAGAAGATATGGCAGCGGCG
AATGCAATGGCATCTCACCTGCGTAAACTTTCCGCCGTATTGGGCCTGCTGGA
GCAAGAACCGGAAGCGTTCCTGCAAAGCGGCGCGCAGGCAGACGACAGCGA
AGTGGCTGAGATTGAAGCGTTAATTCAACAGCGTCTGGATGCCCGTAAAGCG
AAAGACTGGGCGGCGGCAGATGCGGCGCGTGACCGTCTTAATGAGATGGGG
ATCGTGCTGGAAGATGGCCCGCAAGGGACCACCTGGCGTCGTAAGAAACCGG
GGGATCCGAATTCGAGCTCCGTCGACAAGCTTGCGGCCGCACTCGAGCACCA
CCACCACCACCACTGAGATCCGGCTGCTAACAAAGCCCGAAAGGAAGCTGAG
TGGCTGCTCA

Green Fluorescent Protein (GFP) protein sequence:

MetThrSerLysGlyGluGluLeuPheThrGlyValValProIleLeuValGluLeuAspGlyAspValAsn
GlyHisLysPheSerValSerGlyGluGlyGluGlyAspAlaThrTyrGlyLysLeuThrLeuLysPheIleC
ysThrThrGlyLysLeuProValProTrpProThrLeuValThrThrPheSerTyrGlyValGln
CysPheSerArgTyrProAspHisMetLysArgHisAspPhePheLysSerAlaMetProGluGlyTyrVal
GlnGluArgThrIleSerPheLysAspAspGlyAsnTyrLysThrArgAlaGluValLysPheGluGlyAsp
ThrLeuValAsnArgIleGluLeuLysGlyIleAspPheLysGluAspGlyAsnIleLeuGlyHisLysLeuG
luTyrAsnTyrAsnSerHisAsnValTyrIleThrAlaAspLysGlnLysAsnGlyIleLysAlaAsnPheLys
IleArgHisAsnIleGluAspGlySerValGlnLeuAlaAspHisTyrGlnGlnAsnThrProIleGlyAspGl
yProValLeuLeuProAspAsnHisTyrLeuSerThrGlnSerAlaLeuSerLysAspProAsnGluLysAr
gAspHisMetValLeuLeuGluPheValThrAlaAlaGlyIleThrHisGlyMetAspGluLeuTyrLysPro
GlySerAla**TrpSerHisProGlnPheGluLys**

Strep-tag

DNA sequence of GFP in pIVEX2.1:

TCGCGCGTTTCGGTGATGACGGTGAAAACCTCTGACACATGCAGCTCCCGGA
GACGGTCACAGCTTGTCTGTAAGCGGATGCCGGGAGCAGACAAGCCCGTCAG
GGCGCGTCAGCGGGTGTTGGCGGGTGTCGGGGCTGGCTTAACTATGCGGCAT
CAGAGCAGATTGTACTGAGAGTGCACCATATGCGGTGTGAAATACCGCACAG
ATGCGTAAGGAGAAAATACCGCATCAGGCGCCATTCGCCATTCAGGCTGCGC
AACTGTTGGGAAGGGCGATCGGTGCGGGCCTCTTCGCTATTACGCCAGCTGG
CGAAAGGGGGATGTGCTGCAAGGCGATTAAGTTGGGTAACGCCAGGGTTTTC
CCAGTCACGACGTTGTAAAACGACGGCCAGTGCCAAGCTTGCATGCAAGGAG
ATGGCGCCCAACAGTCCCCCGGCCACGGGGCCTGCCACCATACCCACGCCGA
AACAAGCGCTCATGAGCCCGAAGTGGCGAGCCCGATCTTCCCCATCGGTGAT
GTCGGCGATATAGGCGCCAGCAACCGCACCTGTGGCGCCGGTGATGCCGGCC
ACGATGCGTCCGGCGTAGAGGATCGAGATCTCGATCCCGCGAAATTAATACG
ACTCACTATAGGGAGACCACAACGGTTTCCCTCTAGAAATAATTTTGTTTAAC
TTTAAGAAGGAGATATACCATGACTAGCAAAGGAGAAGAACTTTTCACTGGA

GTTGTCCCAATTCTTGTTGAATTAGATGGTGATGTTAATGGGCACAAATTTTC
TGTCAGTGGAGAGGGTGAAGGTGATGCTACATACGGAAAGCTTACCCTTAAA
TTTATTTGCACTACTGGAAAACTACCTGTTCCATGGCCAACACTTGTCACTAC
TTTCTCTTATGGTGTTCAATGCTTTTCCCGTTATCCGGATCATATGAAACGGCA
TGACTTTTTCAAGAGTGCCATGCCCGAAGGTTATGTACAGGAACGCACTATAT
CTTTCAAAGATGACGGGAACTACAAGACGCGTGCTGAAGTCAAGTTTGAAGG
TGATACCCTTGTTAATCGTATCGAGTTAAAAGGTATTGATTTTAAAGAAGATG
GAAACATTCTCGGACACAAACTCGAGTACAACTATAACTCACACAATGTATA
CATCACGGCAGACAAACAAAAGAATGGAATCAAAGCTAACTTCAAAATTCGC
CACAACATTGAAGATGGATCCGTTCAACTAGCAGACCATTATCAACAAAATA
CTCCAATTGGCGATGGCCCTGTCCTTTTACCAGACAACCATTACCTGTCGACA
CAATCTGCCCTTTCGAAAGATCCCAACGAAAAGAGAGACCACATGGTCCTTC
TTGAGTTTGTAACAGCTGCTGGGATTACACATGGCATGGATGAACTATACAA
ACCCGGGAGCGCTTGGAGCCACCCGCAGTTCGAAAAATAATAAGGGCCTCCC
ACTGACTGCTCTTCTGTCAGTGGGCTACTCCTGGACTCGGCACCAGATTGCCT
CATTTTTCTCCTCTGGCATTTTGTATAAATCCACCTTGACTGGGGAAATTCTCC
TGGGGTCAGGTGGCACCAGCCTGGATCCGGCTGCTAACAAAGCCCGAAAGGA
AGCTGAGTTGGCTGCTGCCACCGCTGAGCAATAACTAGCATAACCCCTTGGG
GCCTCTAAACGGGTCTTGAGGGGTTTTTTGCTGAAAGGAGGAACTATATCCG
GATATCCACAGGACGGGTGTGGTCGCCATGATCGCGTAGTCGATAGTGGCTC
CAAGTAGCGAAGCGAGCAGGACTGGGCGGCGGCCAAAGCGGTCGGACAGTG
CTCCGAGAACGGGTGCGCATAGAAATTGCATCAACGCATATAGCGCTAGCAG
CACGCCATAGTGACTGGCGATGCTGTCGGAATGGACGATATCCCGCAAGAGG
CCCGGCAGTACCGGCATAACCAAGCCTATGCCTACAGCATCCAGGGTGACGG
TGCCGAGGATGACGATGAGCGCATTGTTAGATTTCATACACGGTGCCTGACT
GCGTTAGCAATTTAACTGTGATAAACTACCGCATTAAAGCTTATCGATGATAA
GCTGTCAAACATGAGAATTCGTAATCATGGTCATAGCTGTTTCCTGTGTGAAA
TTGTTATCCGCTCACAATTCCACACAACATACGAGCCGGAAGCATAAAGTGT
AAAGCCTGGGGTGCCTAATGAGTGAGCTAACTCACATTAATTGCGTTGCGCT
CACTGCCCGCTTTCCAGTCGGGAAACCTGTCGTGCCAGCTGCATTAATGAATC

GGCCAACGCGCGGGGAGAGGCGGTTTGCGTATTGGGCGCTCTTCCGCTTCCT
CGCTCACTGACTCGCTGCGCTCGGTCGTTCGGCTGCGGCGAGCGGTATCAGCT
CACTCAAAGGCGGTAATACGGTTATCCACAGAATCAGGGGATAACGCAGGA
AAGAACATGTGAGCAAAAGGCCAGCAAAAGGCCAGGAACCGTAAAAAGGCC
GCGTTGCTGGCGTTTTTCCATAGGCTCCGCCCCCCTGACGAGCATCACAAAAA
TCGACGCTCAAGTCAGAGGTGGCGAAACCCGACAGGACTATAAAGATACCA
GGCGTTTCCCCCTGGAAGCTCCCTCGTGCGCTCTCCTGTTCCGACCCTGCCGC
TTACCGGATACCTGTCCGCCTTTCTCCCTTCGGGAAGCGTGGCGCTTTCTCAT
AGCTCACGCTGTAGGTATCTCAGTTCGGTGTAGGTCGTTCGCTCCAAGCTGGG
CTGTGTGCACGAACCCCCCGTTCAGCCCGACCGCTGCGCCTTATCCGGTAACT
ATCGTCTTGAGTCCAACCCGGTAAGACACGACTTATCGCCACTGGCAGCAGC
CACTGGTAACAGGATTAGCAGAGCGAGGTATGTAGGCGGTGCTACAGAGTTC
TTGAAGTGGTGGCCTAACTACGGCTACACTAGAAGGACAGTATTTGGTATCT
GCGCTCTGCTGAAGCCAGTTACCTTCGGAAAAAGAGTTGGTAGCTCTTGATCC
GGCAAACAAACCACCGCTGGTAGCGGTGGTTTTTTTGTTTGCAAGCAGCAGA
TTACGCGCAGAAAAAAAGGATCTCAAGAAGATCCTTTGATCTTTTCTACGGG
GTCTGACGCTCAGTGGAACGAAAACTCACGTTAAGGGATTTTGGTCATGAGA
TTATCAAAAAGGATCTTCACCTAGATCCTTTTAAATTAAAAATGAAGTTTTAA
ATCAATCTAAAGTATATATGAGTAAACTTGGTCTGACAGTTACCAATGCTTAA
TCAGTGAGGCACCTATCTCAGCGATCTGTCTATTTCGTTCATCCATAGTTGCC
TGACTCCCCGTCGTGTAGATAACTACGATACGGGAGGGCTTACCATCTGGCC
CCAGTGCTGCAATGATACCGCGAGACCCACGCTCACCGGCTCCAGATTTATC
AGCAATAAACCAGCCAGCCGGAAGGGCCGAGCGCAGAAGTGGTCCTGCAAC
TTTATCCGCCTCCATCCAGTCTATTAATTGTTGCCGGGAAGCTAGAGTAAGTA
GTTCGCCAGTTAATAGTTTGCGCAACGTTGTTGCCATTGCTACAGGCATCGTG
GTGTCACGCTCGTCGTTTGGTATGGCTTCATTCAGCTCCGGTTCCCAACGATC
AAGGCGAGTTACATGATCCCCCATGTTGTGCAAAAAAGCGGTTAGCTCCTTC
GGTCCTCCGATCGTTGTCAGAAGTAAGTTGGCCGCAGTGTTATCACTCATGGT
TATGGCAGCACTGCATAATTCTCTTACTGTCATGCCATCCGTAAGATGCTTTT
CTGTGACTGGTGAGTACTCAACCAAGTCATTCTGAGAATAGTGTATGCGGCG

ACCGAGTTGCTCTTGCCCGGCGTCAATACGGGATAATACCGCGCCACATAGC
AGAACTTTAAAAGTGCTCATCATTGGAAAACGTTCTTCGGGGCGAAAACTCT
CAAGGATCTTACCGCTGTTGAGATCCAGTTCGATGTAACCCACTCGTGCACCC
AACTGATCTTCAGCATCTTTTACTTTCACCAGCGTTTCTGGGTGAGCAAAAAC
AGGAAGGCAAAATGCCGCAAAAAAGGGAATAAGGGCGACACGGAAATGTTG
AATACTCATACTCTTCCTTTTTCAATATTATTGAAGCATTTATCAGGGTTATTG
TCTCATGAGCGGATACATATTTGAATGTATTTAGAAAAATAAACAAATAGGG
GTTCCGCGCACATTTCCCCGAAAAGTGCCACCTGACGTCTAAGAAACCATTAT
TATCATGACATTAACCTATAAAAATAGGCGTATCACGAGGCCCTTTCGTC

Figure 3. 7 (see page 69)

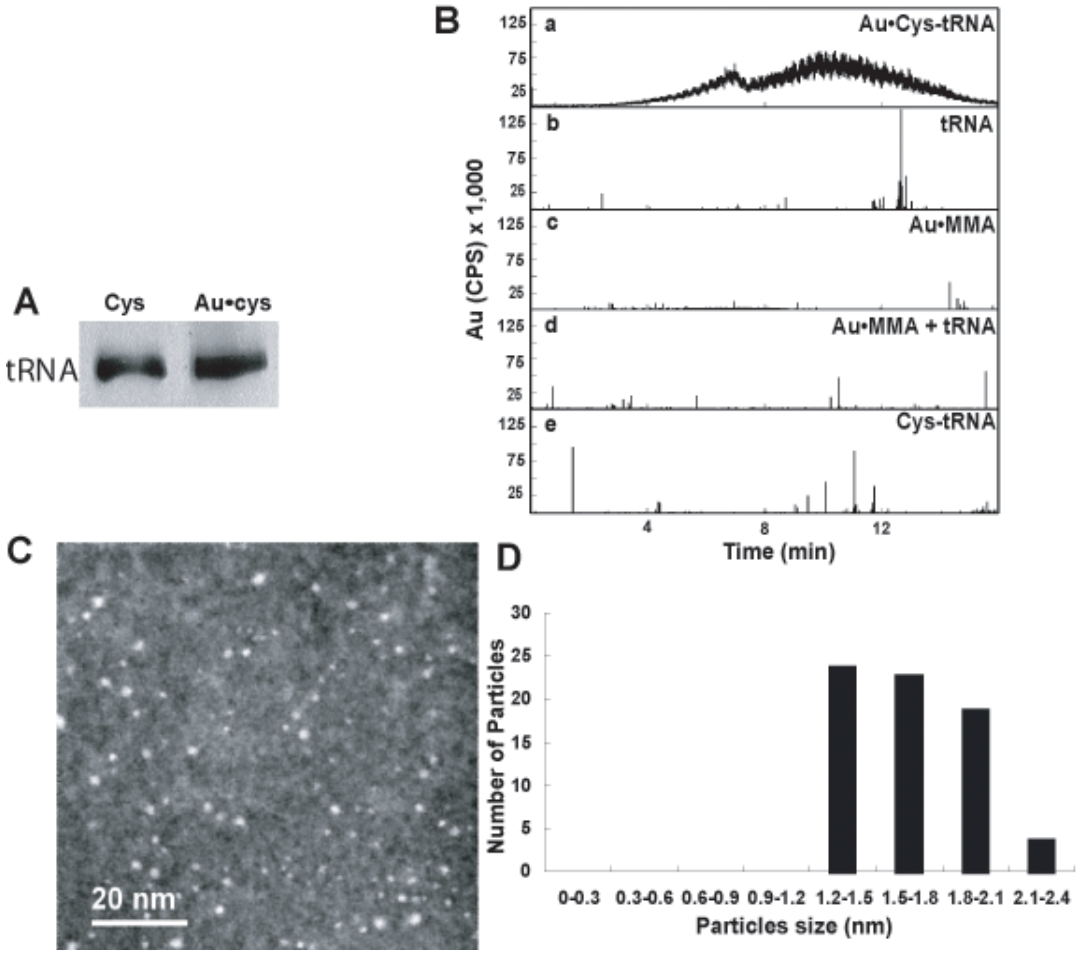

Figure 3. 8 (see page 73)

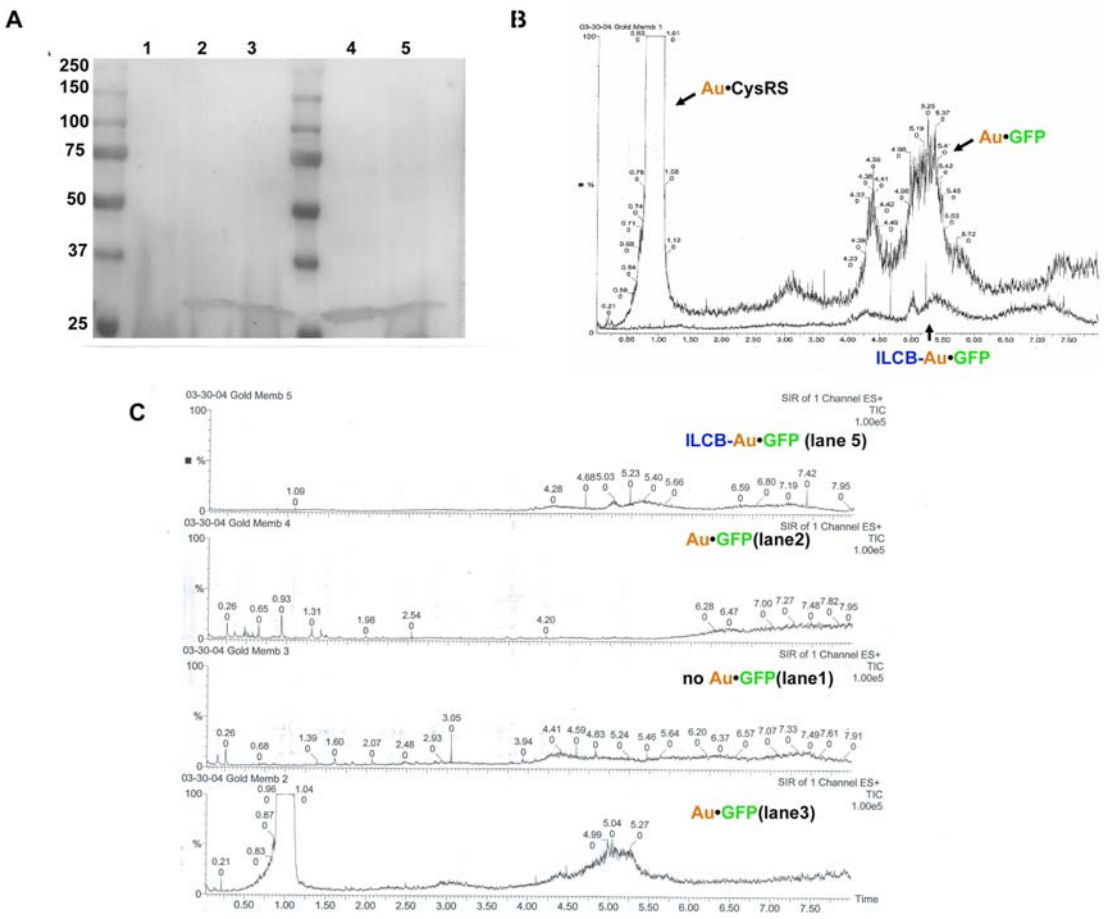

HAADF on Monomaleimido Nanogold (resuspended in water)

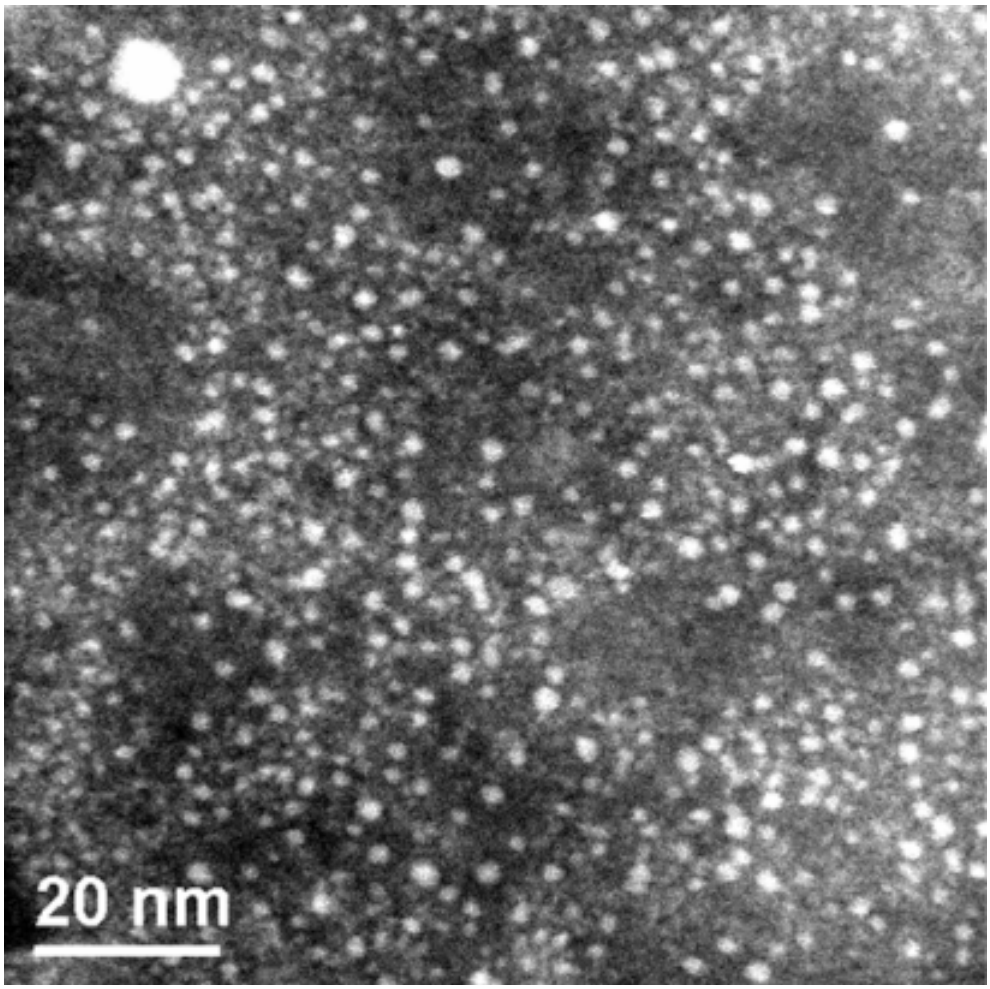

References:

1. Shine, J. and L. Dalgarno, *The 3'-Terminal Sequence of Escherichia coli 16S Ribosomal RNA: Complementarity to Nonsense Triplets and Ribosome Binding Sites.* Proceedings of the National Academy of Sciences, 1974. **71**(4): p. 1342.
2. Dallas, A. and H.F. Noller, *Interaction of Translation Initiation Factor 3 with the 30S Ribosomal Subunit.* Molecular Cell, 2001. **8**(4): p. 855.
3. Pioletti, M., et al., *Crystal structures of complexes of the small ribosomal subunit with tetracycline, edeine and IF3.* The EMBO Journal, 2001. **20**(8): p. 1829.
4. Carter, A.P., et al., *Crystal Structure of an Initiation Factor Bound to the 30S Ribosomal Subunit.* Science, 2001. **291**(5503): p. 498.
5. Rodnina, M.V., et al., *Recognition and selection of tRNA in translation.* FEBS Letters, 2005. **579**(4): p. 938.
6. Katunin, V.I., et al., *Coupling of GTP hydrolysis by elongation factor G to translocation and factor recycling on the ribosome.* Biochemistry, 2002. **41**(42): p. 12806.
7. Peske, F., et al., *Conformational changes of the small ribosomal subunit during elongation factor G-dependent tRNA-mRNA translocation.* J.Mol Biol, 2004. **343**(5): p. 1183.
8. Klaholz, B.P., A.G. Myasnikov, and M. Van Heel, *Visualization of release factor 3 on the ribosome during termination of protein synthesis.* Nature, 2004. **427**(6977): p. 862.
9. Ban, N., et al., *The Complete Atomic Structure of the Large Ribosomal Subunit at 2.4 A Resolution.* Science, 2000. **289**(5481): p. 905-920.
10. Wimberly, B.T., et al., *Structure of the 30S ribosomal subunit.* Nature, 2000. **407**(6802): p. 327.
11. Nissen, P., et al., *The Structural Basis of Ribosome Activity in Peptide Bond Synthesis.* Science, 2000. **289**(5481): p. 920.

12. Barta, A., et al., *Mechanism of Ribosomal Peptide Bond Formation.* Science, 2001. **291**(5502): p. 203a.

13. Green, R. and J.R. Lorsch, *The Path to Perdition Is Paved with Protons.* Cell, 2002. **110**(6): p. 665.

14. Harms, J., et al., *High Resolution Structure of the Large Ribosomal Subunit from a Mesophilic Eubacterium.* Cell, 2001. **107**(5): p. 679.

15. Tenson, T. and M. Ehrenberg, *Regulatory Nascent Peptides in the Ribosomal Tunnel.* Cell, 2002. **108**(5): p. 591.

16. Jenni, S. and N. Ban, *The chemistry of protein synthesis and voyage through the ribosomal tunnel.* Current Opinion in Structural Biology, 2003. **13**(2): p. 212.

17. Wilson, D.N. and K.H. Nierhaus, *The ribosome through the looking glass.* Angew Chem Int Ed Engl, 2003. **42**(30): p. 3464-86.

18. Jenni, S. and N. Ban, *The chemistry of protein synthesis and voyage through the ribosomal tunnel.* Current Opinion in Structural Biology, 2003. **13**(4): p. 533.

19. Ibba, M. and D. Soll, *AMINOACYL-tRNA SYNTHESIS.* Vol. 69. 2000. 617-650.

20. Francklyn, C., et al., *Aminoacyl-tRNA synthetases: versatile players in the changing theater of translation.* RNA., 2002. **8**(11): p. 1363.

21. Zhang, C.M., J.J. Perona, and Y.M. Hou, *Amino acid discrimination by a highly differentiated metal center of an aminoacyl-tRNA synthetase.* Biochemistry, 2003. **42**(37): p. 10931.

22. Avalos, J., L.M. Corrochano, and S. Brenner, *Cysteinyl-tRNA synthetase is a direct descendant of the first aminoacyl-tRNA synthetase.* FEBS Lett., 1991. **286**(1-2): p. 176.

23. Eriani, G., G. Dirheimer, and J. Gangloff, *Cysteinyl-tRNA synthetase: determination of the last E. coli aminoacyl-tRNA synthetase primary structure.* Nucleic Acids Res., 1991. **19**(2): p. 265.

24. Hou, Y.M., et al., *Sequence determination and modeling of structural motifs for the smallest monomeric aminoacyl-tRNA synthetase.* Proc.Natl.Acad.Sci.U.S.A, 1991. **88**(3): p. 976.

25. Lipman, R.S. and Y.M. Hou, *Aminoacylation of tRNA in the evolution of an aminoacyl-tRNA synthetase.* Proc.Natl.Acad.Sci.U.S.A, 1998. **95**(23): p. 13495.

26. Hou, Y.M., et al., *An important 2'-OH group for an RNA-protein interaction.* Nucleic Acids Res., 2001. **29**(4): p. 976.

27. Hauenstein, S., et al., *Shape-selective RNA recognition by cysteinyl-tRNA synthetase.* Nat Struct Mol Biol, 2004. **11**(11): p. 1134.

28. Komatsoulis, G.A. and J. Abelson, *Recognition of tRNA(Cys) by Escherichia coli cysteinyl-tRNA synthetase.* Biochemistry, 1993. **32**(29): p. 7435.

29. Hou, Y.M., E. Westhof, and R. Giege, *An unusual RNA tertiary interaction has a role for the specific aminoacylation of a transfer RNA.* Proc.Natl.Acad.Sci.U.S.A, 1993. **90**(14): p. 6776.

30. Hamann, C.S. and Y.M. Hou, *An RNA structural determinant for tRNA recognition.* Biochemistry, 1997. **36**(26): p. 7967-72.

31. Johnson, A.E., et al., *Nepsilon-acetyllysine transfer ribonucleic acid: a biologically active analogue of aminoacyl transfer ribonucleic acids.* Biochemistry, 1976. **15**(3): p. 569.

32. Crowley, K.S., G.D. Reinhart, and A.E. Johnson, *The signal sequence moves through a ribosomal tunnel into a noncytoplasmic aqueous environment at the ER membrane early in translocation.* Cell, 1993. **73**(6): p. 1101.

33. Johnson, A.E., D.L. Miller, and C.R. Cantor, *Functional covalent complex between elongation factor Tu and an analog of lysyl-tRNA.* Proc.Natl.Acad.Sci.U.S.A, 1978. **75**(7): p. 3075.

34. Johnson, A.E. and P.S.l.D.A.J. Schimmel, *Transfer RNA: Structure, Properties, and Recognition*. 1979, Cold Spring Harbor Laboratory Press, Cold Spring Harbor, N.Y.: New York p. 487.

35. Johnson, A.E. and L.I. Slobin, *Affinity labeling of eukaryotic elongation factors using N epsilon-bromoacetyl-Lys-tRNA.* Nucleic Acids Res., 1980. **8**(18): p. 4185.

36. Krieg, U.C., P. Walter, and A.E. Johnson, *Photocrosslinking of the signal sequence of nascent preprolactin to the 54-kilodalton polypeptide of the signal*

recognition particle. Proc.Natl.Acad.Sci.U.S.A, 1986. **83**(22): p. 8604.

37. Hamman, B.D., et al., *The aqueous pore through the translocon has a diameter of 40-60 A during cotranslational protein translocation at the ER membrane.* Cell, 1997. **89**(4): p. 535.

38. McCallum, C.D., et al., *The interaction of the chaperonin tailless complex polypeptide 1 (TCP1) ring complex (TRiC) with ribosome-bound nascent chains examined using photo-cross-linking.* J.Cell Biol, 2000. **149**(3): p. 591.

39. Wilkinson, D., *Cell-Free And Happy: In Vitro Translation And Transcription/Translation Systems.* The Scientist, 1999. **13**: p. 15.

40. McCormick, D. and R. Mierendorf, in *inNovations*. 1998. p. 1.

41. McCormick, D. and R. Mierendorf, in *inNovations*. 1999. p. 9.

42. Kabat, D., B. Hoffman, and A. Rich, *Synthesis and characterization of a spin-labeled aminoacyl transfer ribonucleic acid.* Biopolymers, 1970. **9**(1): p. 95.

43. Heckler, T.G., et al., *T4 RNA ligase mediated preparation of novel "chemically misacylated" tRNAPheS.* Biochemistry, 1984. **23**(7): p. 1468.

44. Bain, J.D., et al., *Biosynthetic site-specific incorporation of a non-natural amino acid into a polypeptide.* Journal of the American Chemical Society, 1989. **111**(20): p. 8013.

45. Bain, J.D., et al., *Site-specific incorporation of nonnatural residues during in vitro protein biosynthesis with semisynthetic aminoacyl-tRNAs.* Biochemistry, 1991. **30**(22): p. 5411.

46. Noren, C.J., et al., *A general method for site-specific incorporation of unnatural amino acids into proteins.* Science, 1989. **244**(4901): p. 182.

47. Furter, R., *Expansion of the genetic code: site-directed p-fluoro-phenylalanine incorporation in Escherichia coli.* Protein Sci., 1998. **7**(2): p. 419.

48. Liu, D.R. and P.G. Schultz, *Progress toward the evolution of an organism with an expanded genetic code.* Proc.Natl.Acad.Sci.U.S.A, 1999. **96**(9): p. 4780.

49. Bessho, Y., D.R. Hodgson, and H. Suga, *A tRNA aminoacylation system for non-natural amino acids based on a programmable ribozyme.* Nat Biotechnol., 2002.

20(7): p. 723.

50. Murakami, H., N.J. Bonzagni, and H. Suga, *Aminoacyl-tRNA Synthesis by a Resin-Immobilized Ribozyme.* Journal of the American Chemical Society, 2002. **124**(24): p. 6834.

51. Murakami, H., D. Kourouklis, and H. Suga, *Using a Solid-Phase Ribozyme Aminoacylation System to Reprogram the Genetic Code.* Chemistry & Biology, 2003. **10**(11): p. 1077.

52. Murakami, H., H. Saito, and H. Suga, *A Versatile tRNA Aminoacylation Catalyst Based on RNA.* Chemistry & Biology, 2003. **10**(7): p. 655.

53. Ramaswamy, K., et al., *Designer Ribozymes: Programming the tRNA Specificity into Flexizyme.* Journal of the American Chemical Society, 2004. **126**(37): p. 11454.

54. Saito, H. and H. Suga, *A Ribozyme Exclusively Aminoacylates the 3'-Hydroxyl Group of the tRNA Terminal Adenosine.* Journal of the American Chemical Society, 2001. **123**(29): p. 7178.

55. Stromgaard, A., A.A. Jensen, and K. Stromgaard, *Site-specific incorporation of unnatural amino acids into proteins.* Chembiochem., 2004. **5**(7): p. 909.

56. England, P.M., *Unnatural amino acid mutagenesis: a precise tool for probing protein structure and function.* Biochemistry, 2004. **43**(37): p. 11623.

57. Cload, S.T., et al., *Development of improved tRNAs for in vitro biosynthesis of proteins containing unnatural amino acids.* Chem.Biol, 1996. **3**(12): p. 1033.

58. Dougherty, D.A., *Unnatural amino acids as probes of protein structure and function.* Curr.Opin.Chem.Biol, 2000. **4**(6): p. 645.

59. Wang, L. and P.G. Schultz, *Expanding the genetic code.* Angew.Chem.Int.Ed Engl., 2004. **44**(1): p. 34.

60. Wang, L. and P.G. Schultz, *Expanding the genetic code.* Angew.Chem.Int.Ed Engl., 2005. **44**(1): p. 34.

61. Ellman, J., et al., *Biosynthetic method for introducing unnatural amino acids site-specifically into proteins.* Methods Enzymol., 1991. **202:301-36.**: p. 301.

62. Wang, Q., et al., *Icosahedral virus particles as addressable nanoscale building blocks.* Angewandte Chemie, International Edition, 2002. **41**(3): p. 459-462.

63. Xie, J., et al., *The site-specific incorporation of p-iodo-L-phenylalanine into proteins for structure determination.* Nature Biotechnology, 2004. **22**(10): p. 1297-1301.

64. Schwabl, F. and Editor, *Quantum Mechanics*. 1995. 420 pp (approx).

65. Gaponenko, S.V., *Optical Properties of Semiconductor Nanocrystals*. 1998. 240 pp.

66. Ashcroft, N.W. and N.D. Mermin, *Solid State Physics*. 1976. 826 pp.

67. Klimov, V.I., et al., *Electron and hole relaxation pathways in semiconductor quantum dots.* Physical Review B: Condensed Matter and Materials Physics, 1999. **60**(19): p. 13740-13749.

68. Dahan, M., et al., *Time-gated biological imaging by use of colloidal quantum dots.* Optics Letters, 2001. **26**(11): p. 825-827.

69. Hodak, J.H., A. Henglein, and G.V. Hartland, *Photophysics and spectroscopy of metal particles.* Pure and Applied Chemistry, 2000. **72**(1-2): p. 189-197.

70. Mulvaney, P., *Surface Plasmon Spectroscopy of Nanosized Metal Particles.* Langmuir, 1996. **12**(3): p. 788-800.

71. Braun, E. and K. Keren, *From DNA to transistors.* Advances in Physics, 2004. **53**(4): p. 441.

72. Alivisatos, A.P., et al., *Organization of 'nanocrystal molecules' using DNA.* Nature, 1996. **382**(6592): p. 609.

73. Bruchez, M., Jr., et al., *Semiconductor nanocrystals as fluorescent biological labels.* Science, 1998. **281**(5385): p. 2013.

74. Alivisatos, P., *The use of nanocrystals in biological detection.* Nat Biotech, 2004. **22**(1): p. 47.

75. Willard, D.M., et al., *CdSe-ZnS quantum dots as resonance energy transfer donors in a model protein-protein binding assay.[Erratum to document cited in CA135:149544].* Nano Letters, 2001. **1**(10): p. 581.

76. Chan, W.C. and S. Nie, *Quantum dot bioconjugates for ultrasensitive nonisotopic detection.* Science, 1998. **281**(5385): p. 2016.

77. Han, M., et al., *Quantum-dot-tagged microbeads for multiplexed optical coding of biomolecules.* Nat Biotechnol., 2001. **19**(7): p. 631.

78. Chan, W.C., et al., *Luminescent quantum dots for multiplexed biological detection and imaging.* Curr.Opin.Biotechnol., 2002. **13**(1): p. 40.

79. Parak, W.J., et al., *Conjugation of DNA to silanized colloidal semiconductor nanocrystalline quantum dots.* Chemistry of Materials, 2002. **14**(5): p. 2113.

80. Mitchell, G.P., C.A. Mirkin, and R.L. Letsinger, *Programmed Assembly of DNA Functionalized Quantum Dots.* Journal of the American Chemical Society, 1999. **121**(35): p. 8122.

81. Wang, S., et al., *Antigen/antibody immunocomplex from CdTe nanoparticle bioconjugates.* Nano Letters, 2002. **2**(8): p. 817.

82. Paunesku, T., et al., *Biology of TiO2-oligonucleotide nanocomposites.* Nat Mater., 2003. **2**(5): p. 343.

83. Burt, J.L., et al., *Noble-metal nanoparticles directly conjugated to globular proteins.* Langmuir, 2004. **20**(26): p. 11778.

84. Nam, J., S. Park, and C.A. Mirkin, *Bio-barcodes based on oligonucleotide-modified nanoparticles.* Journal of the American Chemical Society, 2002. **124**(15): p. 3820.

85. Chen, Y., J. Aveyard, and R. Wilson, *Gold and silver nanoparticles functionalized with known numbers of oligonucleotides per particle for DNA detection.* Chemical Communications (Cambridge, United Kingdom), 2004(24): p. 2804.

86. Wu, X., et al., *Immunofluorescent labeling of cancer marker Her2 and other cellular targets with semiconductor quantum dots.* Nat Biotechnol., 2003. **21**(1): p. 41.

87. Parak, W.J., et al., *Cell motility and metastatic potential studies based on quantum dot imaging of phagokinetic tracks.* Advanced Materials (Weinheim,

Germany), 2002. **14**(12): p. 882.

88. Taylor, J.R., M.M. Fang, and S. Nie, *Probing specific sequences on single DNA molecules with bioconjugated fluorescent nanoparticles.* Anal.Chem., 2000. **72**(9): p. 1979.

89. Mattoussi, H., et al., *Self-Assembly of CdSe-ZnS Quantum Dot Bioconjugates Using an Engineered Recombinant Protein.* Journal of the American Chemical Society, 2000. **122**(49): p. 12142.

90. Shenton, W., S.A. Davis, and S. Mann, *Directed self-assembly of nanoparticles into macroscopic materials using antibody-antigen recognition.* Advanced Materials (Weinheim, Germany), 1999. **11**(6): p. 449.

91. Naka, K., et al., *Effect of Gold Nanoparticles as a Support for the Oligomerization of L-Cysteine in an Aqueous Solution.* Langmuir, 2003. **19**(13): p. 5546.

92. Hamad-Schifferli, K., et al., *Remote electronic control of DNA hybridization through inductive coupling to an attached metal nanocrystal antenna.* Nature, 2002. **415**(6868): p. 152.

93. Dubertret, B., M. Calame, and A.J. Libchaber, *Single-mismatch detection using gold-quenched fluorescent oligonucleotides.* Nat Biotechnol., 2001. **19**(4): p. 365.

94. Medalia, O., et al., *Gold-tagged RNA-A probe for macromolecular assemblies.* J.Struct Biol, 1999. **127**(2): p. 113.

95. Malecki, M., et al., *Molecular immunolabeling with recombinant single-chain variable fragment (scFv) antibodies designed with metal-binding domains.* Proc.Natl.Acad.Sci.U.S.A, 2002. **99**(1): p. 213.

96. Gestwicki, J.E., L.E. Strong, and L.L. Kiessling, *Visualization of single multivalent receptor-ligand complexes by transmission electron microscopy.* Angewandte Chemie, International Edition, 2000. **39**(24): p. 4567.

97. Niemeyer, C.M., *Nanoparticles, proteins, and nucleic acids: biotechnology meets materials science.* Angewandte Chemie, International Edition, 2001. **40**(22): p. 4128.

98. Soukka, T., et al., *Utilization of kinetically enhanced monovalent binding affinity by immunoassays based on multivalent nanoparticle-antibody bioconjugates.* Anal.Chem., 2001. **73**(10): p. 2254.

99. Sweeney, R.Y., et al., *Bacterial biosynthesis of cadmium sulfide nanocrystals.* Chem.Biol, 2004. **11**(11): p. 1553.

100. Sun, Y. and Y. Xia, *Shape-controlled synthesis of gold and silver nanoparticles.* Science, 2002. **298**(5601): p. 2176.

101. Zheng, J. and R.M. Dickson, *Individual water-soluble dendrimer-encapsulated silver nanodot fluorescence.* J.Am.Chem.Soc., 2002. **124**(47): p. 13982.

102. Zheng, J., J.T. Petty, and R.M. Dickson, *High quantum yield blue emission from water-soluble Au8 nanodots.* J.Am.Chem.Soc., 2003. **125**(26): p. 7780.

103. Liu, Y., et al., *Gold-cluster degradation by the transition of B-DNA into A-DNA and the formation of nanowires.* Angew.Chem.Int.Ed Engl., 2003. **42**(25): p. 2853.

104. Shaffer, A.W., J.G. Worden, and Q. Huo, *Comparison study of the solution phase versus solid phase place exchange reactions in the controlled functionalization of gold nanoparticles.* Langmuir, 2004. **20**(19): p. 8343.

105. Worden, J.G., et al., *Monofunctional Group-Modified Gold Nanoparticles from Solid Phase Synthesis Approach: Solid Support and Experimental Condition Effect.* Chemistry of Materials, 2004. **16**(19): p. 3746.

106. Krieg, U.C., A.E. Johnson, and P. Walter, *Protein translocation across the endoplasmic reticulum membrane: identification by photocross-linking of a 39-kD integral membrane glycoprotein as part of a putative translocation tunnel.* J.Cell Biol, 1989. **109**(5): p. 2033.

107. Shiba, K., et al., *Human lysyl-tRNA synthetase accepts nucleotide 73 variants and rescues Escherichia coli double-defective mutant.* J.Biol Chem., 1997. **272**(36): p. 22809.

108. Shimizu, Y., et al., *Cell-free translation reconstituted with purified components.* Nat Biotechnol., 2001. **19**(8): p. 751.

109. Hermanson, G.T., *Bioconjugate Techniques*. 1996, San Diego, USA.: Academic Press.

110. Kramer, G., et al., *Protein Expression*. 1999, Oxford University Press: Oxford, U K. p. 201-223.

111. Leveque, F., et al., *Homology of lysS and lysU, the two Escherichia coli genes encoding distinct lysyl-tRNA synthetase species.* Nucleic Acids Res., 1990. **18**(2): p. 305.

112. Onesti, S., A.D. Miller, and P. Brick, *The crystal structure of the lysyl-tRNA synthetase (LysU) from Escherichia coli.* Structure., 1995. **3**(2): p. 163.

113. Commans, S., et al., *tRNA anticodon recognition and specification within subclass IIb aminoacyl-tRNA synthetases.* J.Mol Biol, 1998. **278**(4): p. 801.

114. Tamura, K., et al., *In vitro study of E. coli tRNA(Arg) and tRNA(Lys) identity elements.* Nucleic Acids Res., 1992. **20**(9): p. 2335.

115. Cusack, S., A. Yaremchuk, and M. Tukalo, *The crystal structure of the ternary complex of T.thermophilus seryl-tRNA synthetase with tRNA(Ser) and a seryl-adenylate analogue reveals a conformational switch in the active site.* The EMBO Journal, 1996. **15**(11): p. 2834.

116. Alford, B. and S.M. Hecht, *2'-Versus 3'-OH specificity in tRNA aminoacylation. Further support for the "secondary cognition" proposal.* J.Biol Chem., 1978. **253**(14): p. 4844.

117. Ivanova, N., et al., *Ribosome Rescue by tmRNA Requires Truncated mRNAs.* Journal of Molecular Biology, 2004. **338**(1): p. 33.

118. Pavel, I., A. Belcher, and K.S. Browning, *A method for coupled transcription and aminoacylation of cysteinyl-tRNA.* Analytical Biochemistry, 2004. **335**(2): p. 192.

119. *Data Base*. http://paris.chem.yale.edu/extinct.frames.html.

120. Zhang, C.M., et al., *Zinc-mediated amino acid discrimination in cysteinyl-tRNA synthetase.* J.Mol Biol, 2003. **327**(5): p. 911.

121. Ibba, M. and D. Soll, *Aminoacyl-tRNAs: setting the limits of the genetic code.* Genes Dev., 2004. **18**(7): p. 731.

122. Ming, X., et al., *Recognition of tRNA backbone for aminoacylation with cysteine: evolution from Escherichia coli to human.* Journal of Molecular Biology, 2002. **318**(5): p. 1207.

123. Gregori, L., et al., *Binding of Amyloid beta Protein to the 20S Proteasome.* Journal of Biological Chemistry, 1997. **272**(1): p. 58.

124. Boisset, N., et al., *Three-dimensional reconstruction of human a2-macroglobulin and refinement of the localization of thiol ester bonds with monomaleimido nanogold.* Annals of the New York Academy of Sciences, 1994. **737**(Biology of -Macroglobulin, Its Receptor, and Related Proteins): p. 229-44.

125. Milligan, J.F., et al., *Oligoribonucleotide synthesis using T7 RNA polymerase and synthetic DNA templates.* Nucleic Acids Res., 1987. **15**(21): p. 8783.

126. Luc, M., *Applications of mass spectrometry in the trace element analysis of biological materials.* Fresenius' Journal of Analytical Chemistry, 1997. **359**(4 - 5): p. 309.

127. Becker, J.S., *Applications of inductively coupled plasma mass spectrometry and laser ablation inductively coupled plasma mass spectrometry in materials science.* Spectrochimica Acta Part B: Atomic Spectroscopy, 2002. **57**(12): p. 1805.

128. Durrant, S.F., *Laser ablation inductively coupled plasma mass spectrometry: achievements, problems, prospects.* Journal of Analytical Atomic Spectrometry, 1999. **14**(9): p. 1385-1403.

129. Gastel, M., et al., *Determination of long-lived radionuclides in concrete matrix by laser ablation inductively coupled plasma mass spectrometry.* Spectrochimica Acta Part B: Atomic Spectroscopy, 1997. **52**(14): p. 2051.

130. Villeneuve, R.D.E.a.J.Y., *A method for characterization of humic and fulvic acids by gel electrophoresis laser ablation inductively coupled plasma mass spectrometry.* J. Anal. At. Spectrom., 2000. **15**(2): p. 157-161.

131. Hubert Chassaigne, C.C.C., Guy Bordin, Frank Vanhaecke, Adela R. Rodriguez, *2-Dimensional gel electrophoresis technique for yeast selenium-containing proteins—sample preparation and MS approaches for processing 2-D gel protein spots.* J. Anal. At. Spectrom., 2004. **19**(1): p. 85-95.

132. Chery, C.C., et al., *Detection of metals in proteins by means of polyacrylamide gel electrophoresis and laser ablation-inductively coupled plasma-mass spectrometry: Application to selenium.* Electrophoresis, 2003. **24**(19-20): p. 3305-3313.

133. Marshall, P., et al., *The determination of protein phosphorylation on electrophoresis gel blots by laser ablation inductively coupled plasma-mass spectrometry.* Analyst (Cambridge, United Kingdom), 2002. **127**(4): p. 459-461.

134. Neilsen, J.L., et al., *Laser ablation inductively coupled plasma-mass spectrometry in combination with gel electrophoresis: a new strategy for speciation of metal binding serum proteins.* Spectrochimica Acta, Part B: Atomic Spectroscopy, 1998. **53B**(2): p. 339-345.

135. Binet, M.R.B., et al., *Detection and characterization of zinc- and cadmium-binding proteins in Escherichia coli by gel electrophoresis and laser ablation-inductively coupled plasma-mass spectrometry.* Analytical Biochemistry, 2003. **318**(1): p. 30.

136. Teresa W.-M. Fan, E.P., Stephen Shuttleworth, *Speciation of selenoproteins in Se-contaminated wildlife by gel electrophoresis and laser ablation-ICP-MS.* J. Anal. At. Spectrom., 2002. **17**(12): p. 1621-1623.

137. Lee, S.W., et al., *Ordering of quantum dots using genetically engineered viruses.* Science, 2002. **296**(5569): p. 892.

138. Mao, C., et al., *Viral assembly of oriented quantum dot nanowires.* Proc.Natl.Acad.Sci.U.S.A, 2003. **100**(12): p. 6946.

139. Mao, C., et al., *Virus-based toolkit for the directed synthesis of magnetic and semiconducting nanowires.* Science, 2004. **303**(5655): p. 213.

140. Whaley, S.R., et al., *Selection of peptides with semiconductor binding specificity for directed nanocrystal assembly.* Nature, 2000. **405**(6787): p. 665.

141. Sherlin, L.D., et al., *Chemical and enzymatic synthesis of tRNAs for high-throughput crystallization.* RNA, 2001. **7**(11): p. 1671.

Vita

Ioana Simona Pavel was born in Oradea, Bihor, Romania on March 1, 1972, to Marioara and Aurel Ioan Negru. She attended the "Babes-Bolyai" University were she received in 1996 a bachelor degree in Chemistry with a minor in Physics. In 1997, she received a Master in Science in Inorganic Chemistry from the same university. In 1998, she enrolled in the graduate program at University of Texas at El Paso, under the supervision of Dr. Keith H Pannell where she received a Master in Science in Organometallic Chemistry in 2000. In 2000, she went on to pursue her doctoral studies in bioinorganic chemistry at University of Texas at Austin under the supervision of Professors Karen S. Browning and Angela Belcher. Dr. Angela Belcher has since moved to the Massachusetts Institute of Technology.

Permanent address: 1333 Arena Dr. Apt 205, Austin, Texas 78741

This dissertation was typed by the author